

THESIS FOR THE DEGREE OF DOCTOR OF PHILOSOPHY (PHD)

Novel inducers of human adipocyte browning;  
Utilization of population scale cellular analysis

by

Endre Károly Kristóf

Supervisor: Prof. Dr. László Fésüs



UNIVERSITY OF DEBRECEN  
DOCTORAL SCHOOL OF MOLECULAR CELL AND IMMUNE BIOLOGY

DEBRECEN, 2016

# TABLE OF CONTENTS

<b>1. Abbreviations .....</b>	<b>3</b>
<b>2. Introduction .....</b>	<b>6</b>
2.1. The unique mammalian heat producing organ: Brown adipose tissue (BAT) ...	6
2.1.1. Morphology of BAT .....	6
2.1.2. Uncoupling protein 1 (UCP1) .....	8
2.1.3. Induction of BAT thermogenesis .....	10
2.2. Heat-generating fat depots: “Classical brown” and “beige” adipocyte development .....	11
2.2.1. Origin of “classical brown” adipocytes .....	11
2.2.2. “Beige” adipocytes – inducible thermogenic fat cells .....	13
2.2.3. Markers of browning .....	16
2.2.4. UCP1-independent thermogenesis .....	17
2.3. Implications of “browning” for metabolic health in humans .....	18
2.3.1. Obesity – a global health issue .....	18
2.3.2. Browning adipocytes exist in adult humans – Can we find and activate them? .....	20
2.4. Activators of brown and “beige” fat development and function .....	23
2.4.1. Hormones which regulate browning by central and peripheral actions ....	23
2.4.2. Physical exercise and non-shivering thermogenesis (NST) .....	25
2.4.3. Browning-inducers which directly target adipose tissue .....	28
<b>3. Aims of the study .....</b>	<b>30</b>
<b>4. Materials and methods.....</b>	<b>31</b>
4.1. Ethics statement.....	31
4.2. Materials .....	31
4.3. Isolation and cultivation of hADMSCs .....	33
4.4. Induction of white and “beige” adipocyte differentiation <i>ex vivo</i> .....	34
4.5. Treatments of hADMSCs and differentiated white and “beige” adipocytes with browning-inducers or activators .....	35
4.6. RNA Preparation and TaqMan reverse transcription-coupled quantitative PCR (RT-qPCR).....	35
4.7. Quantification of mitochondrial (mt) DNA by quantitative PCR .....	36
4.8. Western blotting .....	36
4.9. Vital and immunofluorescence staining of differentiated adipocytes .....	37
4.10. Image acquisition by laser-scanning cytometry (LSC), recognition of cellular objects.....	37

4.11. Texture analysis, quantification of Ucp1 and Cidea protein content of single cells and population scale analysis of human adipocyte browning.....	40
4.12. Determination of cellular oxygen consumption (OC).....	42
4.13. Determination of cytokine release.....	43
4.14. Statistical analysis .....	43
<b>5. Results .....</b>	<b>44</b>
5.1. A previously described brown adipogenic protocol induced a “beige”-like gene expression pattern in differentiating human adipocytes.....	44
5.2. Laser-scanning cytometry (LSC) can quantify human adipocyte browning ....	48
5.3. Irisin and BMP7 induce browning of human adipocytes .....	51
5.4. Clozapine enhances browning of human adipocytes detected by LSC .....	53
5.5. Irisin and BMP7 administration during adipocyte differentiation results in different gene expression patterns .....	55
5.6. Clozapine enhances “beige” potential of human adipocytes via inhibiting 5HT-receptor mediated signaling.....	61
5.7. The “beige” adipogenic cocktail, irisin and BMP7 induce a functional browning program while clozapine treated adipocytes are less capable of responding to thermogenic cues .....	72
5.8. Differentiating human browning adipocytes secrete cytokines (“batokines”).....	79
<b>6. Discussion.....</b>	<b>83</b>
6.1. Methodological overview of analysis of <i>ex vivo</i> browning – an unsolved problem.....	83
6.2. Combined analysis of texture and Ucp1 by laser-scanning cytometry (LSC) effectively identifies browning adipocytes .....	85
6.3. Gene expression pattern and “batokine” secretion distinguish irisin and BMP7 induced browning .....	88
6.4. Clozapine, an unexpected novel inducer of browning .....	90
<b>7. Summary .....</b>	<b>96</b>
Összefoglalás (in Hungarian) .....	98
<b>8. References .....</b>	<b>100</b>
<b>9. Keywords.....</b>	<b>125</b>
<b>10. Acknowledgements.....</b>	<b>126</b>
<b>11. Publications, conferences.....</b>	<b>128</b>

## 1. ABBREVIATIONS

ACADM - Acyl-CoA Dehydrogenase, C-4 To C-12 Straight Chain  
ACOX2 - Acyl-CoA Oxidase 2, Branched Chain  
ADMSC - Adipose tissue-derived mesenchymal stem cells  
ADP/ATP - Adenosine diphosphate/Adenosine triphosphate  
AMPK - 5' adenosine monophosphate-activated protein kinase  
ANOVA - Analysis of variance  
ANP - Atrial natriuretic peptide  
ATF2 - Activating Transcription Factor 2  
ATP5G1 - ATP Synthase, H<sup>+</sup> Transporting, Mitochondrial Fo Complex Subunit C1 (Subunit 9)  
BAT - Brown adipose tissue  
BDNF - Brain-derived neurotrophic factor  
β-GPA – β/3-Guanidinopropionic acid  
BMI - Body mass index  
BMP - Bone morphogenetic protein  
cAMP/cGMP - 3',5'-cyclic adenosine monophosphate/3',5'-cyclic guanosine monophosphate  
C/EBPα/β - CCAAT/Enhancer Binding Protein Alpha/Beta  
CIDEA - Cell Death-Inducing DFFA-Like Effector A  
CITED1 - Cbp/P300 Interacting Transactivator With Glu/Asp Rich Carboxy-Terminal Domain 1  
CKMT1/2 - Creatine Kinase, Mitochondrial 1/2  
CNS - Central nervous system  
COX2/5B - Cytochrome C Oxidase Subunit 2/5B  
CPT - Carnitine Palmitoyl-transferase  
CREB - cAMP Response Element Binding Protein  
Ct - Threshold cycle  
CYC1 - Cytochrome C1  
DIO2 - Deiodinase, Iodothyronine, Type II  
DMEM - Dulbecco's modified Eagle's medium  
DMSO - Dimethyl sulfoxide  
EBF2 - Early B-Cell Factor 2  
EDTA - Ethylenediaminetetraacetic acid disodium salt dehydrate  
EHMT1 - Euchromatic Histone-Lysine N-Methyltransferase 1  
ELISA - Enzyme-linked immunosorbent assay  
ELOVL3 - ELOVL Fatty Acid Elongase 3  
ERK - Extracellular signal-regulated kinase

FABP4 - Fatty Acid Binding Protein 4  
 FAD/FADH2 - Flavin adenine dinucleotide  
 FBS - Fetal bovine serum  
 FC - Fold change  
<sup>18</sup>F-FDG - Fluorine-18 fluorodeoxyglucose  
 FGF - Fibroblast growth factor  
 Fndc5 - Fibronectin Type III Domain Containing 5  
 FOXC2 - Forkhead Box C2  
 FTO - Fat Mass and Obesity Associated  
 GAPDH - Glyceraldehyde-3-Phosphate Dehydrogenase  
 Gi/Gs/Gq - Guanine nucleotide-binding proteins  
 GLUT4 - Glucose transporter type 4  
 5HT - Serotonin  
 IBMX - 3-Isobutyl-1-methylxantin  
 IL - Interleukin  
<sup>123</sup>I-MIBG - Iodine-123 metaiodobenzylguanidine (Iobenguane)  
 IRF4 - Interferon Regulatory Factor 4  
 IRX3/5 - Iroquois Homeobox 3  
 KCNK3 - Potassium Two Pore Domain Channel Subfamily K Member 3  
 LHX8 - LIM Homeobox 8  
 LSC - Laser-scanning cytometry  
 MAPK - Mitogen-activated protein kinase  
 MCP-1 - Monocyte Chemotactic Protein-1 (C-C Motif Chemokine Ligand 2)  
 2-MEA - 2-mercaptoethanol  
 Metrnl - Meteorin-like  
 MΦ - Macrophage  
 MTUS1 - Microtubule Associated Tumor Suppressor 1  
 NAD<sup>+</sup>/NADH - Nicotinamide adenine dinucleotide  
 NDUFS1 - NADH:Ubiquinone Oxidoreductase Core Subunit S7  
 NE - Norepinephrine  
 NO - Nitric oxide  
 NST - Non-shivering thermogenesis  
 OC - Oxygen consumption  
 OCR - Oxygen consumption rate  
 PBS - Phosphate Buffered Saline  
 PCr – Phospho-creatine  
 PCR - Polymerase chain reaction

PDGFR $\alpha$  - Platelet Derived Growth Factor Receptor Alpha  
 PET/CT - Positron emission tomography/computed tomography  
 PGC-1 $\alpha$  - PPAR $\gamma$  Coactivator-1 $\alpha$   
 PKA/PKC - Protein Kinase A/C  
 PPAR $\gamma$  - Peroxisome Proliferator Activated Receptor Gamma  
 pRB - Retinoblastoma protein  
 PRDM16 - PR Domain 16  
 PVDF - Polyvinylidene fluoride  
 RNA - Ribonucleic acid  
 SD - Standard deviation  
 SDS - Sodium dodecyl-sulfate (or Sodium lauryl-sulfate)  
 SERCA - Sarco/endoplasmic reticulum Ca<sup>2+</sup>-ATPase  
 SGA - Second-generation antipsychotic drug  
 SMI - Severe mental illnesses  
 SNS - Sympathetic nervous system  
 SPECT/CT - Single-photon emission computed tomography  
 SRC - Proto-oncogene tyrosine-protein kinase Src  
 SV - Sum variance  
 SVF - Stromal-vascular fraction  
 T3 - 3,3',5-Triiodo-L-thyronine  
 TBX1 - T-Box 1  
 TGF- $\beta$  - Transforming growth factor-beta  
 TLE3 - Transducin Like Enhancer Of Split 3  
 TMEM26 - Transmembrane Protein 26  
 TNF $\alpha$  - Tumor necrosis factor alpha  
 TPH1 - Tryptophan Hydroxylase 1  
 TRR - therapeutic reference range  
 TZD - Thiazolidinedione  
 UCP1 - Uncoupling Protein 1  
 WAT - White adipose tissue  
 Wnt - Wingless type  
 ZFP516 - Zinc Finger Protein 516  
 ZIC1 - Zic Family Member 1

## 2. INTRODUCTION

### 2.1. The unique mammalian heat producing organ: Brown adipose tissue (BAT)

#### 2.1.1. Morphology of BAT

BAT was first described in marmots by Konrad Gessner in the 16<sup>th</sup> century [1]. The fact that BAT is found in all mammals and its major function is heat production was identified 400 years later [2,3]. The acquirement of BAT may have been the one development that gave us as mammals the evolutionary advantage to survive the periods of nocturnal or hibernation cold or the cold stress of birth [4]. In rodents maintained at thermoneutral conditions, BAT is mainly localized in the interscapular, subscapular, axillary and cervical areas [5]. Brown adipocytes can be also found in a smaller amount in the periaortal part of the mediastinal and in the perirenal fat depots [6] (**Figure 1**).

Both white and brown adipocytes accumulate triglycerides in their cytoplasm. White adipocytes form a single large lipid vacuole (30-100  $\mu\text{m}$ ) *in vivo* and contain only a thin rim of cytoplasm around it. This appearance is often referred to as unilocular morphology. In contrast to white adipocytes, brown fat cells accumulate numerous smaller lipid droplets in a multilocular arrangement. Brown adipocytes have polygonal or ellipsoid shape and contain a larger amount of mitochondria-rich cytoplasm. The morphology of mitochondria visualized by electron microscopy in white and brown adipocytes is also markedly different. While the white cells contain small and elongated mitochondria; brown adipocytes have large, round-shaped mitochondria which are abundantly rich in cristae [6-8] (**Figure 2**).

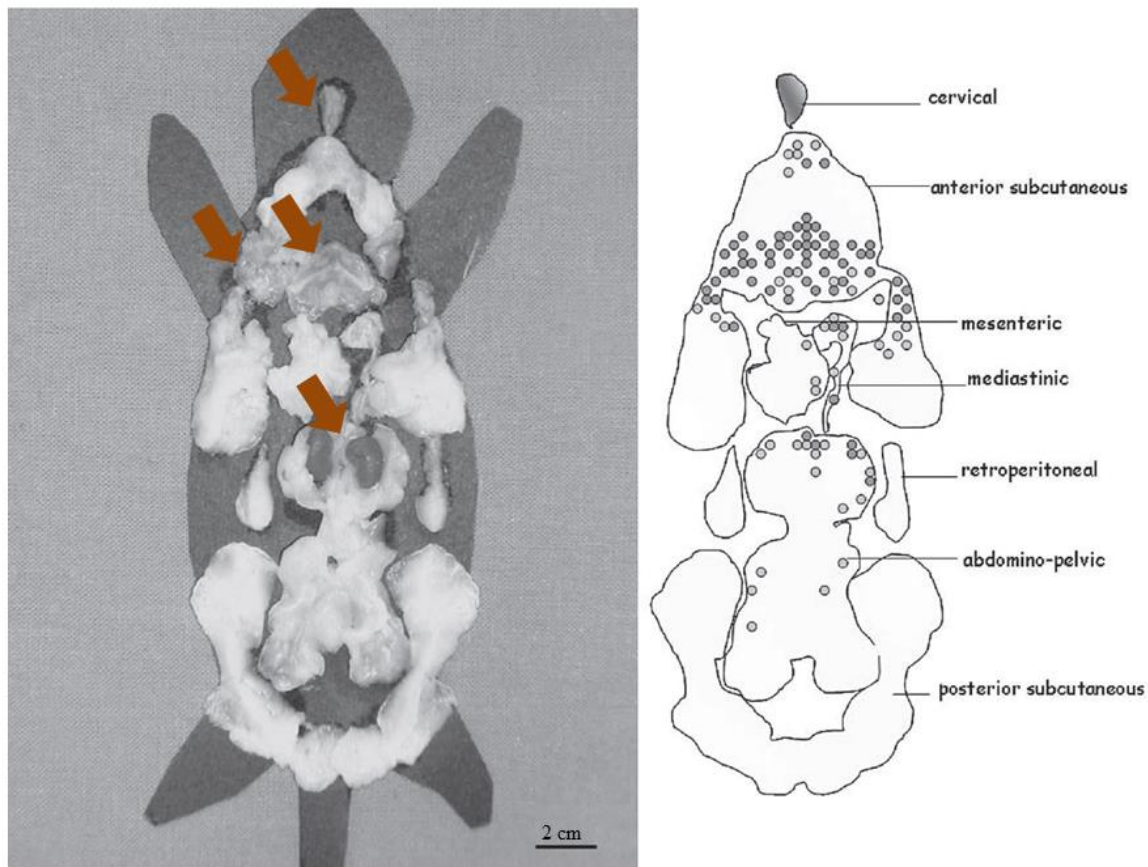


**Figure 1.** The adipose organ of a lean Sv 129 female mouse maintained at thermoneutral conditions. BAT depots are marked with brown arrows (left panel) or with circles (right panel) [6].

In this context, it must be outlined that in most of the cases clear anatomical borders between BAT and the surrounding white adipose tissue (WAT) depots do not exist. Furthermore, it should be emphasized that 20-50% of the cells in any fat depot are not adipocytes and constitute the so called stromal-vascular fraction (SVF), which contains vascular elements, adipose tissue-derived mesenchymal stem cells (ADMSCs), other progenitors, fibroblasts, macrophages (MΦs), lymphocytes, mast cells and nerves [9,10].



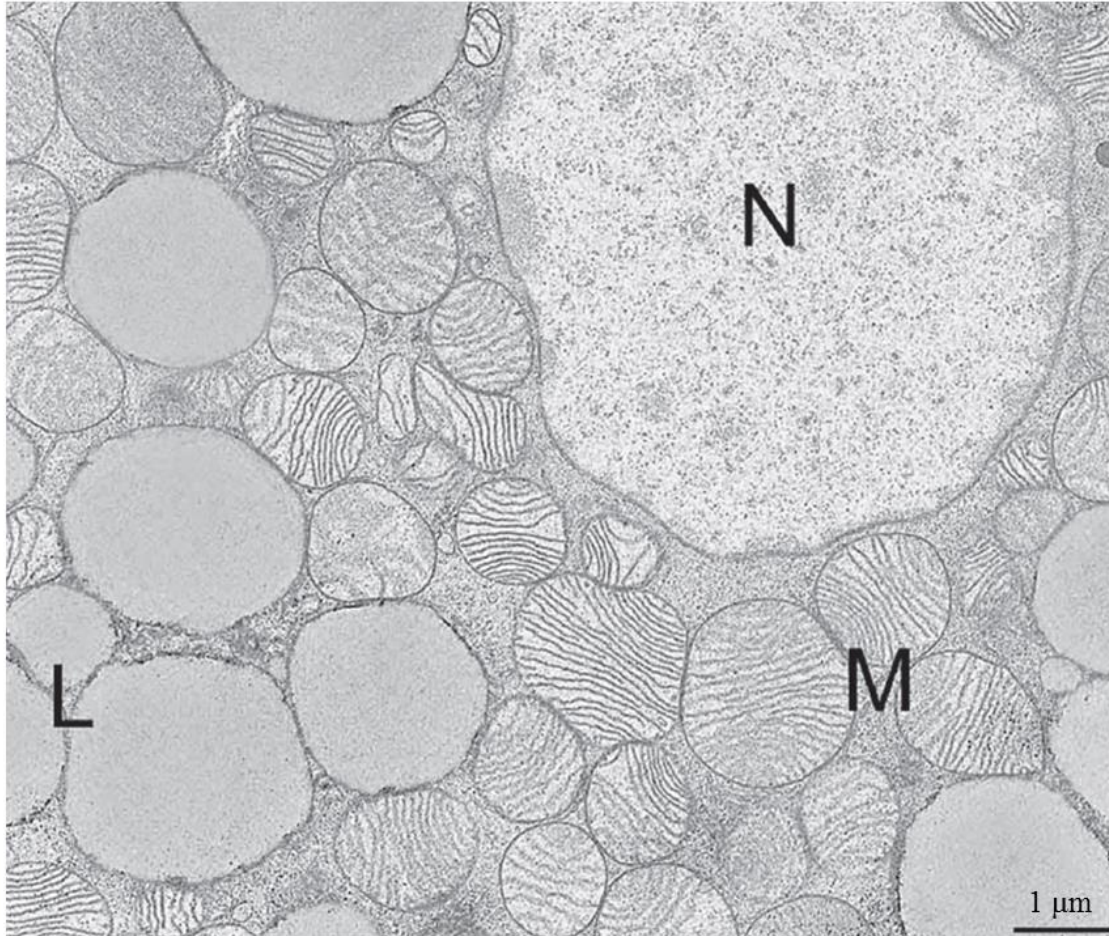


**Figure 2.** *Electron microscopy image of a murine brown adipocyte. Multilocular lipid droplets (L), typical mitochondria (M) and the cell nucleus (N) are visualized [6].*

### **2.1.2. Uncoupling protein 1 (UCP1)**

The mitochondrial protein which is responsible for the unique function of BAT, Ucp1 (Uncoupling protein 1, or known as Thermogenin) was discovered in 1978 [11]. Ucp1 is a member of the mitochondrial carrier protein family that uncouples mitochondrial ATP synthesis from the respiratory chain activity and therefore decreases the proton gradient generated through the internal mitochondrial membrane by the electron transfer system [12-17]. In line with this,

mitochondria in BAT contain high amounts of the mitochondrial respiratory chain enzymes but remarkably low amounts of the F<sub>1</sub>F<sub>o</sub>-ATPase because of the low expression level of the nuclear ATP5G1 gene, which encodes the mitochondrial membrane-bound c subunit of the F<sub>o</sub> oligomer [18-21]. Ucp1 is activated by long-chain fatty acids which are cleaved by the hormone-sensitive lipase from triglycerides stored in the cytoplasmic lipid droplets of brown adipocytes as a result of  $\beta$ 3-adrenergic stimulation [22-25]. Fatty acids which are permanently associated with Ucp1 by hydrophobic interactions carry protons within the Ucp1 protein through the inner mitochondrial membrane. Then, protons are released in the mitochondrial matrix but the fatty acid anion stays associated with Ucp1 and returns to initiate another H<sup>+</sup> translocation cycle [26].

This mechanism leads to the dissipation of energy mainly generated by  $\beta$ -oxidation of fatty acids as heat. For the proper adrenergic activation, Cys253 residue of Ucp1 is sulfenylated by mitochondrial reactive oxygen species which are generated during hypothermic stress conditions [27].

Therefore, BAT plays a major role in maintaining the constant core body temperature of hibernating, small and newborn animals (as well as in humans, discussed in detail in 2.3.) without shivering [16,28,29]. The crucial role of Ucp1-dependent non-shivering thermogenesis (NST) mediated by BAT in rodents was further proven when the first UCP1<sup>-/-</sup> mice were generated which were unable to maintain their body temperature when transferred from normal animal house temperatures of approximately 23°C to 5°C (acute cold exposure) [30]. On the other hand, UCP1<sup>-/-</sup> mice acclimated at 18°C before the prolonged cold exposure, were able to survive [31]. The same effect was observed when the ambient temperature of UCP1<sup>-/-</sup> mice was gradually reduced [32]. In these cases, the increase of other mechanisms of NST or the elevated endurance capacity for shivering might compensate for the loss of Ucp1-dependent heat production [33,34].

The possibility that the thermogenic activity of BAT might combat metabolic disturbances (and its functional disorders might cause severe metabolic inefficiency), e.g. weight gain, was initially addressed in 1979, when the first induced thermogenic process, diet-induced thermogenesis (thermogenic capacity to combust excess energy in the diet) was described [35]. It was an unexpected observation that UCP1-/- mice even on a high-fat diet did not develop obesity [30,36]. However, in these experiments mice were kept at normal animal house temperatures (18-23 °C) which resulted in a chronic thermal stress. Therefore, these mice had already an increased thermogenic activity which subsequently induced their metabolism [37]. Contrarily, when the thermal stress was eliminated (UCP1-/- mice were housed at thermoneutral conditions, at 30 °C) obesity was developed even on a regular chow diet [38]. Moreover, several other studies indicated that experimental increases in the amount or function of BAT in mice promote a lean and healthy phenotype [39-42].

### **2.1.3. Induction of BAT thermogenesis**

The first experiments that linked the sympathetic nervous system (SNS) to the control of NST were conducted in the 1950s in rodents [43,44]. The organ generating heat without shivering remained unrevealed for a long time after the major mediator, norepinephrine (NE) was identified. Later, it was also demonstrated that the blood flow to BAT, which is directly innervated by sympathetic nerves, surges following the injection of NE in rats [45,46]. In differentiated rodent brown adipocytes  $\alpha 1$ ,  $\alpha 2$  and  $\beta 3$  adrenergic receptors are expressed [4,47-51]. In brown fat progenitors  $\beta 1$ , in vascular elements of BAT  $\beta 2$  receptors are also present [52-54]. The  $\beta 3$ -adrenergic signaling cascade is mediated via adenylyl cyclase activation by Gs proteins; then 3',5'-cyclic adenosine monophosphate (cAMP) and Protein Kinase A (PKA) transmit the thermogenic signal [55-57]. That is the reason why PKA activators (e.g. forskolin)

and cell permeable cAMP analogues (e.g. dibutyryl-cAMP) are able to model natural thermogenic cues during the experiments [58-60]. Among others, PKA activation directly stimulates lipolysis and leads to characteristic gene expression changes (including UCP1 upregulation) facilitated by the phosphorylation of cAMP Response Element Binding Protein (CREB) or by the induced MAP kinase pathways (Erk1/2, p38, JNK) [61-64]. The  $\alpha 2$  adrenergic receptors are coupled to Gi proteins and modulate the aforementioned pathway negatively, in contrast to  $\alpha 1$  receptors which activate Gq proteins and phospholipase C resulting in the generation of inositol 1,4,5-trisphosphate and diacyl-glycerol [65,66]. This signal transduction pathway results in elevated intracellular  $\text{Ca}^{2+}$  levels, increased protein kinase C (PKC) activity and subsequent CREB phosphorylation or MAP kinase (Erk1/2) activation which further facilitate heat production [67-70]. Moreover, NE has a major role not only in the acute induction of Ucp1-dependent NST but also (among other mediators, discussed in details in 2.4.) in the long-term regulation of proliferation and differentiation processes in BAT [71-74]. The developmental pathways resulting in heat generating adipocytes will be summarized in the next section.

## **2.2. Heat-generating fat depots: “Classical brown” and “beige” adipocyte development**

### **2.2.1. Origin of “classical brown” adipocytes**

Both white and brown adipocytes are able to store and liberate triglycerides, express a common set of genes and undergo a similar differentiation process controlled by Peroxisome Proliferator Activated Receptor Gamma ( $\text{PPAR}\gamma$ ) and members of the CCAAT/Enhancer Binding Protein (C/EBP) family of transcription factors [75-80]. Because of these common features, brown cells were termed as adipocytes and they were assumed to be originated from the same precursors as

white adipocytes for a very long period of time [81,82]. Studies focusing on BAT development in rodents found that these “classical brown” adipose cells originate from a dermatomyotomal precursor and they are developmentally much closer to skeletal muscle cells than to white adipocytes [83,84]. These multipotent precursors express Engrailed-1, MYF5 or PAX7 and are equipped with the potential to differentiate into “classical brown” adipocytes and skeletal myocytes [83,85,86]. In response to certain stimuli, e.g. bone morphogenetic protein 7 (BMP7), the dermatomyotomal precursors are committed to differentiate into brown preadipocytes which are marked by the upregulation of early B cell factor-2 (EBF2) [87-89]. This process is negatively regulated by the wingless (Wnt) signaling pathway [90,91]. Of note, later it turned out that some subsets of white adipocytes could also be able to be differentiated from the MYF5 positive precursors [92].

The transcriptional cascades that control the process of “classical brown” adipocyte differentiation from the aforementioned preadipocytes were extensively studied in rodents (reviewed in ref. 93-97 and in **Figure 3**). PR Domain 16 (PRDM16) is one of the key mediators that specifies brown adipocyte identity and differentiation by direct interactions with several key adipogenic transcription factors (PPAR $\alpha$ , PPAR $\gamma$ , PGC-1 $\alpha$ , C/EBP $\beta$ , etc.) resulting in their transcriptional co-activation [85,98,99]. However, its absence can be compensated by other factors, e.g. EHMT1 (stabilizes PRDM16 protein through direct interaction) or EWS (activates BMP7 production). In parallel, these transcriptional co-regulators also suppress white adipocyte and skeletal muscle-specific genes effectively [99-101]. The cold-induced, cAMP-dependent long-term thermogenic program which stimulates brown adipocyte differentiation and vascularization of BAT is potentiated by PRDM16 and FOXC2 resulting in the elevated expression of PPAR $\gamma$  Coactivator-1 $\alpha$  (PGC-1 $\alpha$ ) [98,102,103]. PGC-1 $\alpha$  is a transcriptional co-activator which interacts with IRF4 and nuclear hormone receptors including PPAR $\gamma$  and serves

as a key regulator of adaptive NST due to the induction of genes involved in mitochondrial biogenesis and oxidative metabolic pathways [104-107]. Of note, PGC-1 $\alpha$  does not determine the identity of “classical brown” adipocytes directly and it has a broad range of effects including the upregulation of mitochondrial genes in other types of tissues as well [108-113]. On the other hand, Retinoblastoma protein (pRB) and some members of the SRC-family were described as negative regulators of “classical brown” adipocyte differentiation and activation in mouse models [114-116].

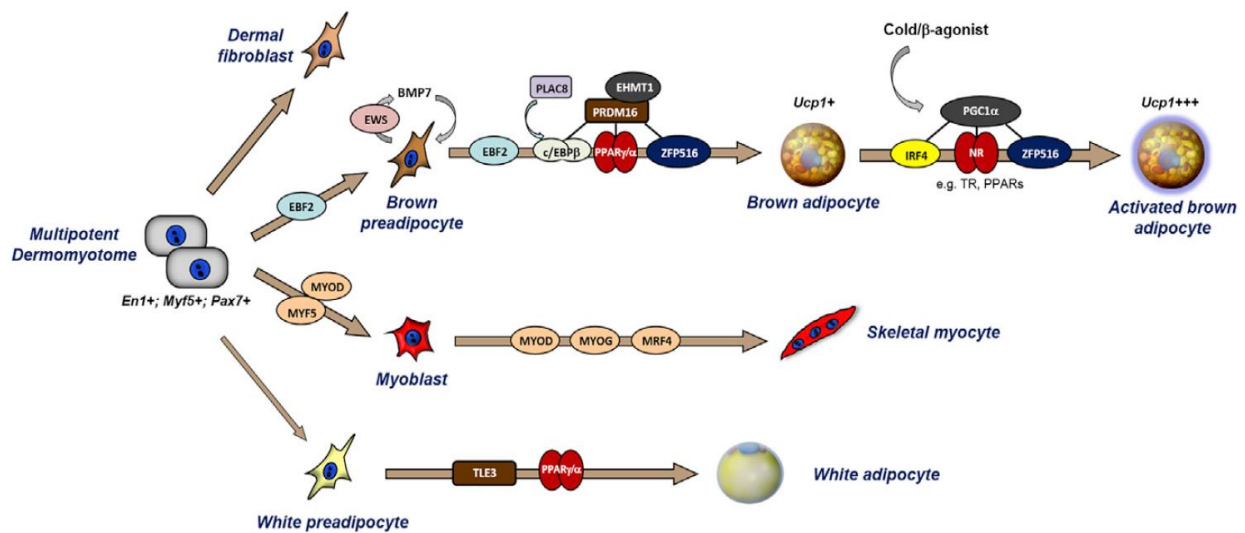


**Figure 3.** Key factors of “classical brown” adipocyte development in mice [96].

### 2.2.2. “Beige” adipocytes – inducible thermogenic fat cells

More than 30 years ago, “brown adipocyte-like” cells were detected in rodent WAT depots as a result of cold- induced thermogenesis mediated by the SNS [117-120]. These cells contained multilocular lipid droplets (usually with a predominant central droplet surrounded by several smaller ones at the periphery of the cells) and high amount of Ucp1 expressing mitochondria [6,118]. This phenomenon, which was assumed to be the reversible transdifferentiation

(transformation of a differentiated cell into another cell type with different morphological features and functions) of white adipocytes into brown fat cells [119-121], was associated with the improvement of obesity and insulin resistance [122-124]. Later, experiments using mouse models (and human samples, discussed in detail in 2.3.) suggested that the differentiation of these “brown adipocyte-like” cells arose from a distinct precursor as a result of several stimuli (e.g. cold, physical exercise, diet) at least partially regulated by the  $\beta$ 3-adrenergic signaling pathway [125-131]. These inducible cell populations which are generated mostly in subcutaneous WAT from preadipocytes (marked with PDGFR $\alpha$  and EBF2 expression) in a process called “browning” were termed as “beige” (or “brite”) adipocytes [89,125,126,132-134].

“Beige” adipocyte development can be highly enhanced by several neuro-endocrine or paracrine factors (discussed in detail in 2.4.) and shares numerous common regulatory transcriptional mechanisms with “classical brown” adipocyte differentiation [95,96,101,126,127] (**Figure 4**). The ratio of energy-dissipating “beige” and energy-storing white adipocytes is determined, at least partially, during early differentiation of mesenchymal progenitors into adipocyte subtypes [96,130,131,135]. A crucial mechanism regulating this process was described recently. When a repressor binds to a mesenchymal super enhancer in one of the intronic regions of the Fat Mass and Obesity Associated (FTO) gene, resulting in the downregulation of IRX3 and IRX5 expression, this drives the progenitors toward a “beige” cell fate, elevated thermogenesis and reduced lipid storage [131]. PRDM16 is also a key regulator that determines “beige” adipocyte fate; it can directly interact with ZFP516, a transcription factor leading to the upregulation of the UCP1 and PGC-1 $\alpha$  genes during “browning” of WAT [126,136,137]. Contrarily, RIP140, p107 or TLE3 inhibit “browning” in mice by antagonizing the functions of PRDM16 or PGC-1 $\alpha$  [138-140]. Casein kinase 2 phosphorylates and activates class I Histone deacetylases, which results in downregulation of PGC-1 $\alpha$  expression and reduced “beige” fat biogenesis and heat production

[141,142]. In addition, several micro RNAs (e.g. miR-26, miR-30, miR-133, miR-155, miR-193b, miR-196a, miR-365, miR-378) and long non-coding RNAs (e.g. lnc-BATE1, Blinc1) were described recently to fine tune the control of “classical brown” and “beige” adipocyte differentiation in rodents and humans [143-153]. Of note, some of the “beige” adipocytes arise from smooth muscle precursors [154] and the regulatory network that controls “beige” adipogenesis may significantly vary in different fat depots [96,128,155].

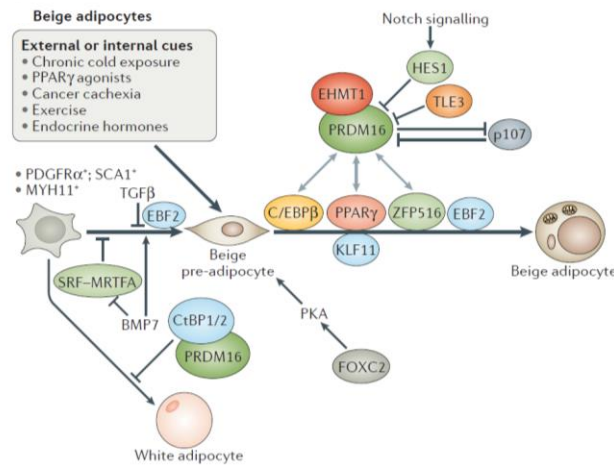


**Figure 4.** Transcriptional regulation of “beige” adipocyte differentiation in mice [97].

In contrast to “classical brown” adipocytes, “mature beige” cells express thermogenic genes at low levels under basal unstimulated conditions [125,128]. In addition, when a thermogenic stimulus subsides, “masked beige” cells persist that have a white adipocyte-like morphology *in vivo* [96,130]. Both “mature” and “masked beige” adipocytes are able to strongly activate UCP1 expression and their thermogenic capacity in response to recurring  $\beta$ -adrenergic stimuli [96,127,130]. In summary, “beige” adipocytes are able to switch on and off their UCP1-dependent thermogenic program in response to external cues. On the other hand, the possibility of reversible transdifferentiation of mature white adipocytes into heat producing “beige” cells, at

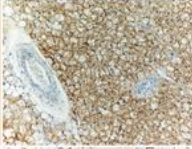
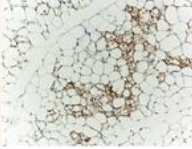


least under special conditions, has never, to our knowledge, been completely excluded [95,96,156].

### **2.2.3. Markers of browning**

Although many similarities and differences between the two thermogenic fat cell types have been elucidated recently (**Figure 5**), there is no clear consensus (especially in human studies) on the criteria of classification of “browning” adipocytes into “classical brown” or “beige”. Higher expression of thermogenic genes (e.g. UCP1, PGC-1 $\alpha$ , CIDEA, ELOVL3, PRDM16, DIO2) and mitochondrial markers (e.g. CYC1, COX2, COX5B, ATP5B, ATP6V02, NDUFS1) compared to white adipocytes can be found in both heat producing cell types, especially when they are stimulated for thermogenesis [126,129,130,136,138,157]. In mice, “classical brown” adipocytes express ZIC1, LHX8, MYLPF, PDK4, EBF3, MPZL2, FBXO31, miR-206 etc. at elevated levels compared to white or “beige” adipocytes [84,98,155,158]. Among these genes only ZIC1 and LHX8 were validated in infant and adult human samples as “classical brown” markers so far [159,160]. Of note, the constitutive expression of UCP1 is always higher in classical BAT than in “beige” fat depots [155,159]. To recognize “beige” adipocytes in mice, the most accepted gene expression markers are TBX1, TMEM26, HOXC9, CD137, SHOX2, CITED1 and TNFRSF9 [125,127,155,161]. In a recent study, using clonally derived adult human adipocytes with “beige” characteristics, KCNK3 and MTUS1 variant 3 were identified as new molecular markers for human “beige” adipocytes [162]. Furthermore cell surface proteins, ASC-1, PAT2 and P2RX5 were found to be highly accumulated on white, “classical brown” and “beige” adipocytes, respectively [163]. However, to date, widely accepted surface markers that can discriminate between these adipose cell types have not been described, which limit the possibility to specifically identify and sort out different types of thermogenic adipocytes in a heterogeneous

cell population. Furthermore, to our knowledge, “masked beige” cells cannot be detected among white adipocytes by specific molecular markers.

	Immunohistochemistry with anti-Ucp1	Location in humans	Location in mice	Developmental origin in mice	Enriched markers	Key transcription factors	Activators
Brown		Neck Interscapular (newborns) (Perirenal?)	Interscapular Cervical Axillary Perirenal (Endocardial?)	Myf5 <sup>+</sup> cells (dermomyotome)	<i>Zic1</i> <i>Lhx8</i> <i>Eva1</i> <i>Pdk4</i> <i>Epsti1</i> <i>miR-206</i> , <i>miR-133b</i>	<i>C/ebpβ</i> <i>Prdm16</i> <i>Pgc-1α</i> <i>Ppar-α</i> <i>Ebf2</i> <i>TR</i>	Cold Thiazolidinediones Natriuretic peptides Thyroid hormone Fgf21, Bmp7, Bmp8b Orexin
Beige		Supraclavicular (Paraspinal?)	Interspersed within WAT subcutaneous fat > visceral fat	Myf5 <sup>-</sup> cells <i>Pdgfr-α</i> <sup>+</sup> (perigonadal)	<i>Cd137</i> <i>Tbx1</i> <i>Tmem26</i> <i>Cited1</i> <i>Shox2</i>	<i>C/ebpβ</i> <i>Prdm16</i> <i>Pgc-1α</i> ( <i>Ppar-α</i> ?)	Cold Thiazolidinediones Natriuretic peptides (Thyroid hormone?) Fgf21 Irisin

**Figure 5.** Main features of “classical brown” and “beige” adipocytes [129].

#### 2.2.4. UCP1-independent thermogenesis

Isolated mitochondria of murine classical BAT and “beige” fat depots were both able to efficiently perform UCP1-dependent thermogenesis connected with a limited capacity to produce ATP through oxidative phosphorylation [20,21,164]. In mice, however, NST mediated by classical BAT is approximately three fold higher than the maximal UCP1-dependent heat production of activated total “beige” fat [164]. In parallel with the UCP1-mediated uncoupling, it is becoming clear, that thermogenic adipocytes contain other, UCP1-independent energy dissipating pathways. The glycerol-3-phosphate shuttle regularly allows the NADH synthesized in the cytosol by glycolysis to contribute to oxidative phosphorylation in the mitochondria to generate ATP. Primarily, cytosolic glycerol-3-phosphate dehydrogenase converts dihydroxyacetone phosphate to glycerol 3-phosphate by oxidizing one molecule of NADH to NAD<sup>+</sup>. Glycerol-3-phosphate is converted back to dihydroxyacetone phosphate by an inner membrane-bound mitochondrial glycerol-3-phosphate dehydrogenase, reducing one molecule of enzyme-bound FAD to FADH<sub>2</sub> [165-168]. When these reactions are continuously coupled to

each other resulting in a substrate cycle, as it was shown in BAT of rodents, metabolic inefficiency is caused, because of the production of only two instead of three ATPs/mol of NADH generated by glycolysis [33,169]. Another thermogenic futile cycle is based on the cycling of  $\text{Ca}^{2+}$  by the SERCA  $\text{Ca}^{2+}$ -ATPase which pumps  $\text{Ca}^{2+}$  into the sarcoplasmic reticulum and the subsequent leakage of  $\text{Ca}^{2+}$  into the cytoplasm [170,171].  $\text{Ca}^{2+}$  cycling uncoupled to muscle contraction, which is regulated by phosphorylation of sarcolipin or phospholamban small regulatory proteins, mainly functions in skeletal muscle cells but has been suggested to be an additional UCP1-independent thermogenic mechanism in BAT [32,172,173]. In addition, synergistic enhancement of both lipid synthesis and oxidation, another thermogenic mechanism based on lipid turnover was also proposed to be active in BAT [174,175]. Recent findings revealed a novel futile cycle of creatine metabolism which enhances energy expenditure in the mitochondria of “beige” (and in a smaller extent in “classical brown”) adipocytes. Mitochondrial creatine kinase 1 or 2 (CKMT1/2) catalyzes the conversion of creatine and utilizes ATP to create phosphocreatine (PCr) and ADP, before Phospho1 liberates the high-energy phosphate group from PCr [176-179]. However, how these energy dissipating pathways relatively contribute to heat production in different fat depots and which regulatory mechanisms switch on and off the aforementioned substrate cycles, especially in humans, remain elusive.

## **2.3. Implications of “browning” for metabolic health in humans**

### **2.3.1. Obesity – a global health issue**

Obesity is one of the major risk factors of metabolic syndrome, coronary heart disease and cancer which are leading causes of morbidity and mortality today [180,181]. In Europe, approximately four million people die each year as a result of cardiovascular diseases [182]. Even though, the

rate of cardiovascular mortality in Hungary (640/10000 inhabitants) has been continuously decreasing in the recent years, it is still more than two-fold higher than the mean cardiovascular mortality of the EU-25 countries [183]. In Hungary, the mean prevalence of chronic heart failure was 1.6% between 2004 and 2010 (in Western-Europe and North-America: 0.4-2%). The majority of the patients suffering in chronic heart failure are older than 60 years. Above 75 years of age, the prevalence of chronic heart failure is more than 10%. These patients have the worst prognosis; the mortality of those is 30% in 3 years and more than 50% in 5 years after the diagnosis [184]. In our country, the prevalence of overweight people (BMI: 25-29.9 kg/m<sup>2</sup>) is 58%. Approximately half of them are obese (BMI: >30 kg/m<sup>2</sup>). Obese patients have 2-3 times higher relative morbidity risk than people with normal body weight (BMI: 18-24.9 kg/m<sup>2</sup>) for the other components of metabolic syndrome [185]. In 2012, the public expenditure in regard to obesity was more than 200 billion HUF (700 million USD) in Hungary [186,187].

Although the prevalence of overweight and obesity is as high as 40-50% in most of the developed countries, the effective therapeutic potentials against obesity are very limited. The idea to increase mitochondrial uncoupling to burn off the excess fat as heat is dated back for a long time. Therefore, 2,4-dinitrophenol was administered broadly to obese patients in order to increase their metabolic rate. However, 2,4-dinitrophenol treatment was later withdrawn because of severe side-effects [188]. The presence of BAT in humans was first described more than 50 years ago. Newborn infants have a significant amount of interscapular BAT that shares common morphological features with rodent brown fat and provides a “thermogenic jacket” after birth [28,189,190]. A recent study revealed that this brown fat depot contains mostly “classical brown” adipocytes [160]. Multilocular brown adipocytes, which are usually surrounded by white fat cells, were found in several other anatomical sites in infants including the “deep neck”, mediastinal and perirenal regions [191]. Although some studies proposed that BAT depots exist in a smaller

amount in adult humans as well, it has been generally believed for decades that NST mediated by BAT disappears in childhood or adolescence and therefore lacks significance in adults [191,192]. It was also suggested long time ago that inactive brown adipocytes which have a unilocular morphology might persist during the later stages of life [191].

### **2.3.2. Browning adipocytes exist in adult humans – Can we find and activate them?**

Studies using positron or gamma radiation emitting radiolabelled metabolic substrates ( $^{18}\text{F}$ -FDG,  $^{123}\text{I}$ -MIBG) in nuclear medicine detected high incidence of metabolically active BAT, which can dissipate energy directly into heat as a result of a cold challenge, in healthy adult humans of different ethnic groups. These thermogenic fat depots, which were three dimensionally visualized by PET/CT or SPECT/CT, can be found interspersed in the human body and are mostly enriched in the supraclavicular, “deep neck” and paravertebral regions (**Figure 6**) [193-200]. Furthermore, independent trials proved the strong negative correlation between obesity or glucose intolerance and the amount of metabolically active BAT in humans [201-206]. The activity of these heat producing, anti-obesity fat depots was predicted to account for up to 5% of basal metabolic rate in adult humans, which could cumulatively support more than 4 kg of fat loss per year [95,207]. However, the amount of thermogenic BAT is reduced as a result of aging both in mice and humans [208,209]. Thus, the importance of BAT in controlling the energy homeostasis of the entire human body has become increasingly evident in the past few years, highlighting the possibility of therapeutic application of BAT stimulation in the treatment of obesity and diabetes mellitus [210-213].

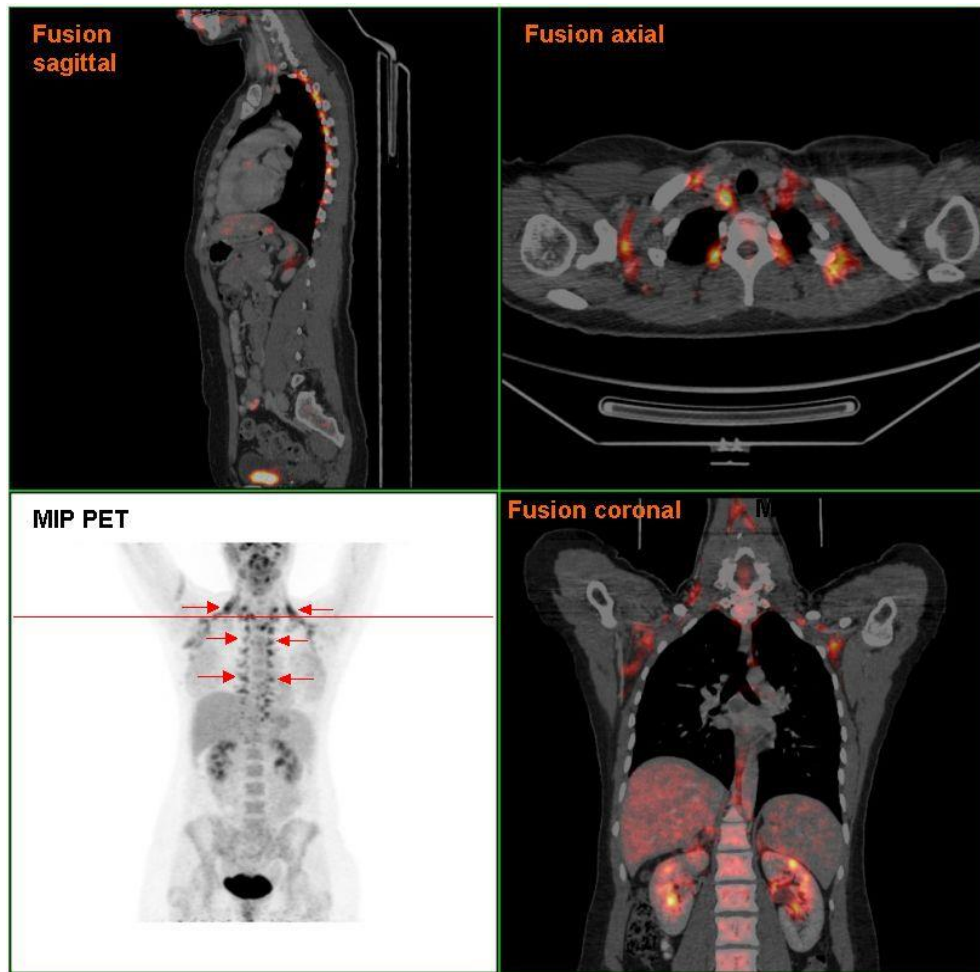


**Figure 6.** Metabolically active brown and “beige” adipose tissue depots can be found interspersed in adult humans [200].

Although adipocytes which express “classical brown” markers were found in the “deep neck” fat of adult humans, most of the obtained data suggest that the energy expenditure of thermogenic adipose depots in the entire body is less pronouncedly mediated by the *ab ovo* differentiated “classical brown” adipocytes [159,214]. The development of “beige” cells which can be found interspersed in WAT and generated in a process called “browning” seems to play a more significant role. Several studies suggest that a large proportion of the thermogenic fat depots in adult humans is mostly composed of “beige” cells. However, there is only limited information

about the origin of “beige” adipocytes and the regulators of “beige” adipogenesis in humans [127,162,215]. “Beige” adipocytes are developed either from distinct precursors or from mature white adipocytes as discussed in details in the previous section.

This “browning” process which results in unstimulated, slightly active “beige” cells would determine a “beige” potential or the “thermogenic competency” of each individual [135]. The “beige” potential is fundamentally defined by the proportion of the differentiated energy-dissipating “beige” and energy-storing white adipocytes in each person. Those who carry the risk-allele of the FTO locus fail to drive the adipocyte progenitors toward a “beige” cell fate and harbor a strong genetic association with obesity. This recent discovery proposed to date the first strong genetic link in humans between obesity and thermogenic competency generated by “beige” fat development [131]. The thermogenic competency might be increased pharmacologically by “browning-inducers” (discussed in details in 2.4.) or by implants of “masked” or activated “beige” adipocyte depots [216]. After a complete “browning”, both mature and “masked beige” adipocytes are able to enhance UCP1 expression and heat production (both in a UCP1 dependent and independent manner) in response to anti-obesity cues, such as an adrenergic stimulus, in a process called “thermogenic activation” [127,130,135]. As a natural thermogenic stimulus, cold exposure causes the SNS to release NE and induce heat production of brown and “beige” fat in humans through consumption of fatty acids and glucose [196]. Since non-specific  $\beta$ -adrenergic agonists have striking effects on the cardiovascular system, selective induction of the  $\beta_3$ -receptor mediated pathway (e.g. by mirabegron) can be a promising future therapeutic target that boosts “thermogenic activation” [217-219]. On the other hand, various food ingredients can mimic a cold challenge and activate transient receptor potential channels on sensory neurons resulting in the stimulation of NST by the SNS. Therefore, capsaicin in chili pepper, catechins in green tea, piperine in black and white pepper, gingerols in ginger or

cinnamaldehyde in cinnamon might be safely applicable to our daily life for preventing weight gain [220-224].

It is also becoming clear that brown and “beige” adipocytes are not only heat-generating cells. Recent results suggest that “beige” adipocytes contribute significantly to the regulation of whole body energy expenditure and systemic metabolic homeostasis not exclusively by thermogenesis and mitochondrial uncoupling [205,206,225]. For example, BAT-derived Interleukin-6 (IL-6) is required for the profound effects of BAT on glucose homeostasis and insulin sensitivity in mice [226,227]. There is, however, only limited information about the secreted factors by brown and “beige” adipocytes („batokines”) in humans. Some of them contribute to the direct induction of “thermogenic competency and activation” as a paracrine-autocrine mediator, as discussed in the next section.

## **2.4. Activators of brown and “beige” fat development and function**

### **2.4.1. Hormones which regulate browning by central and peripheral actions**

It has been known for a long time from rodent experiments, and was later proven in humans, that cold exposure facilitates NE release from the SNS which not only induces a rapid thermogenic program but also enhances BAT development [71-74,196,228]. Recently it was discovered that alternatively activated (or M2) MΦs which are recruited during “browning” secrete also catecholamines to sustain NST [229]. Insulin (as well as cholecystokinin and enterostatin) were also described in rodents as meal-induced, centrally acting, acute thermogenic cues decades ago [230-233]. Then, it was demonstrated that insulin signaling, which stimulates the upregulation and transfer of Glucose transporter type 4 (GLUT4) to the plasma membrane, plays a crucial role in mediating the uptake of glucose and storage of lipid droplets not only in white but also in



brown adipocytes [234-236]. Later, insulin and Insulin-like growth factor-1, which suppress Wnt signaling and the expression of *necln* (functionally similar to the pRB that binds to and represses the activity of cell cycle-promoting proteins) were directly linked to fetal brown adipocyte development in rodents [237-240]. Contrarily, Transforming growth factor-beta (TGF- $\beta$ ) induced Smad3 signaling negatively regulates thermogenesis and mitochondrial energetics by decreased activation of the insulin receptor signaling pathway in “browning” adipocytes [241,242].

Leptin, which reduces appetite as a circulating hormone secreted by adipocytes, also enhances BAT thermogenesis by inducing SNS via the release of melanocyte-stimulating hormone in the hypothalamus [243-247]. However, the thermogenesis-inducing effect of leptin was debated recently [248]. In contrast to centrally acting glucocorticoids which decreased the effect of leptin *in vivo*, dexamethasone treatment on primary cultures of murine brown adipocytes resulted in the upregulation of ELOVL Fatty Acid Elongase 3 (ELOVL3 or Cig30) and promoted their differentiation [157,249,250]. Previously, the metabolic effects of thyroid hormones including elevated heat production have been suggested to be peripherally mediated [251-254]. However, recent studies revealed that T3 inhibits AMPK in the ventromedial hypothalamus resulting in the activation of SNS that leads to increased “thermogenic competency” and induction in mice. The central effects of thyroid hormones seem to be more significant than their peripheral action on the regulation of energy balance by NST [255-258].

Central serotonin (5HT) is known to regulate energy balance by decreasing appetite and increasing BAT thermogenesis through effects on the nervous system [259,260]. These actions were exploited by appetite-suppressing drugs, e.g fenfluramine or sibutramine, in the treatment of obesity [261]. However, these drugs were later withdrawn, because of frequent cardiovascular side effects [262,263]. Recently two groups reported independently that peripheral 5HT has an opposing effect. In mice, 5HT reduced the “beige” potential and the sensitivity of brown and

“beige” adipocytes to thermogenic induction in a cell autonomous manner [264-266]. Second-generation antipsychotic drugs (SGAs), including clozapine, bind to different 5HT, muscarinic and histamine receptors and antagonize adrenergic  $\alpha 1$  and 2 or various dopamine receptors [267-269]. SGAs, especially clozapine, olanzapine, risperidone and quetiapine increase the incidence of weight gain and metabolic syndrome in patients with severe mental illnesses (SMI) with diverse but not completely revealed molecular mechanisms [270-273].

#### **2.4.2. Physical exercise and non-shivering thermogenesis (NST)**

Physical exercise has well-known beneficial metabolic effects and protects against several pathological conditions, such as metabolic syndrome, neurodegenerative disorders, or cancer [274,275]. Skeletal and cardiac muscle cells secrete various hormones, which were termed as “myokines”, in response to physical activity [276,277]. These factors significantly contribute to the crosstalk between the brain, muscle and adipose tissue, by which “browning” is also regulated **(Figure 7)** [278,279].

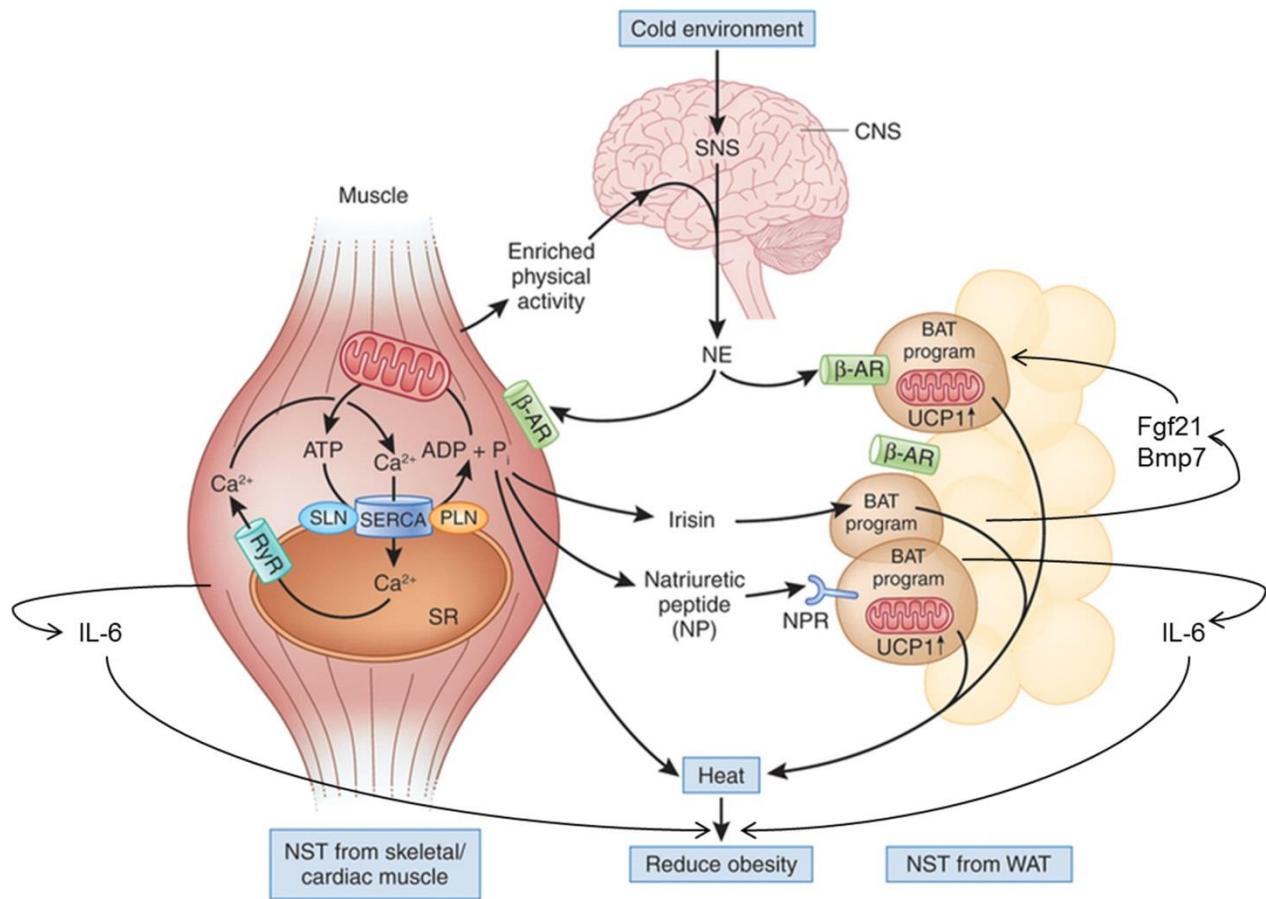


**Figure 7.** Regulation of non-shivering thermogenesis by muscle and brown or “beige” adipose tissue [modified from ref. 280].

Irisin was discovered as a “myokine” which is cleaved from the Fibronectin Type III Domain Containing 5 (Fndc5) transmembrane protein and induced a “beige” program of subcutaneous WAT in mouse models. Physical exercise (as well as shivering) induced the upregulation of Fndc5 and the subsequent secretion of irisin in skeletal myocytes driven by PGC-1 $\alpha$  [113]. The production of irisin by cardiac muscle was also demonstrated in rats [281]. Then, irisin acts as a “browning-inducer” in a cell-autonomous manner, presumably through an unknown selective receptor, via the p38 MAPK and ERK pathways [113,282]. In the ATG start codon of the Fndc5 gene the A was replaced by G in humans compared to the mouse genome. This change probably results in a shorter Fndc5 protein lacking the part from which irisin is generated [283]. However,

several studies have demonstrated the presence of irisin in human blood plasma, using mass spectrometry or many different antibodies, as a function of exercise or other metabolic parameters [284-288]. Of note, the specificity of some antibodies against human Fndc5 or irisin has been later debated [289]. Furthermore, more than 10-fold higher irisin plasma concentrations were detected in rodents ( $>100$  ng/ $\mu$ l) than in humans ( $<10$  ng/ $\mu$ l) by mass spectrometry [290]. Fndc5 is expressed in distinct areas of the brain and central effects of circulating irisin were described recently as well [291]. For example, irisin is able to potentiate “browning” via SNS by inducing the production of hypothalamic brain-derived neurotrophic factor (BDNF) [292]. Stimulation of physical and social activity (“enriched environment”) also leads directly to the upregulation of BDNF in the hypothalamus [293]. In addition, this central Fndc5/irisin-BDNF pathway was hypothetically connected to beneficial cognitive functions, such as learning or motivation [294].

In response to exercise, skeletal muscle cells secrete Meteorin-like (Metrnl) hormone which promotes eosinophil granulocyte infiltration and alternative activation of M $\Phi$ s in adipose tissue and regulates immune-adipose interactions to stimulate “beige” fat thermogenesis in mice [295]. Lactate and  $\beta$ -aminoisobutyric acid, which are also released by myocytes after exercise, induce “browning” in the subcutaneous WAT depots of rodents and in differentiating human adipocytes [296,297]. Recent findings suggest that IL-6 not only acts as a crucial mediator of inflammatory processes but also serves as an endocrine modulator of metabolism for the entire body [298]. IL-6, as a “myokine”, targets several tissues including liver, skeletal muscle, pancreas, brain, WAT and BAT, and seems to balance exercise-associated catabolic pathways in order to mediate glycemic control during recovery [299-302]. Furthermore, IL-6 can mediate some of the long-term systemic beneficial effects of physical training. In accordance with the homeostatic roles of IL-6, it can contribute to the exercise-induced alternative activation of M $\Phi$ s and the induction of

“thermogenic competency” in mice [303,304]. Group 2 innate lymphoid cells, which infiltrate “browning” adipose tissue in response to IL-33, produce IL-5 that prompts eosinophils to secrete IL-4. This paracrine signaling of the innate immune system, similarly to the endocrine effects of *Metnl*, also contributes to the induction of “beige” thermogenesis via the alternative activation of MΦs [305,306]. In addition, activated group 2 innate lymphoid cells secrete methionine-enkephalin peptide which directly enhances “browning” acting on the opioid receptors of “beige” adipocytes [307].

#### **2.4.3. Browning-inducers which directly target adipose tissue**

Another key endocrine factor, atrial natriuretic peptide (ANP), which is produced by cardiomyocytes and switches on p38 MAPK signaling and phosphorylation of ATF2, directly increasing UCP1 transcription, promotes “thermogenic activation” and mitochondrial biogenesis in murine “beige” fat and in human adipocytes [308,309]. Nitric oxide (NO), similarly to ANP, increases intracellular cGMP amount and locally induces heat production of classical BAT in rats [310]. In addition, pharmacological stimulation of soluble guanylyl cyclase protects against diet-induced obesity by increasing the “thermogenic competency” in mice [311,312].

p38 MAPK signaling is also induced by distinct BMPs which are key endocrine-paracrine regulators of “thermogenic competency and activation”. BMP7 was described earlier as a locally acting mediator in mice that both drives “classical brown” adipogenesis and recruits “beige” adipocytes [87,313]. Then, the effect of BMP8b and BMP4 was connected to increased “thermogenic induction” of BAT and accelerated “beige” adipocyte differentiation, respectively [314,315]. Growth differentiation factor-5 (GDF5), which acts in a paracrine-autocrine manner, also induced “browning” in mice via BMP receptor complex and Smad5 to activate the PGC-1 $\alpha$  promoter [316].

Fibroblast growth factor 21 (FGF21) is secreted by hepatocytes and “beige” adipocytes and binds to a receptor complex in which  $\beta$ Klotho interacts with FGF receptors 1c and 4. Then, FRS2 $\alpha$  docking protein and ERK1/2 are phosphorylated which improves insulin sensitivity and induces “browning” in WAT [317-320]. Because of the beneficial effects of FGF21 on the liver and adipose tissue, which results in decreased blood sugar levels and increased energy expenditure, its analogues are being tested in preclinical and clinical trials for the management of diabetes and obesity [321,322].

Recently it was demonstrated, that “beige” adipocytes secrete Slit2 which is post-translationally cleaved into fragments in the extracellular matrix. Then, its C-terminal fragment promptly induces “beige” fat thermogenesis in an autocrine-paracrine manner by activating PKA signaling [323]. Adenosine, a locally acting purine nucleoside secreted by adipocytes or generated from the released ATP by SNS, activates ADORA2A receptor, leading also to increased cAMP- and PGC-1 $\alpha$ -dependent signaling, that enhances thermogenesis and lipolysis in murine and human brown and “beige” adipocytes [324]. Moreover, prostaglandins were also proposed to locally regulate “browning” in mice without any effects on classical BAT [325].

As discussed above, there is growing evidence, that “browning” is regulated by several factors which might not affect the central nervous system (CNS). Some of these mediators are released by “browning” adipocytes and act in a paracrine-autocrine manner. These might open up better strategies to stimulate “browning” specifically or to establish an *in vitro* “engineered BAT” that helps the treatment of obese or diabetic patients more effectively. However, most of these factors were tested only in rodent models and their effects on human adipocyte “browning” are unrevealed. Therefore, we aimed to quantify human brown and “beige” adipocyte differentiation in response to different “browning-inducers” *ex vivo* at a single cell level in a highly replicative manner by using a slide-based image cytometry approach.

### 3. AIMS OF THE STUDY

- To quantify human brown and “beige” adipocyte differentiation *ex vivo* at a single cell level in a highly replicative manner by using a slide-based image cytometry approach.
- To clarify the direct effect of irisin and BMP7, two potent browning-inducers described in mice, on the induction of browning in our *ex vivo* human model system.
- To identify novel effects of drugs on human browning by complementing gene expression and oxygen consumption measurements (OC) with the laser-scanning cytometry (LSC) based population scale analysis of *ex vivo* brown adipogenic differentiation.
- To learn the molecular mechanism that can explain the unexpected browning effect of clozapine.
- To investigate the secretion of cytokines (“batokines”) by primary human brown and “beige” adipocytes.

## **4. MATERIALS AND METHODS**

### **4.1. Ethics statement**

Human adipose-derived mesenchymal stem cells (hADMSCs) were isolated from subcutaneous abdominal adipose tissue of healthy volunteers (body mass index < 29.9) aged 20–65 years who underwent a planned surgical treatment (herniotomy). Written informed consent from all participants was obtained before the surgical procedure. The study protocol was approved by the Ethics Committee of the University of Debrecen, Hungary (No. 3186-2010/DEOEC RKEB/IKEB). All experiments were carried out in accordance with the approved ethical guidelines and regulations.

### **4.2. Materials**

- Anti-Glyceraldehyde-3-Phosphate Dehydrogenase (GAPDH) Antibody, clone 6C5 (Merck-Millipore; MAB374)
- Antimycin A from Streptomyces sp. (Sigma-Aldrich; U8674)
- Anti-mouse IgG (H+L) antibody [HRP] (Covalab; lab0252)
- Anti-rabbit IgG (H+L) antibody [HRP] (Covalab; lab0273)
- Anti-UCP-1 antibody produced in rabbit (Sigma-Aldrich; U6382)
- Apo-Transferrin human (Sigma-Aldrich; T2252)
- Biotin (Sigma-Aldrich; B4639)
- CIDE A (aa200-217) antibody (Covalab, pab70665)
- Clozapine (Sigma-Aldrich; C6305)
- Collagenase from Clostridium histolyticum (Sigma-Aldrich; C1639)



- cOmplete™ Protease Inhibitor Cocktail (Roche Diagnostics; 11873580001)
- Dexamethasone (Sigma-Aldrich; D1756)
- N6,2'-O-Dibutyryl-adenosine 3',5'-cyclic monophosphate sodium salt (dibutyryl-cAMP) (Sigma-Aldrich; D0627)
- Dimethyl sulfoxide (DMSO) (Sigma-Aldrich; D2650)
- Dulbecco's modified Eagle's medium (DMEM) Nutrient mixture F-12 (Sigma-Aldrich; D8437)
- DuoSet ELISA (R&D Systems; DY 201, DY206, DY208, DY210, DY279)
- Ethylenediaminetetraacetic acid disodium salt dehydrate (EDTA) (Sigma-Aldrich; E5134)
- (+)-Etomoxir sodium salt hydrate (Sigma-Aldrich; E1905)
- Fetal bovine serum (FBS) (Gibco; 10270)
- Goat anti-Rabbit IgG (H+L) Secondary Antibody, Alexa Fluor® 488 conjugate (Thermo Fisher Scientific; A-11034)
- 3-Guanidinopropionic acid ( $\beta$ -GPA) (Sigma-Aldrich; G6878)
- High Capacity cDNA Reverse Transcription Kit (Applied Biosystems; 4368813)
- Hoechst 33342, Trihydrochloride, Trihydrate (Thermo Fisher Scientific; H1399)
- Hydrocortisone (Sigma-Aldrich; H0888)
- 3-Isobutyl-1-methylxanthin (IBMX) (Sigma-Aldrich; I5879)
- Immobilon®-P PVDF Membrane (Merck-Millipore; IPVH00010)
- Immobilon Western Chemiluminescent HRP Substrate (Merck-Millipore; WBKLS0500)
- Insulin solution human (Sigma-Aldrich; I9278)
- Irisin (human recombinant) (Cayman Chemicals; 11451)
- Maxima SYBR Green/ROX qPCR Master Mix (2X) (Thermo Fisher Scientific; K0221)

- 2-mercaptoethanol (2-MEA) (Sigma-Aldrich; M3148)
- $\mu$ -slide 8 well plate (Ibidi GmbH; 80826)
- Nile Blue A (Sigma-Aldrich; N0766)
- Oligomycin (Enzo Life Sciences; ALX-380-037)
- Pantothenic acid (Sigma-Aldrich; P5155)
- Paraformaldehyde (Sigma-Aldrich; P6148)
- PCR Mycoplasma Test Kit I/C (PromoKine; PK-CA91)
- Penicillin-Streptomycin (Sigma-Aldrich; P4333)
- Recombinant Human BMP-7 Protein (R&D systems; 354-BP)
- Rosiglitazone (Cayman Chemicals; 71740)
- Saponin (Sigma-Aldrich; 47036)
- Serotonin hydrochloride (5HT) (Sigma-Aldrich; H9523)
- Taq DNA Polymerase, recombinant (5 U/ $\mu$ L) (Thermo Fisher Scientific; EP0401)
- 3,3',5-Triiodo-L-thyronine sodium salt (T3) (Sigma-Aldrich; T6397)
- TRI Reagent (Molecular Research Center, Inc.; TR118)
- Triton X-100 (Sigma-Aldrich; T8787)
- Trypsin-EDTA solution (Sigma-Aldrich; T3984)
- TWEEN® 20 (Sigma-Aldrich; P1379)
- XF96 FluxPak mini (Seahorse Biosciences; 102312-100)

#### **4.3. Isolation and cultivation of hADMSCs**

Subcutaneous abdominal adipose tissue samples were immediately transported in sterile PBS to the laboratory following herniotomy. Adipose tissue specimens were dissected from fibrous

material and blood vessels, minced into small pieces and digested in PBS with 120 U/ml collagenase for 60 min in a 37 °C water bath with gentle agitation. The completely disaggregated tissue was filtered (pore size 140 µm) to remove any remaining tissue. The cell suspension was centrifuged for 10 min at 200 g, and the pellet of SVF was re-suspended in DMEM-F12 medium containing 10% FBS, 100 U/ml penicillin-streptomycin, 33 µM biotin and 17 µM pantothenic acid. hADMSCs were seeded into 6-well plates or Ibidi eight-well µ-slides at a density of 15000 cells/cm<sup>2</sup> and cultured in the same medium at 37 °C in 5% CO<sub>2</sub> for 24 h to attach. Floating cells were washed away with PBS and the remaining hADMSCs were cultured until they became confluent. The absence of mycoplasma was checked by polymerase chain reaction (PCR) analysis.

#### **4.4. Induction of white and “beige” adipocyte differentiation *ex vivo***

After the cell culture became confluent, adipogenic differentiation was initiated. White adipocyte differentiation was induced for four days using the following medium: DMEM-F12 supplemented with 33 µM biotin, 17 µM pantothenic acid, 10 µg/ml human apo-transferrin, 20 nM human insulin, 100 nM hydrocortisone, 200 pM T3, 2 µM rosiglitazone, 25 nM dexamethasone and 500 µM IBMX. After four days rosiglitazone, dexamethasone and IBMX were omitted from the differentiation medium [326,327]. “Beige” adipogenic differentiation was carried out for three days using the following medium: DMEM-F12 containing 33 µM biotin, 17 µM pantothenic acid, 10 µg/ml apo-transferrin, 0.85 µM human insulin, 200 pM T3, 1 µM dexamethasone and 500 µM IBMX. Three days later, the medium was changed (dexamethasone and IBMX were omitted) and 500 nM rosiglitazone was added [328]. From this point on media were changed every other day and cells were assayed after 14 days of differentiation.

#### **4.5. Treatments of hADMSCs and differentiated white and “beige” adipocytes with browning-inducers or activators**

Where indicated, white or browning adipocytes were differentiated in the presence of potent browning-inducers: 250 ng/ml human recombinant irisin or 50 ng/ml human recombinant BMP7 [113,283]. Irisin or BMP7 was administered during the whole differentiation procedure, or in the last 4 days of the differentiation. Cells were treated with clozapine (dissolved in DMSO) every day at 100 ng/mL concentration on the last 2 and 4 days or during the whole adipogenic differentiation process. Browning-inducers were administered for 12 h to hADMSCs and to fully differentiated white or brown adipocytes for short-term treatments. Where indicated, cells were treated with 5HT every day at 10  $\mu$ M concentration during the whole adipocyte differentiation [265]. To investigate the response of differentiated adipocytes to thermogenic induction, cells received a single bolus of dibutyl-cAMP at 500  $\mu$ M final concentration for 4 hours [159].

#### **4.6. RNA Preparation and TaqMan reverse transcription-coupled quantitative PCR (RT-qPCR)**

Total cellular RNA was isolated from hADMSCs and differentiated adipocytes using TRI Reagent. Total RNA concentrations were quantified by spectrometry after DNase treatment. TaqMan reverse transcription reagent was applied for generating cDNA according to manufacturer's instructions. An ABI Prism 7700 sequence detection system (Applied Biosystems) or a LightCycler 480 (Roche Diagnostics) was used to determine normalized gene expression of “classical brown”, “beige”, white and general adipocyte markers. Validated TaqMan qPCR assays designed and supplied by Applied Biosystems were used according to the manufacturer's instructions under which conditions PCR efficiency differed negligibly from 2. Human GAPDH was used as endogenous control. In line with a recent publication, GAPDH

expression levels did not vary between cell types and treatments [329]. All samples were run in triplicate. Gene expression values were calculated by the comparative Ct method.  $\Delta C_t$  represents the threshold cycle (Ct) of the target minus that of GAPDH. Normalized gene expression levels equal  $2^{-\Delta C_t}$ .

#### **4.7. Quantification of mitochondrial (mt) DNA by quantitative PCR**

Total cellular DNA was isolated by a conventional phenol-chloroform method from hADMSCs and differentiated white or browning adipocytes using TRI Reagent. Quantitative PCR was carried out in triplicates on diluted DNA using 10  $\mu$ M each primer (mtDNA specific PCR, forward 5'-CTATGTCGCAGTATCTGTCTTTG-3', reverse 5'-GTTATGATGTCTGTGTGGAAAG-3'; and nuclear specific PCR (SIRT1 gene), forward 5'-CTTTGTGTGCTATAGATGATATGGTAAATTG-3', reverse 5'-GATTAAACAGTGTACAAAAGTAG-3') and Maxima SYBR Green/ROX qPCR Master Mix in a LightCycler 480 with a program of 20 min at 95  $^{\circ}$ C, followed by 50 cycles of 15 sec at 95  $^{\circ}$ C, 20 sec at 58  $^{\circ}$ C and 20 sec at 72  $^{\circ}$ C. Single-product amplification was proved by an integrated post-run melting curve analysis. Results were calculated from the difference in Ct values for mtDNA and nuclear specific amplification. Data were expressed as mitochondrial genomes per diploid nuclei [330].

#### **4.8. Western blotting**

hADMSCs and differentiated adipocytes were washed with ice cold PBS and collected followed by lysing in 50 mM Tris-HCl; 0.1% Triton X-100; 1 mM EDTA; 15 mM 2-MEA and protease inhibitors. Insoluble cellular material was removed by centrifugation. Then, the protein concentration was determined by using Bradford reagent and the lysates were mixed with 5 $\times$

Laemmli loading buffer, boiled for 10 min and loaded onto a 10% SDS polyacrylamide gel. Proteins were transferred onto PVDF Immobilon-P Transfer Membranes followed by blocking in Tris-buffered saline containing 0.05% Tween-20 (TBS-T) and 5% skimmed milk for 1h. Membranes were probed by polyclonal anti-Ucp1 and monoclonal anti-GAPDH antibodies overnight at 4°C, followed by incubation with horseradish-peroxidase-conjugated species-corresponding secondary antibodies for 1 h at room temperature. Immunoblots were developed with Immobilon Western chemiluminescent substrate. Densitometry analysis of immunoblots was performed using Image J software.

#### **4.9. Vital and immunofluorescence staining of differentiated adipocytes**

hADMSCs were plated on Ibidi eight-well  $\mu$ -slides and differentiated as described in 4.4. On the day of measurement, cells were washed once with PBS and then kept in fresh medium for subvital scanning with 50  $\mu$ g/ml Hoechst 33342 for 60 minutes and 750  $\mu$ g/ml Nile Blue for 20 minutes. Next, cells were washed and fixed in 4% paraformaldehyde for 5 min followed by blocking in 5% skimmed milk for 2h and staining with anti-Ucp1 or anti-Cidea primary antibodies for 6h at room temperature. Alexa 488 goat anti-rabbit IgG was applied as a secondary antibody. Antibodies were used and additional washing steps between and after Ab usage were carried out in the presence of 0.1% saponin in PBS for effective cell permeabilization.

#### **4.10. Image acquisition by laser-scanning cytometry (LSC), recognition of cellular objects**

Images were collected with an iCys Research Imaging Cytometer (iCys, Thorlabs Imaging Systems) following the protocol of Doan-Xuan et al [331]. Sample slides were attached on a computer-controlled stepper-motor driven stage. An area with optimal confluence was defined in

low-resolution scout scan with a  $\times 10$  magnification objective and a 10- $\mu\text{m}$  scanning step. As a next step, high-resolution images were consequently obtained by using a  $\times 40$  objective and a 0.25- $\mu\text{m}$  scanning step. The size of a pixel was set to 0.25  $\mu\text{m} \times 0.245 \mu\text{m}$  at  $\times 40$  magnification. Laser lines were separately operated, namely a 405-nm diode laser was used to excite Hoechst 33342, a solid-state 488-nm laser was used for Alexa 488 goat anti-rabbit IgG and a 633-nm HeNe gas laser for Nile Blue. Emissions were collected by three photomultiplier tubes; Hoechst was detected at  $450 \pm 20 \text{ nm}$ , Alexa 488 at  $530 \pm 15 \text{ nm}$  and Nile Blue at above 650 nm.

Transmitted laser light was captured by diode photodetectors in which light loss and shaded relief signals were measured to gain information about light absorption, light scattering and texture of the objects. Then, images were processed and analyzed by our high throughput automatic cell recognition protocol using the iCys companion software (iNovator Application Development Toolkit, CompuCyte Corporation) and CellProfiler (The Broad Institute of MIT).

A two step process was used to identify adipocytes in the mixed cultures. Hoechst-stained nuclei were first identified and defined as primary objects. Based on parent nuclei, the secondary objects, a whole cell, were then identified according to its Nile Blue fluorescence (**Figure 8**). The texture feature was used to characterize the lipid droplet content of the cells, therefore cells which contained lipids above a preset threshold value were considered as adipocytes and included in further analysis. On texture “sum variance” (SV) vs. Ucp1 expression plots undifferentiated progenitors segregated from the rest of the cells and were narrowly confined around the (0, 0) coordinates. Image regions occupied by these cells were excluded from further analysis.

*[The images were analyzed by Dr. Quang-Minh Doan-Xuan and Dr. Zsolt Bacsó (Department of Biophysics and Cell Biology, University of Debrecen). These results are shown in Figures 11-14]*

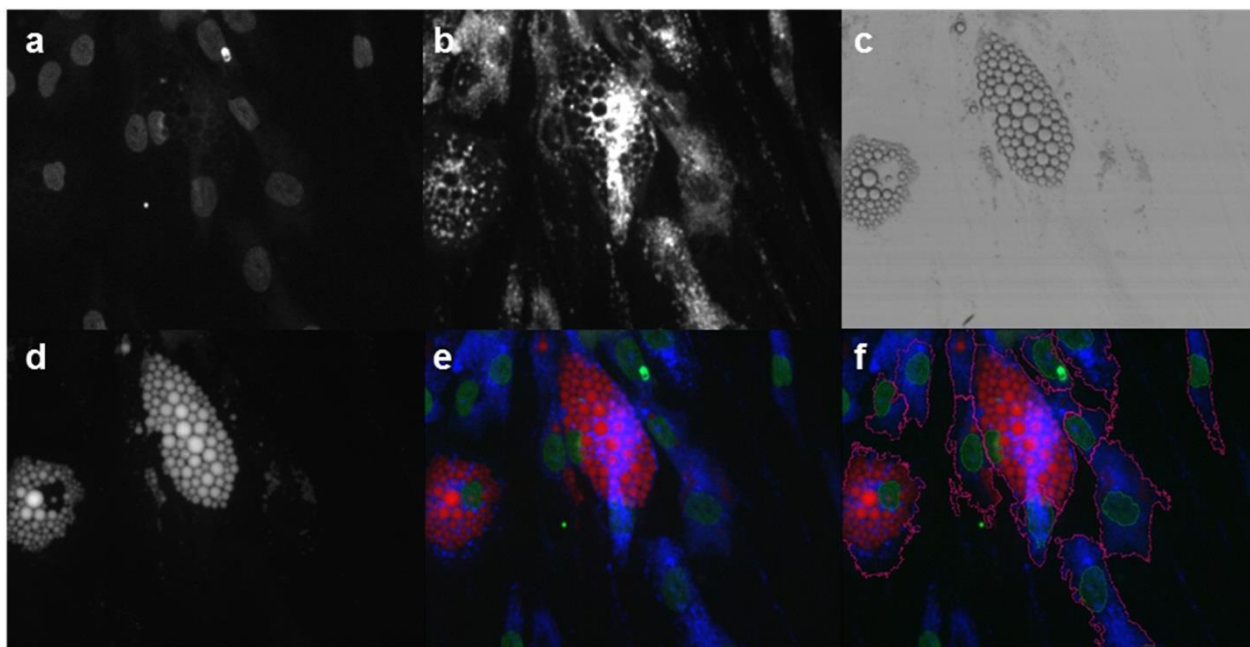


**Figure 8.** Segmentation and automated recognition of adipocytes and preadipocytes by LSC. (a) Hoechst-stained nuclei of differentiated adipocytes and preadipocytes. (b) Phospholipid specific Nile Blue labelling. (c) Transmitted light images by which texture analyses were performed. (d) Nile Red staining as an alternative approach to visualize and analyze lipid droplets. (e) Merged image of Hoechst, Nile Blue and Nile Red channels. (f) Nuclei were identified as primary objects, contoured with green lines. Then, secondary objects as adipocytes and preadipocytes were detected using Nile Blue signal in close association with the predefined primary objects and bordered with red lines. Cell recognition was performed by the automated segmentation module of CellProfiler software. This Figure was prepared by Dr. Quang-Minh Doan-Xuan.



#### **4.11. Texture analysis, quantification of Ucp1 and Cidea protein content of single cells and population scale analysis of human adipocyte browning**

2000-3000 cells per sample were collected for image analysis. Clustered, detached or dead cells were omitted and 1000-2000 cells were quantified per data set. We sought to render the difference that is obvious to the observer between the appearance of white adipocytes containing a few large lipid droplets and “beige”/brown adipocytes containing many small droplets in the form of a computable measure. Pictorial information may be grasped in spectral, textural or contextual terms. A textural description concerns itself with spatial distribution of tonal variations within an image. Textural parameters were calculated per identified objects using a built-in module of the CellProfiler software based on the approach of Haralick et al. [332] After segmentation the images of individual adipocytes were treated as a function which assigns a grey-tone value to each one in the 'x' by 'y' array of resolution cells, or pixels, based on their levels of brightness in a transmitted light image. From these quantized levels of grey shades of the pixels a nearest-neighbor grey-tone spatial dependence matrix was derived the entries of which are the numbers of adjacent pixel pairs with grey tone values exactly m,n where  $m,n = \{1, 2, 3 \dots, N_g\}$  and  $N_g$  is the number of distinct grey levels in the image. CellProfiler paired any pixel with the one to its right. The spatial dependence matrix was frequency normalized by dividing it with R, the total number of possible neighboring resolution cell pairs in the image. Haralick et al. [332] extract 14 different features from matrices of this sort which either relate to specific textural characteristics of the image or characterize the complexity of and the grey-tone transitions in the image. From among the latter we selected texture SV as it could well separate the white and “beige” populations. Note, that it is not possible to identify in everyday terms (such as homogeneity, contrast, coarseness, boundaries, etc.) the property which this feature represents. Texture SV was calculated as:

$$SV = \sum_{i=2}^{2Ng} \left( i - \sum_{i=2}^{2Ng} i p_{x+y}(i) \right)^2 p_{x+y}(i)$$

where

$p_{x+y}(i) = \sum_{m=1}^{Ng} \sum_{n=1}^{Ng} P(m, n) i = \{2, 3, \dots, 2Ng\}$  is the  $i^{\text{th}}$  entry in the probability matrix obtained by summing of  $p(m, n)$  of pixel pairs with a sum intensity of  $i$

$p(m, n) = P(m, n)/R$  is the  $(m, n)^{\text{th}}$  entry in the normalized grey-tone spatial-dependence matrix

$P(m, n)$  is the number of adjacent pixel pairs with grey tone values exactly  $m, n$  where  $m, n = \{1, 2, 3, \dots, Ng\}$

$Ng$  is the number of distinct grey levels in the image and

$R$  is the total number of possible neighboring resolution cell pairs in the image

Beside texture parameters, the other major profiles that were also extracted are: Integral, which is the sum of the pixel intensities for a given event that provides information about the expression level of the labelled protein; and Area, which is the area enclosed by the boundary contour of the object, in square micrometers. From these parameters, Ucp1 or Cidea immunofluorescence intensity per cell (Ucp1 or Cidea protein content of each adipocyte) could be evaluated as the value of the Integrated intensity relative to the Area of each event. Ucp1 intensities and texture SV of each differentiated adipocyte were then plotted. On the density contour plots cells were identified as browning adipocytes if their texture SV was lower than 4.5. This value corresponds to the local minimum between the peaks of a lower and higher SV group, when the frequency of SV of equal numbers of cells differentiated with the white and the “beige” protocols is plotted together. In our experience this invariably well discriminated two intuitively recognizable distinct populations throughout all experiments. For the Ucp1 immunostaining, where the efficiency of staining varied from experiment to experiment and no constant threshold could be set, low and

high expressing populations were demarcated by the highest fluorescence value in the cells that had the highest 10% of texture SV in the high SV group, of which it was most reasonable to believe that they represented white adipocytes.

Thus, adipocytes with morphological characteristics of browning were recognized as the ones that contained small lipid droplets (their texture SV was low) and high levels of Ucp1 protein (lower right quadrant of density plot images), in contrast to white adipocytes, which accumulated large lipid droplets (their texture SV was high) and expressed low amount of Ucp1 (upper left quadrant of density plot images) (**Figures 12-14**).

#### **4.12. Determination of cellular oxygen consumption (OC)**

OC was determined using an XF96 oximeter (Seahorse Biosciences). Cells were seeded and differentiated in 96-well XF96 assay plates. On the day of measurement, after recording the baseline OC for 30 min, adipocytes received a single bolus dose of dibutyryl-cAMP (at 500  $\mu$ M final concentration) modelling adrenergic stimulation. Then, stimulated OC was measured every 30 minutes. The final reading took place at 5 h post-treatment [60,330]. Adipocytes were treated with 5  $\mu$ M etomoxir or with 2 mM  $\beta$ -GPA to block beta-oxidation and creatine-driven substrate cycle [179]. Next, proton leak respiration was recorded after adding oligomycin at 2  $\mu$ M concentration to block ATP synthase activity. As a last step, cells received a single bolus dose of Antimycin A (10  $\mu$ M final concentration) for baseline correction. The oxygen consumption rate (OCR) was normalized to protein content and normalized readings were shown. For statistical analysis, the fold change of OC levels were determined comparing basal, cAMP stimulated and oligomycin inhibited (both in unstimulated and stimulated cells) OCRs of each sample to the basal OCR of untreated white adipocytes.

#### **4.13. Determination of cytokine release**

During regular replacement of differentiation media, culture supernatants were harvested and stored for cytokine measurements. Then, conditioned differentiation media from the same donor and differentiated sample were pooled. Where indicated, media were changed and culture supernatants were collected every day. The concentration of IL-6, IL-1 $\beta$ , IL-8, Tumor necrosis factor alpha (TNF $\alpha$ ) and Monocyte Chemotactic Protein-1 (MCP-1) was measured from the collected cell culture media using ELISA DuoSet Kit [327].

#### **4.14. Statistical analysis**

Each experiment was repeated 3-10 times with SVFs from independent healthy donors. Results are expressed as the mean  $\pm$  SD for the number of assays indicated in the Figure captions. Sample sizes were chosen to ensure adequate statistical power following the practice of similar studies. For multiple comparisons of groups statistical significance was calculated and evaluated by one-way Analysis of variance (ANOVA) followed by Tukey post-hoc test. In comparison of two groups two-tailed, paired Student's t-test was used. The data were analyzed using Prism 6.01 (GraphPad Software).

## 5. RESULTS

### 5.1. A previously described brown adipogenic protocol induced a “beige”-like gene expression pattern in differentiating human adipocytes

hADMSCs were isolated from the SVF of abdominal subcutaneous WAT and previously described differentiation regimens were applied to induce white [326,327] and brown [328] adipocyte differentiation. We selected to examine the expression of a core set of BAT-specific genes (UCP1, CIDEA, PGC-1 $\alpha$  and ELOVL3) and a marker of mitochondrial enrichment (CYC1). The expression of PRDM16 and C/EBP $\beta$  which are key transcriptional regulators of browning was also measured. A “beige”-selective (TBX1) and a “classical brown” adipocyte marker gene (ZIC1) were also investigated. Finally, key drivers of the adipogenic program (C/EBP $\alpha$ , PPAR $\gamma$ ) and general (LEPTIN, FABP4) adipocyte marker genes were assessed. The expression of UCP1 was not detectable in undifferentiated hADMSCs and showed a basal level in adipocytes differentiated by the white adipogenic cocktail for two weeks. Significantly higher expression of UCP1, both at mRNA and protein level, and increased mitochondrial DNA amount were found in whole cell lysates of adipocytes differentiated in the presence of the brown compared to the white protocol (**Figure 9**).

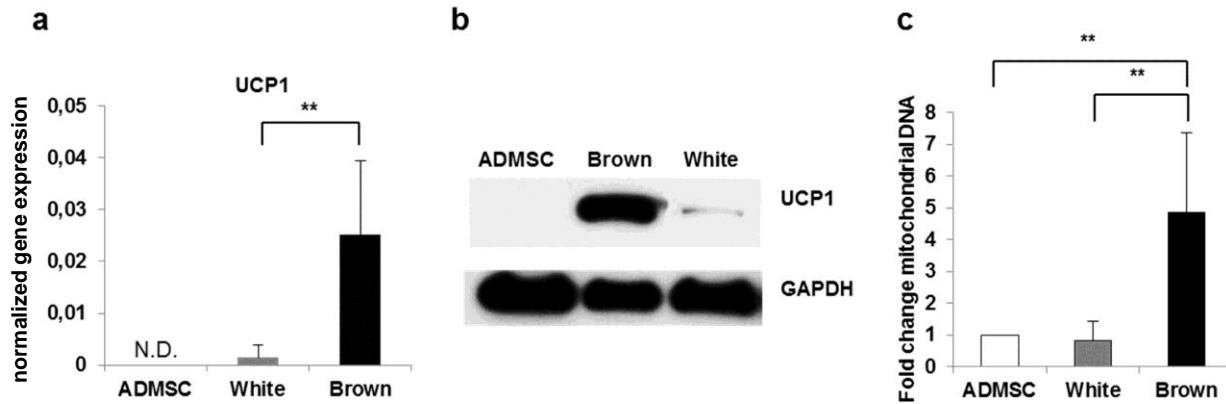


**Figure 9.** *UCP1 expression and mitochondrial DNA content of primary human adipocytes. ADMSCs were differentiated for two weeks to white or brown adipocytes. (a) Ucp1 expression at mRNA level, detected by RT-qPCR; n=10. (b) Ucp1 protein expression in one representative adipocyte donor. (c) Relative mitochondrial DNA amount (as compared to undifferentiated ADMSCs), determined by qPCR; n=7. Results are expressed as the mean  $\pm$  SD for the number of assays (adipocytes of n different SVF donors) indicated. For multiple comparisons of groups statistical significance was evaluated by one-way ANOVA followed by Tukey post hoc test.*

**\*\*** $p < 0.01$

In line with the increased UCP1 expression, we found upregulated browning marker genes (CIDEA, ELOVL3, CYC1 and PGC-1 $\alpha$ ) in response to the brown differentiation cocktail. The expression of ZIC1 remained at a low level after 14 days of brown adipogenic differentiation excluding that this protocol induces “classical brown” adipocyte phenotype. Contrarily, the significant upregulation of TBX1, a “beige” marker gene, suggests that human primary adipocytes from abdominal subcutaneous fat follow the „beige” pathway when differentiated according to the protocol developed by Elabd et al. [328] (**Figure 10**). From this point forward, we are referring to these cells as “beige” adipocytes.

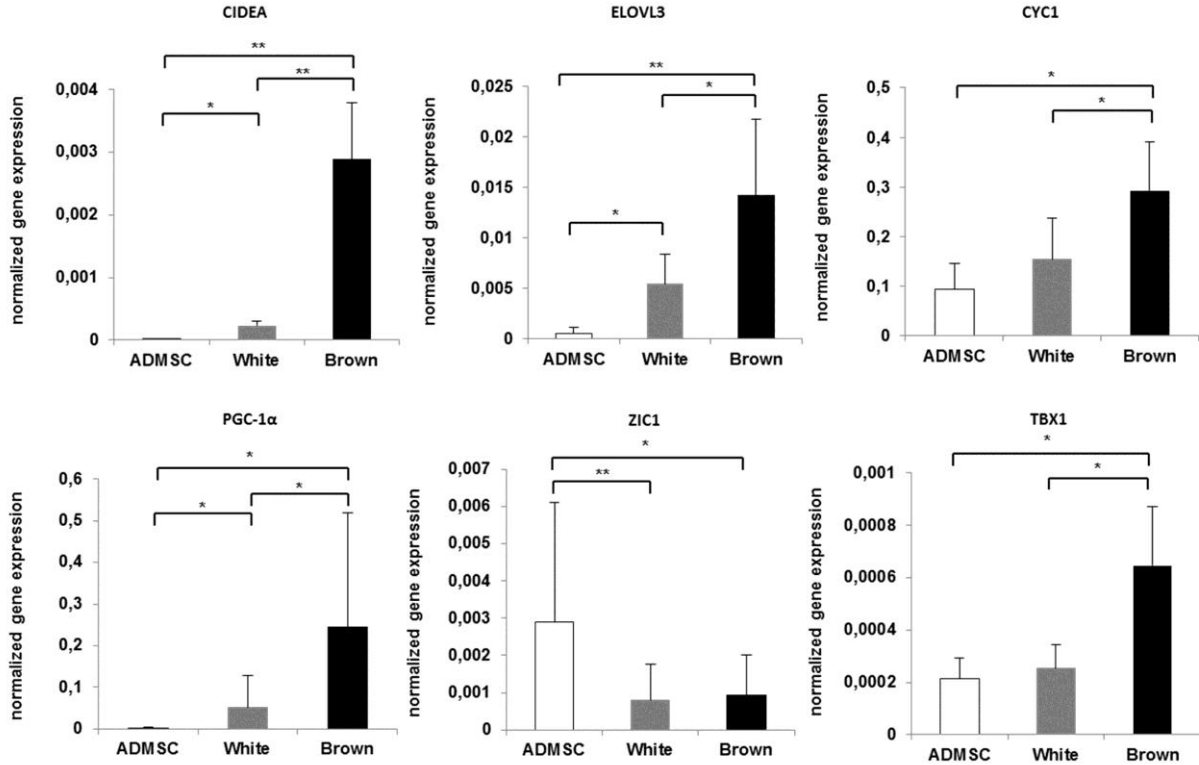


**Figure 10.** Changes in expression levels of browning marker genes in primary human adipocytes during *ex vivo* brown adipocyte differentiation. ADMSCs of 10 different donors were differentiated for two weeks to white or brown adipocytes. (Gene expression was determined by RT-qPCR, target genes were normalized to GAPDH) Results are expressed as the mean  $\pm$  SD; for multiple comparisons of groups statistical significance was evaluated by one-way ANOVA followed by Tukey post hoc test. \* $p < 0.05$ , \*\* $p < 0.01$

In general, adipogenic markers were hardly detected in undifferentiated progenitors. However, both adipocyte differentiation regimens induced a robust upregulation of well-accepted adipogenic marker genes. Gene expression changes in response to the aforementioned protocols are summarized in **Table 1**.

GENES	ADMSC Average	SD	White Average	SD	FC (W/ADMSC)	Brown Average	SD	FC (B/ADMSC)	FC (B/W)
UCP1	N.D.	-	0.0036	0.0048	N.D.	0.026	0.014	N.D.	7.26
ELOVL3	0.00051	0.00018	0.0055 *	0.0027	10.71	0.014 **	0.0062	27.95	2.61
CYC1	0.094	0.041	0.15	0.059	1.65	0.29 *	0.087	3.12	1.89
CIDEA	0.000018	0.0000076	0.00023 *	0.000082	12.72	0.0029 **	0.00071	159.13	12.51
PGC-1 $\alpha$	0.0023	0.0011	0.054 *	0.072	23.85	0.25 **	0.34	111.86	4.69
PRDM16	0.00046	0.00065	0.00072	0.00023	1.58	0.00077	0.00038	1.69	1.07
C/EBP $\beta$	0.092	0.044	0.12	0.056	1.47	0.15	0.062	1.96	1.33
ZIC1	0.0029	0.0032	0.00079 **	0.00098	0.27	0.00092 *	0.0011	0.32	1.16
TBX1	0.00022	0.000069	0.00025	0.000093	1.18	0.00065 *	0.00018	2.99	2.54
LEPTIN	0.0087	0.0042	0.061 **	0.038	7.02	0.026 *	0.016	2.99	0.43
C/EBP $\alpha$	0.0023	0.00078	0.029 **	0.017	12.61	0.027 **	0.015	11.74	0.93
FABP4	0.00073	0.00034	3.61 ***	2.84	4945.52	6.27 ***	4.67	8589.56	1.72
PPAR $\gamma$	0.0018	0.00073	0.0096 *	0.0081	4.51	0.0094 *	0.011	5.27	0.98

**Table 1.** Numerical data of changes in expression levels of adipogenic genes in primary human adipocytes during ex vivo white or brown adipocyte differentiation. Table shows average normalized expression levels of ADMSCs, white and brown adipocytes, their SD and fold changes (FC) as a ratio of expression levels of white adipocytes and ADMSCs (W/ADMSC); brown adipocytes and ADMSCs (B/ADMSC); brown adipocytes and white adipocytes (B/W). The experiment was repeated ten times with SVFs from independent healthy donors. For comparison of the sample pairs White average vs. ADMSC average and Brown average vs. ADMSC average statistical significance was evaluated by Student's *t*-test. \**p*<0.05, \*\**p*<0.01, \*\*\* *p*<0.001. (Gene expression was determined by RT-qPCR, target genes were normalized to GAPDH)



## 5.2. Laser-scanning cytometry (LSC) can quantify human adipocyte browning

To date, white, “classical brown” or “beige” adipocyte differentiation has mostly been evaluated based on the detection of mRNA or protein expression in whole cell lysates. However, up to 50% of precursor cells remain undifferentiated in human cellular models of adipocyte development. In line with other studies, depending on individual donors, 40-60% of the hADMSCs were able to accumulate lipid droplets as a result of 14 days long adipocyte differentiation; this phenomenon was quantified at consecutive time points using LSC formerly by Doan-Xuan et al [331]. Since the cell cultures of both white and “beige” adipocytes were heterogeneous, we intended to quantify adipocyte browning *ex vivo* at a single cell level in a highly replicative manner by the abovementioned slide-based image cytometry approach.

In our experiments, following the differentiation process and staining, fluorescently labelled nuclei of cells were identified and then cellular morphology, lipid accumulation and major brown adipogenic marker protein expression were inspected simultaneously, as described in details in section 4.11. We found significantly lower texture SV along with the accumulation of smaller lipid droplets as a result of “beige” differentiation. Immunofluorescent staining showed that Ucp1 was mostly distributed between the lipid droplets of “beige” adipocytes, while Cidea accumulated highly in the perinuclear lipid-free region of these cells. When images, which captured 1000-2000 cells per donor, were quantified, we found that “beige” differentiation compared to white lead to a two-fold higher Ucp1 and Cidea protein content in single human adipocytes (**Figure 11**).

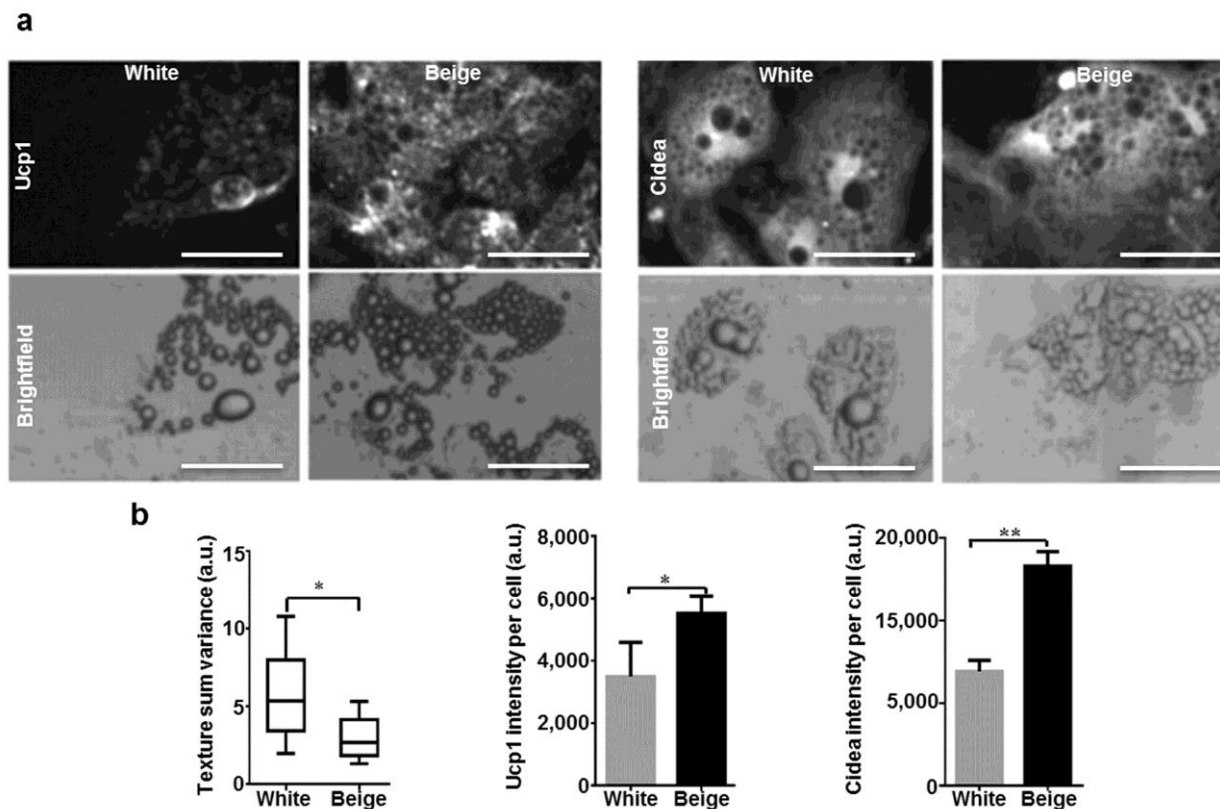


**Figure 11.** Immunostaining and texture analysis of human adipocytes. ADMSCs were differentiated as in Figures 9-11. **(a)** Distribution of lipid droplets and browning marker proteins in adipocytes. “Beige” cells accumulated smaller lipid droplets and more Ucp1 or Cidea than the white adipocytes. Bars represent 50  $\mu$ m. **(b)** Texture “sum variance”, Ucp1 and Cidea protein content of adipocytes per cell.  $n=6$ , 1000-2000 cells per each donor. For comparison of two groups statistical significance was evaluated by Student’s *t*-test. \* $p<0.05$ , \*\* $p<0.01$ .

Next, we plotted Ucp1 protein content and texture SV for each differentiated adipocyte (undifferentiated progenitors were omitted from the analysis). Adipocytes with morphological characteristics of browning were recognized as the ones that contained small lipid droplets and high levels of Ucp1 (lower right quadrant of density plot images), contrary to white adipocytes, which accumulated large lipid droplets and expressed low amount of browning marker protein

(upper left quadrant of density plot images). Our results show that the population of differentiated adipocytes remains heterogeneous regardless of whether white or “beige” program was induced. Furthermore, we could detect a significant amount of cells (15-30% of the adipocytes) with the characteristic morphological features of browning even in response to the white adipogenic cocktail. However, when adipocytes were differentiated in the presence of the aforementioned “beige” regimen, the rate of browning cells increased strongly, depending on individual donors, by approximately 3-fold (**Figure 12**).

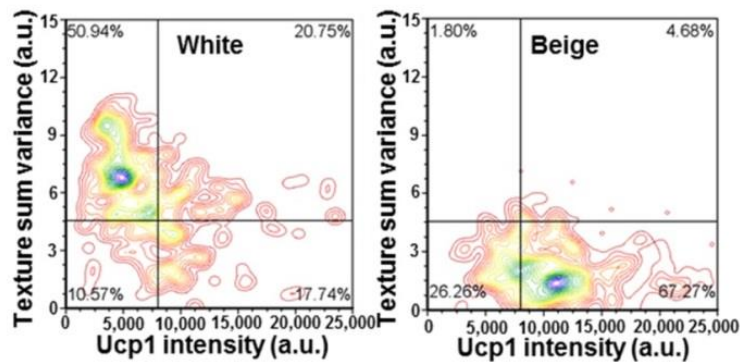


**Figure 12.** Density plot images of one representative donor based on which browning adipocytes (lower right quadrants) can be identified as cells containing small lipid droplets and high levels of Ucp1 protein. SVF derived ADMSCs were differentiated as in Figures 9-12.

In summary, complementing measurements of gene expression changes from total cell lysates with the presented LSC based texture analysis and detection of Ucp1 content in adipocytes resulted in an effective population scale analysis of human „beige” (or brown) adipogenic differentiation. As far as we are aware, our LSC based method was the first approach that can clearly discriminate between human white and brown adipocytes in the heterogeneous cell culture conditions in a high throughput manner.

### 5.3. Irisin and BMP7 induce browning of human adipocytes

Our next aim was to clarify whether human recombinant irisin and BMP7, two potent endogenous browning-inducers described in mice, were able to shift the adipocyte differentiation towards browning. Using the LSC approach described above, we determined that irisin and BMP7 treated differentiating white adipocytes contained smaller lipid droplets and higher amount of Ucp1 and Cidea protein than the untreated cells. When we analyzed Ucp1 immunofluorescence intensity and texture SV of 2000 differentiated cells in 3 different donors, following the practice demonstrated on **Figure 12**, we found that 30-60% of adipocytes had the characteristic morphological features of browning in response to irisin or BMP7 treatment (**Figure 13**). The biological variance among donors of hADMSCs is described in **Table 2**. Thus, by using a slide-based image cytometry approach we could validate mouse data in human samples demonstrating the effectiveness of irisin and BMP7 to induce a browning program in human subcutaneous adipocytes.

	White differentiation protocol		Beige differentiation protocol		White differentiation protocol + Irisin		White differentiation protocol + BMP7	
Donors	% of differentiated adipocytes							
	Texture↑ Ucp1↓	Texture↓ Ucp1↑	Texture↑ Ucp1↓	Texture↓ Ucp1↑	Texture↑ Ucp1↓	Texture↓ Ucp1↑	Texture↑ Ucp1↓	Texture↓ Ucp1↑
1	43.89	10.56	33.89	24.44	16.68	42.10	12.17	26.97
2	50.94	17.74	1.80	67.27	5.84	53.25	12.33	47.00
3	36.54	9.62	6.78	55.93	10.53	37.78	8.86	31.58

**Table 2.** LSC based population scale analysis of ex vivo adipogenic differentiation by texture parameters and Ucp1 protein content of adipocytes showing the biological variance of different donors. Browning adipocytes are identified as they contain small lipid droplets (Texture↓) and high amount of Ucp1 protein (Ucp1↑).

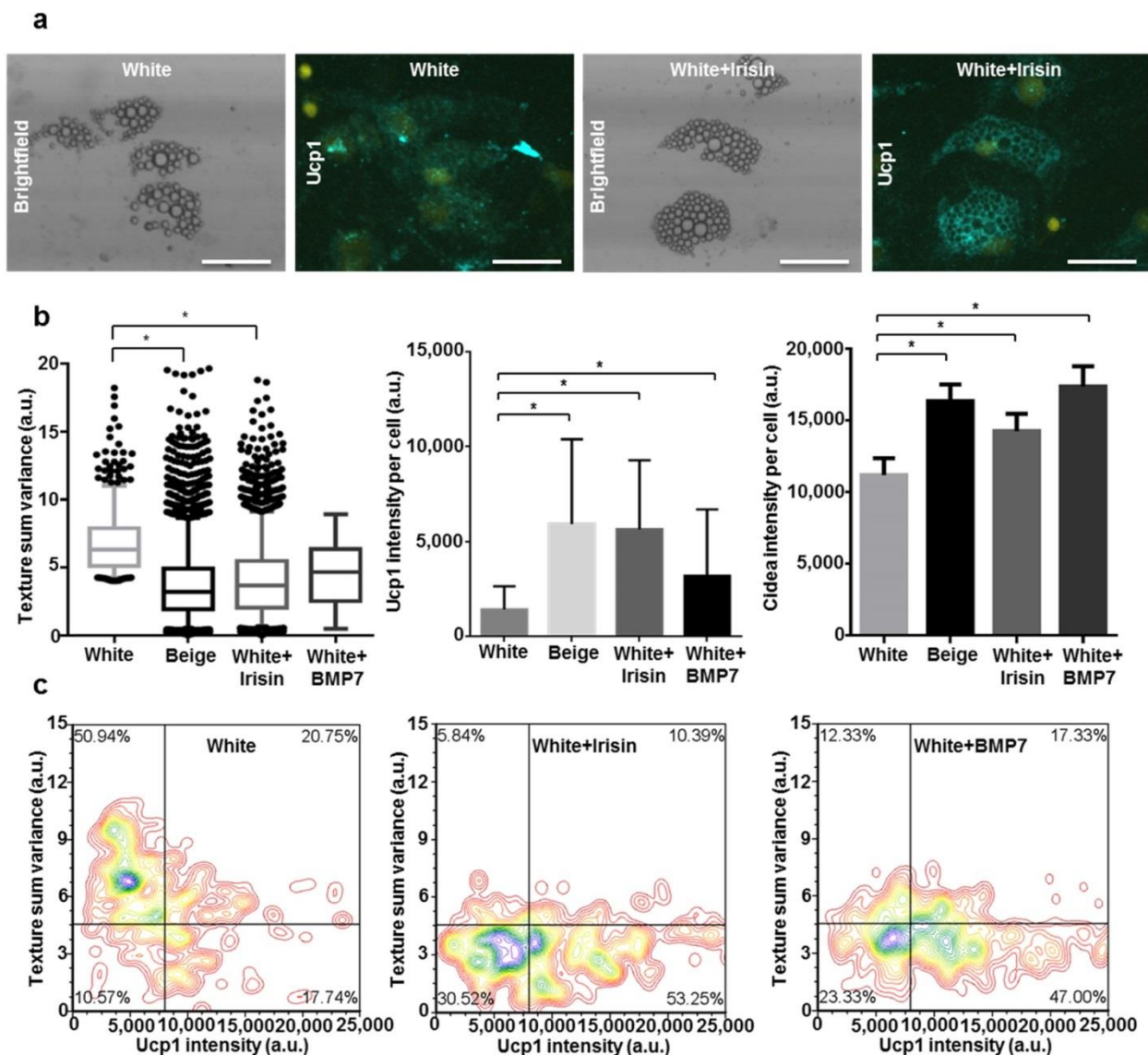


**Figure 13.** Population scale analysis of adipocytes treated with irisin or BMP7 for 14 days. **(a)**

Distribution of lipid droplets and Ucp1 in irisin treated white adipocytes. Irisin treated cells accumulated smaller lipid droplets and more Ucp1 protein then the untreated white adipocytes.

Bars represent 50  $\mu\text{m}$ . **(b)** Texture “sum variance”, Ucp1 and Cidea protein content of adipocytes per cell.  $*p < 0.05$ ,  $n = 3$ , 1000-2000 cells per each donor **(c)** Density plot images showing texture “sum variance” and Ucp1 content of differentiated cells in one representative donor. Browning adipocytes were identified as in **Figure 12**.

#### **5.4. Clozapine enhances browning of human adipocytes detected by LSC**

Next, we aimed to apply our slide-based image cytometry method to test the effect of exogenous drugs on the induction of human adipocyte browning. Only a few studies investigated the direct effect of SGAs on differentiating human adipocytes so far. To fill this hiatus and to follow-up the previous study by Sárvári et al. [333] where expression of selected adipogenic, cell cycle-related and pro-inflammatory genes in SGA-treated human white adipocytes were investigated, we examined how the propensity of hADMSCs to differentiate into heat-generating browning cells is influenced by clozapine. Surprisingly, we found that the long-term clozapine administration on top of the white adipogenic cocktail resulted in the occurrence of more and smaller lipid droplets in the differentiated adipocytes, similarly but less extensively than in the case of “beige” adipocytes described in section 5.2. In addition, elevated Ucp1 protein content was observed simultaneously in single adipocytes. Following the practice shown on **Figure 12**, we demonstrated that, depending on individual donors, 30-40% of differentiating adipocytes had the characteristic morphological features of browning cells in response to clozapine treatment. The proportion of browning adipocytes was increased by approximately 1.5-fold compared to white fat cells (**Figure 14**). The biological variance among donors of hADMSCs was summarized in **Table 3**.

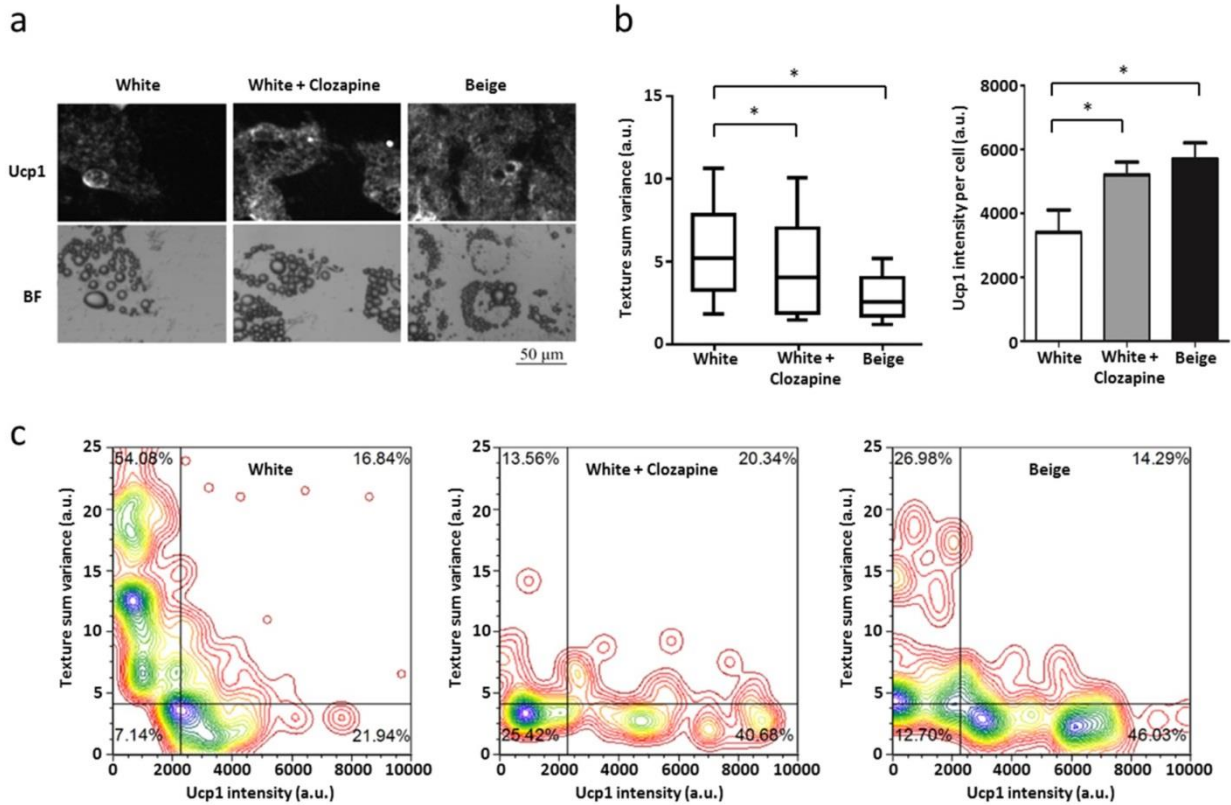


**Figure 14.** LSC based population scale analysis of browning by texture parameters and Ucp1 protein content of ex vivo differentiated single primary adipocytes treated with clozapine. **(a)** Distribution of Ucp1 in clozapine treated adipocytes. Images were collected with an iCys Research Imaging Cytometer. **(b)** Texture “sum variance” and Ucp1 protein content of adipocytes per cell. \* $p < 0.05$ ,  $n = 3$ , 1000-2000 cells per each donor. **(c)** Density plot images showing texture “sum variance” and Ucp1 content of differentiated cells in one representative donor. Browning adipocytes were identified as in **Figure 12**.

	White differentiation protocol		Beige differentiation protocol		White differentiation protocol + Clozapine	
Donors	% of differentiated adipocytes					
	Texture↑ Ucp1↓	Texture↓ Ucp1↑	Texture↑ Ucp1↓	Texture↓ Ucp1↑	Texture↑ Ucp1↓	Texture↓ Ucp1↑
1	42.34	29.20	26.98	46.03	13.56	40.66
2	56.64	17.60	8.60	44.09	14.55	25.45
3	54.08	21.94	8.62	58.62	28.89	33.23

**Table 3.** LSC based population scale analysis of clozapine effect on ex vivo adipogenic differentiation by texture parameters and Ucp1 protein content of adipocytes showing the biological variance of different donors. Browning adipocytes are identified as they contain small lipid droplets (Texture↓) and high amount of Ucp1 protein (Ucp1↑).

### 5.5. Irisin and BMP7 administration during adipocyte differentiation results in different gene expression patterns

As a next step, irisin or BMP7 was administered on the last 4 days or during the whole white or “beige” differentiation process. Then, whole cell lysates were collected and the expression of a panel of marker genes described in section 5.1 was determined by RT-qPCR. We found that, both irisin and BMP7 treatment during white adipocyte differentiation significantly upregulated UCP1, CIDEA, ELOVL3, CYC1 and PGC-1 $\alpha$  genes (**Figure 15**). Furthermore, elevated expression of C/EBP $\beta$ , PRDM16, C/EBP $\alpha$  and PPAR $\gamma$  was detected in whole cell lysates of BMP7 treated adipocytes. There was no difference between the effect of irisin and BMP7 in regard of LEPTIN and FABP4 expression (**Figure 16**).



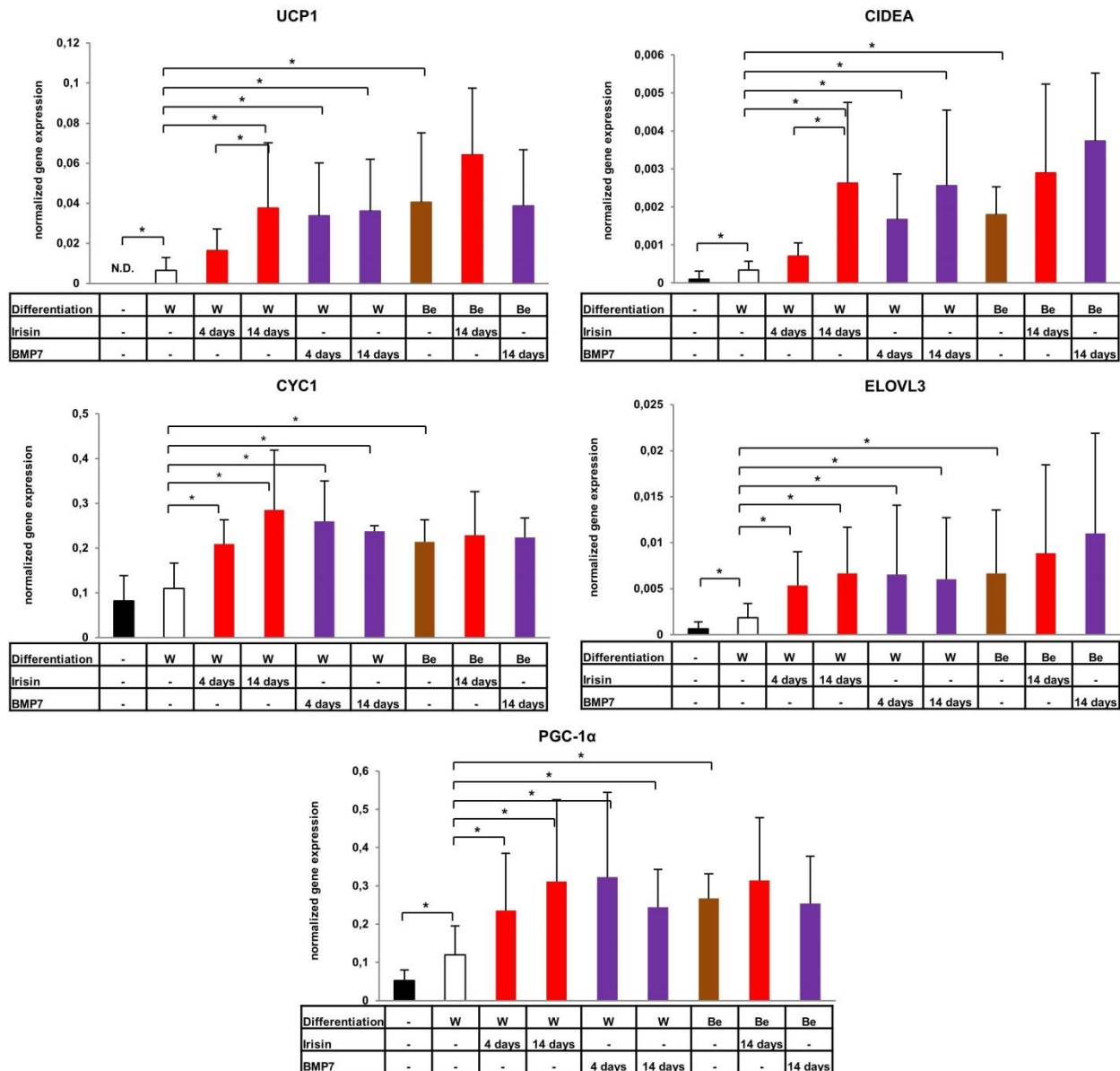


**Figure 15.** Expression of brown adipogenic marker genes in ex vivo differentiated human adipocytes treated with irisin or BMP7, detected by RT-qPCR. ADMSCs were differentiated for two weeks to white (W) or “beige” (Be) adipocytes. 250 ng/ml irisin (red bars) or 50 ng/ml BMP7 (blue bars) was administered on the last 4 days or during the whole differentiation process. Target genes were normalized to GAPDH.  $n=5$ ; Results are expressed as the mean  $\pm$  SD for the number of assays indicated. For multiple comparisons of groups statistical significance was evaluated by one-way ANOVA followed by Tukey post-hoc test.  $*p<0.05$ .

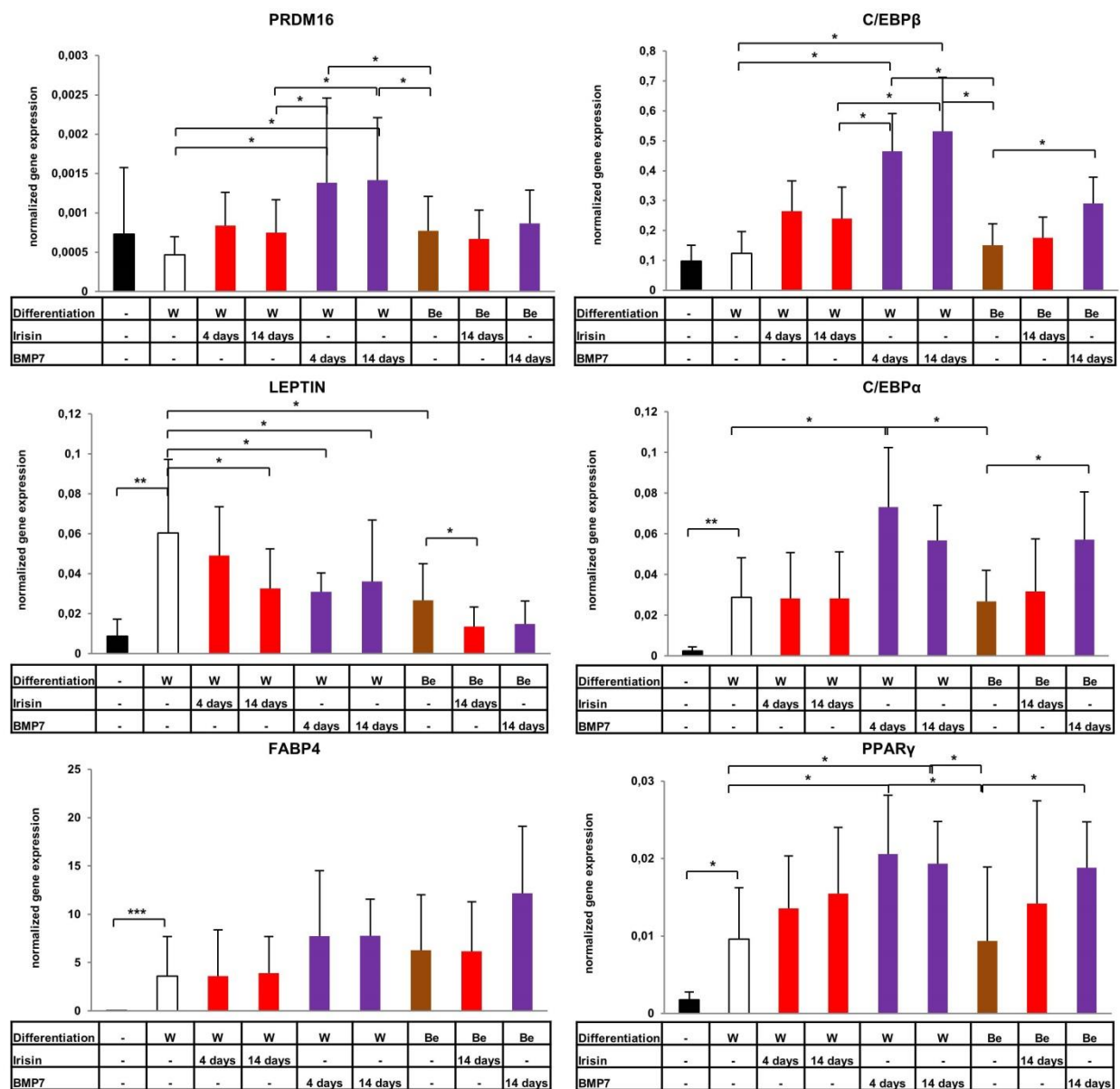


**Figure 16.** Expression of key transcriptional regulators of brown adipocyte development and general adipogenic marker genes in *ex vivo* differentiated human adipocytes treated with irisin or BMP7, detected by RT-qPCR. ADMSCs were differentiated and treated as in Figure 15. Target genes were normalized to GAPDH. Results are expressed as the mean  $\pm$  SD for the number of assays (adipocytes of 5 different SVF donors) indicated. For multiple comparisons of groups statistical significance was evaluated by one-way ANOVA followed by Tukey post-hoc test.

\* $p < 0.05$ , \*\* $p < 0.01$ , \*\*\* $p < 0.001$ .

The expression of ZIC1 remained at a low level after irisin administration excluding that irisin induces “classical brown” adipocyte differentiation. However, expression of the “beige” marker, TBX1 increased selectively as a result of irisin treatment. When, on the other hand, we applied BMP7 on top of both the white and “beige” adipogenic protocol, we found that BMP7 resulted in the upregulation of the “classical brown”-specific ZIC1 (**Figure 17**). In summary, our results suggest that irisin is able to induce a “beige” program in differentiating human primary subcutaneous white adipocytes, while BMP7 induces a “classical brown” adipocyte-like phenotype.

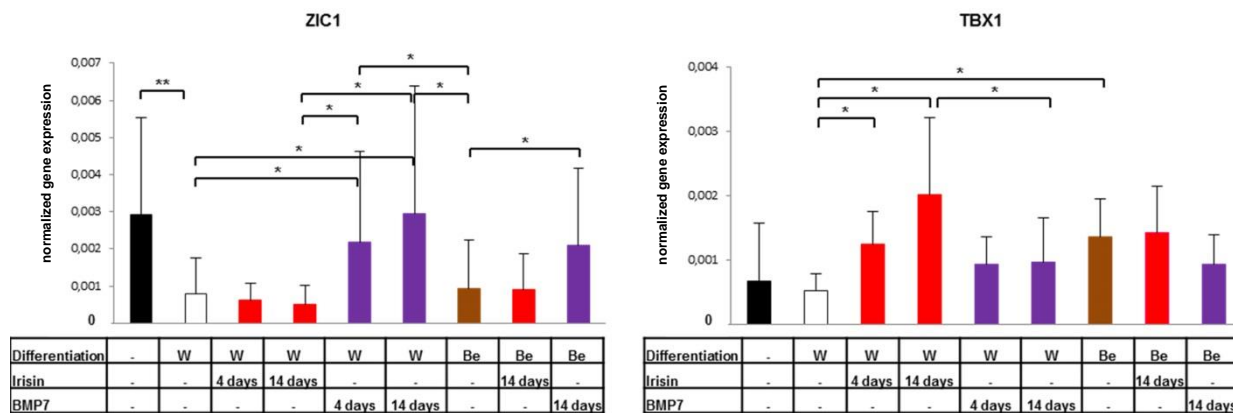


**Figure 17.** Expression of a classical brown and a “beige” marker gene in ex vivo differentiated human adipocytes treated with irisin or BMP7, detected by RT-qPCR. ADMSCs were differentiated and treated as in Figure 15. Target genes were normalized to GAPDH. Results are expressed as the mean  $\pm$  SD for the number of assays (adipocytes of 5 different SVF donors) indicated. For multiple comparisons of groups statistical significance was evaluated by one-way ANOVA followed by Tukey post-hoc test.  $*p<0.05$ ,  $**p<0.01$ .

Then, we investigated how short-term administration of the browning-inducers affected the gene expression patterns of hADMSCs and completely differentiated adipocytes (**Figures 18 and 19**).

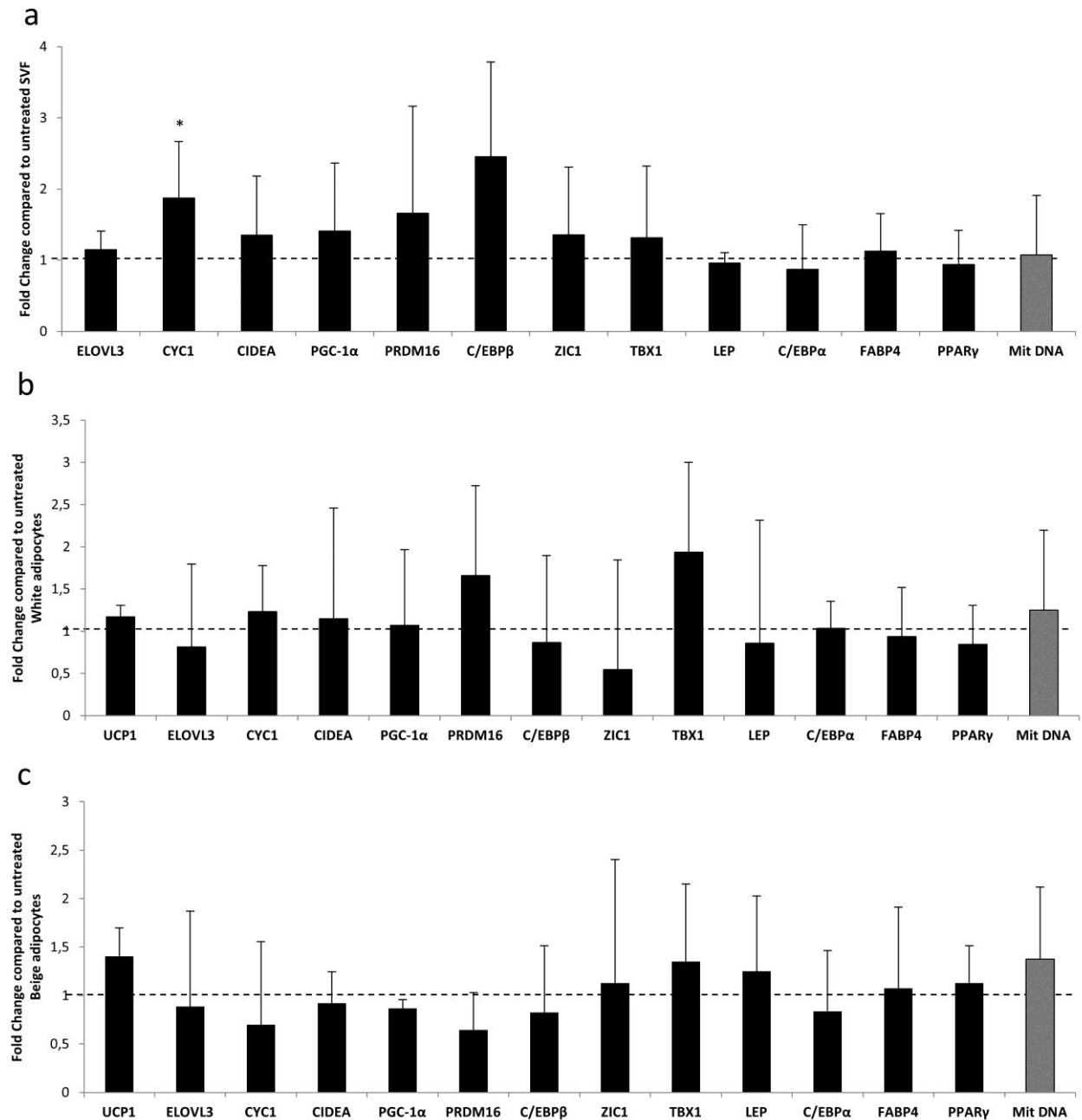


**Figure 18.** Effect of short-term irisin treatment on the expression of selected adipocyte marker genes and mitochondrial DNA amount in primary human SVF, white and “beige” adipocytes (as compared to untreated cells). 250 ng/mL irisin was administered for 12 hours to undifferentiated SVF (a) or to fully differentiated white (b) or “beige” (c) adipocytes.  $n=4$ ,  $*p<0.05$  (The expression of UCP1 could not be detected in SVF). [Unpublished data]

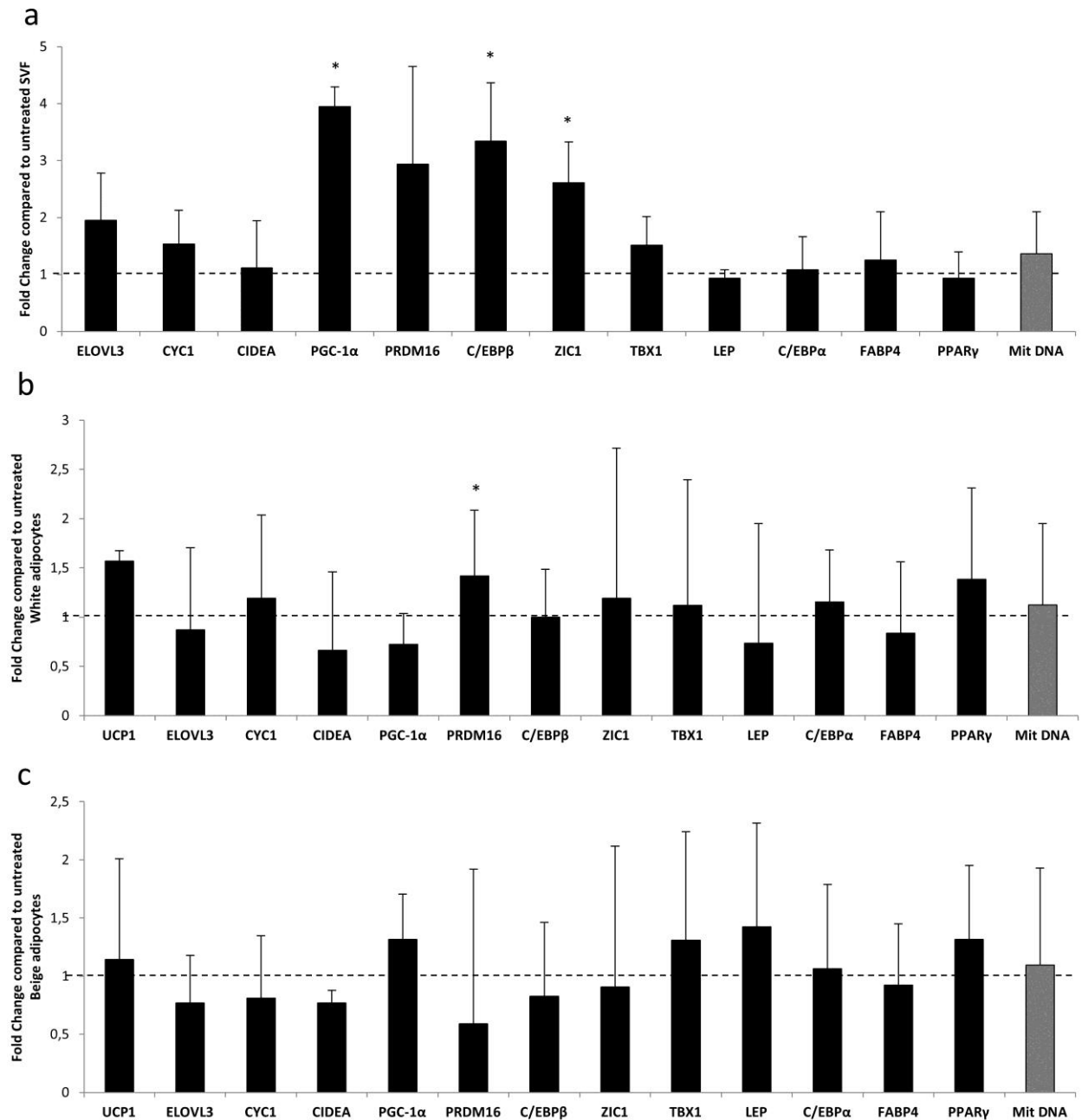


**Figure 19.** Effect of short-term BMP7 treatment on the expression of selected adipocyte marker genes and mitochondrial DNA amount in primary human SVF, white and “beige” adipocytes (as compared to untreated cells). 50 ng/mL BMP7 was administered for 12 hours to undifferentiated SVF (**a**) or to fully differentiated white (**b**) or “beige” (**c**) adipocytes.  $n=4$ ,  $*p<0.05$  (The expression of UCP1 could not be detected in SVF). [Unpublished data]

Undifferentiated progenitors or completely differentiated white or “beige” adipocytes did not respond to the 12 h long irisin treatment (except for the slight upregulation of CYC1 in hADMSCs), suggesting that the adipogenic differentiation program is required for the browning effect of irisin (**Figure 18**). However, the expression of several key transcriptional regulators (C/EBP $\beta$ , PGC-1 $\alpha$  and PRDM16) of brown adipocyte differentiation and ZIC1 was enhanced by a bolus dose of BMP7 in undifferentiated preadipocytes or in white fat cells (**Figure 19**).

#### **5.6. Clozapine enhances “beige” potential of human adipocytes via inhibiting 5HT-receptor mediated signaling**

As a next step, we intended to examine the gene expression changes underlying the browning effect of clozapine by RT-qPCR. Therefore, differentiating white adipocytes were treated with clozapine on the last 2 and 4 days or during the whole differentiation process at a dose comparable to its therapeutic plasma concentration [333]. We found that UCP1 was expressed 5-fold higher at mRNA level as a result of clozapine administration in each case. In line with the upregulation of UCP1 gene, significantly elevated expression of CIDEA, CYC1, ELOVL3 and PGC-1 $\alpha$  was found compared to white adipocytes. The expression of PRDM16 was not changed by *ex vivo* clozapine treatment. However, the white protocol and clozapine treatment was less effective (but still significant as compared to white adipocytes) in the induction of brown and “beige”-related genes than the browning protocol described in the section 5.1 (**Figure 20**).

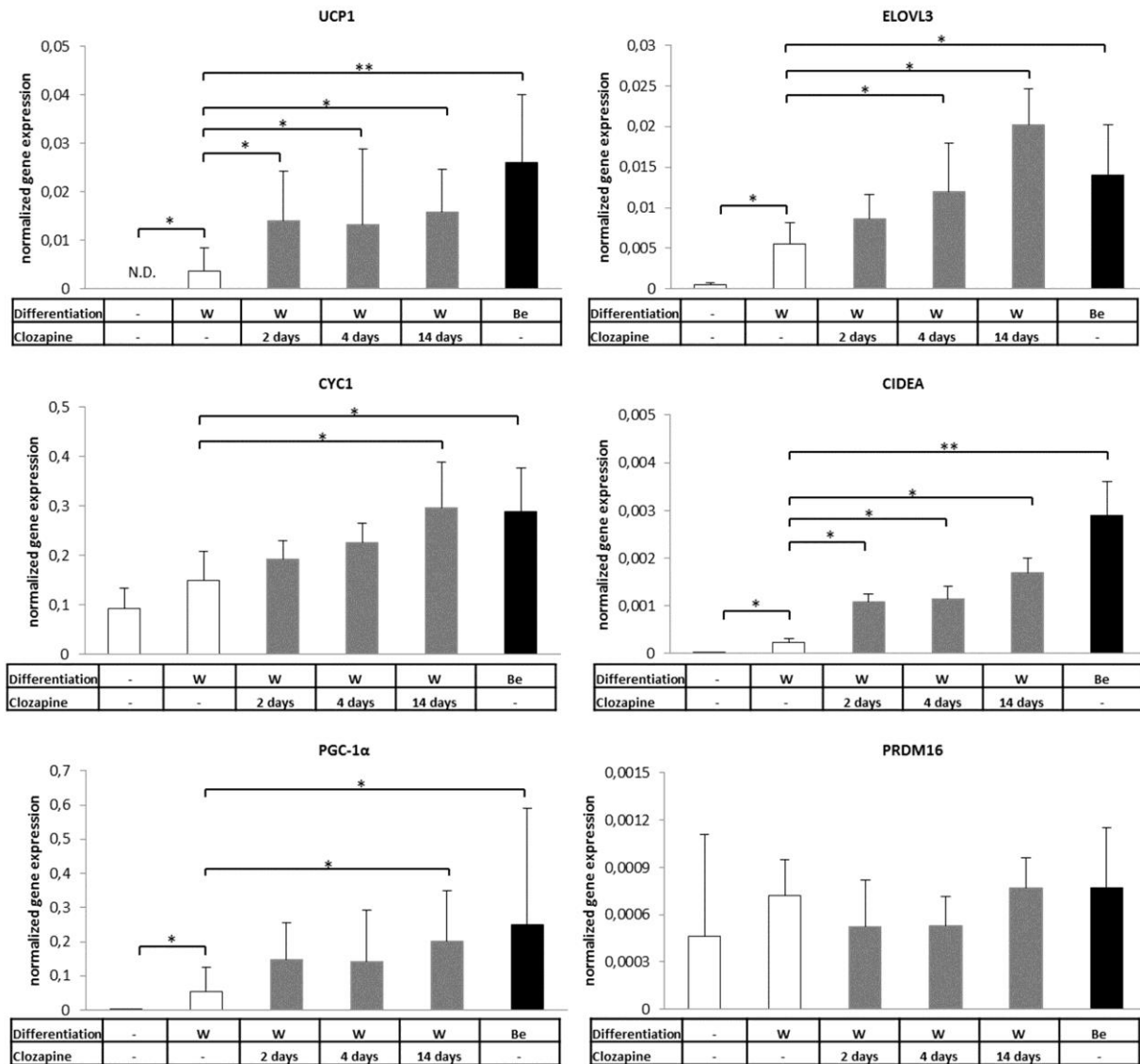


**Figure 20.** Normalized expression of browning markers in primary human adipocytes as a result of clozapine treatment during ex vivo white or “beige” adipocyte differentiation. SVF derived ADMSCs were differentiated for two weeks to white (W) or “beige” (Be) adipocytes. 100 ng/mL clozapine (grey bars) was administered on the last 2 and 4 days or during the whole white adipogenic differentiation process. (Gene expression was determined by RT-qPCR, target genes were normalized to GAPDH) For multiple comparisons of groups statistical significance was evaluated by one-way ANOVA followed by Tukey post-hoc test.  $n=6$ ,  $*p<0.05$ ,  $**p<0.01$ .

Furthermore, clozapine treatment moderately induced the expression of beta-oxidation related mitochondrial genes (ACOX2, CPT1A, CPT2 and ACADM) (**Figure 21**). On the other hand, C/EBP $\beta$ , C/EBP $\alpha$ , FABP4, LEPTIN and PPAR $\gamma$  genes were expressed at the same level in adipocytes differentiated in the presence of clozapine compared to the untreated ones (**Figure 22**).

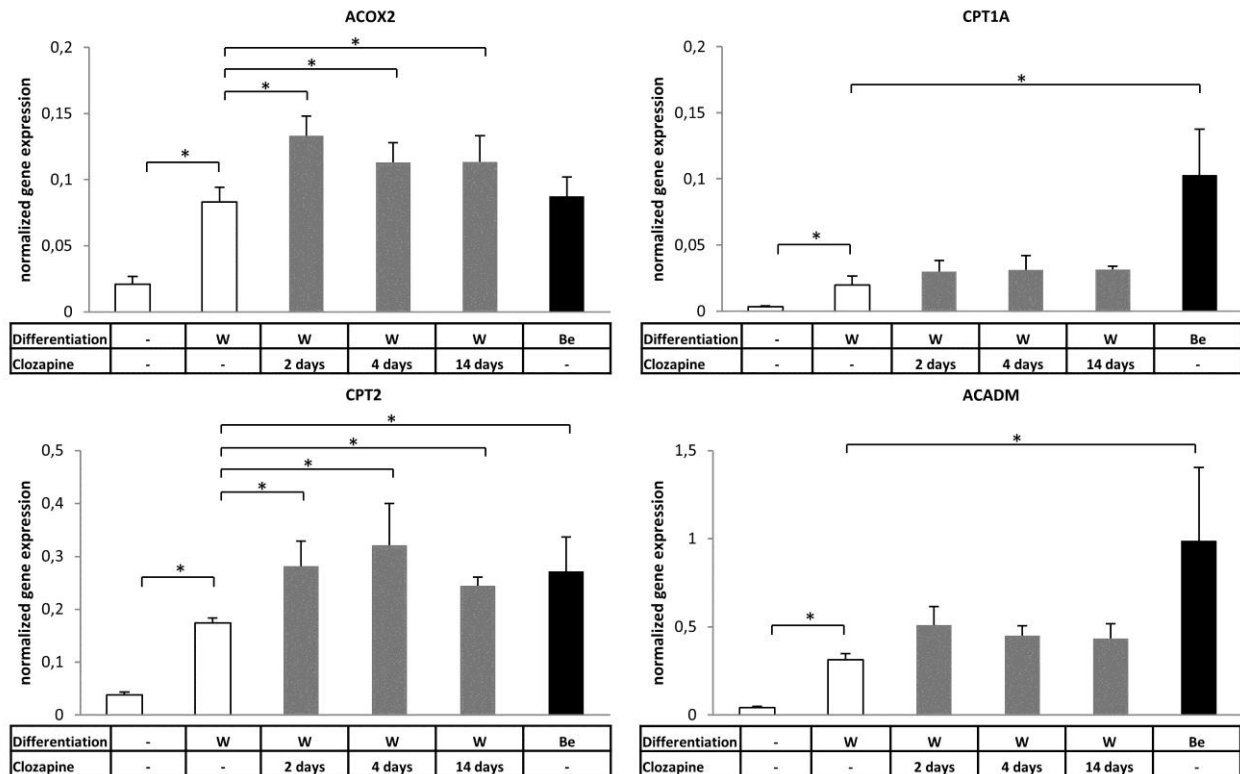


**Figure 21.** Normalized expression of beta-oxidation related genes in primary human adipocytes as a result of clozapine treatment during *ex vivo* white or “beige” adipocyte differentiation. SVF derived ADMSCs were differentiated and treated as in Figure 20. (Gene expression was determined by RT-qPCR, target genes were normalized to GAPDH) For multiple comparisons of groups statistical significance was evaluated by one-way ANOVA followed by Tukey post-hoc test.  $n=4$ ,  $*p<0.05$ .



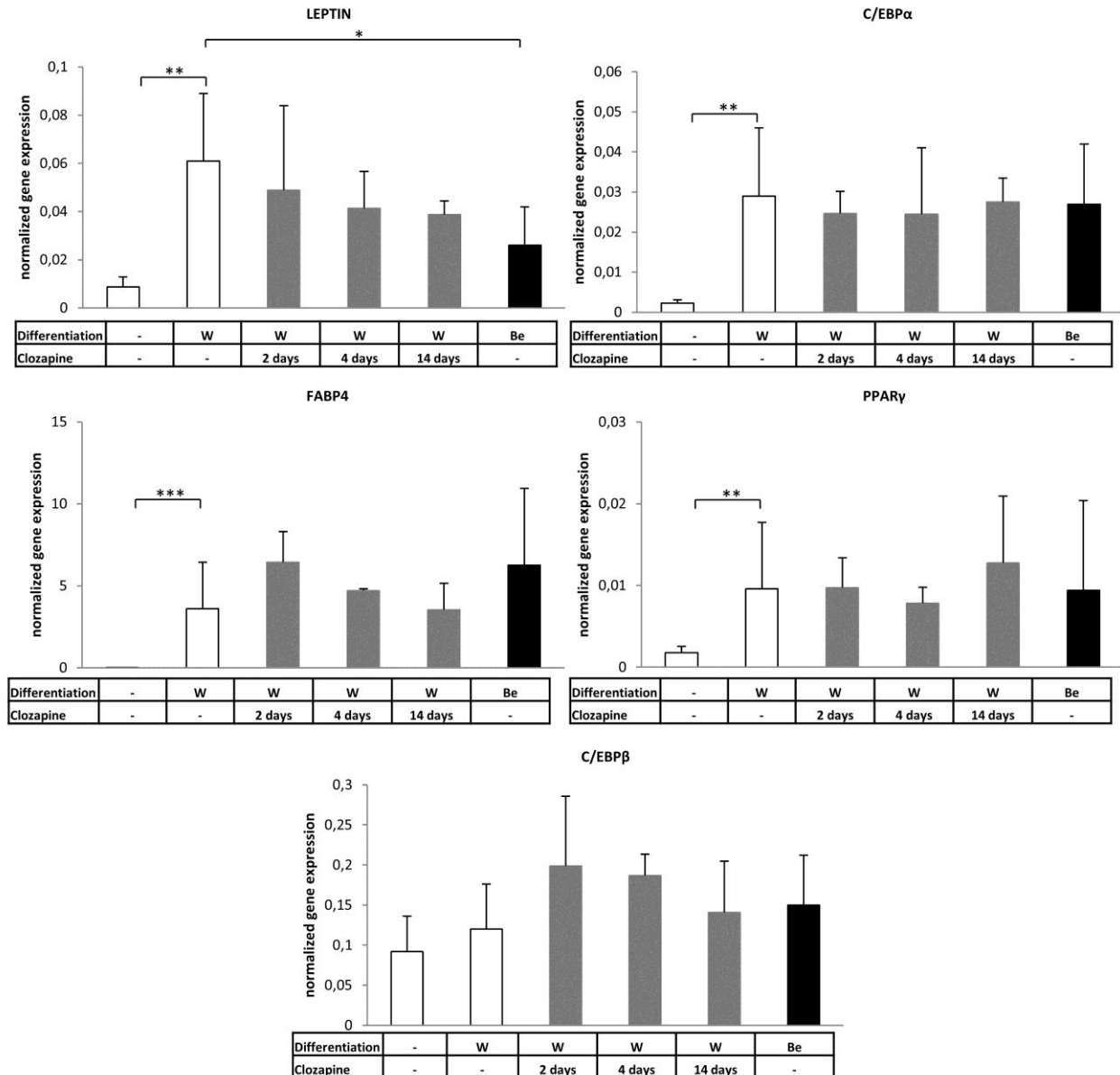


**Figure 22.** Normalized expression of general adipogenic marker genes in primary human adipocytes as a result of clozapine treatment during *ex vivo* white or “beige” adipocyte differentiation. SVF derived ADMSCs were differentiated and treated as in Figure 20-21. (Gene expression was determined by RT-qPCR, target genes were normalized to GAPDH) For multiple comparisons of groups statistical significance was evaluated by one-way ANOVA followed by Tukey post-hoc test.  $n=6$ ,  $*p<0.05$ ,  $**p<0.01$ ,  $***p<0.001$ .

The expression of ZIC1 remained at a low level after clozapine administration excluding that clozapine induces a “classical brown” adipocyte phenotype. Contrarily, the “beige” indicator TBX1 was upregulated when we applied clozapine on top of the white adipogenic protocol suggesting that the drug could shift the adipocyte differentiation towards browning, with gene expression changes indicating the “beige” program (**Figure 23**). Dose-response curves which show the concentration dependent browning effect of clozapine are displayed in **Figure 24**.

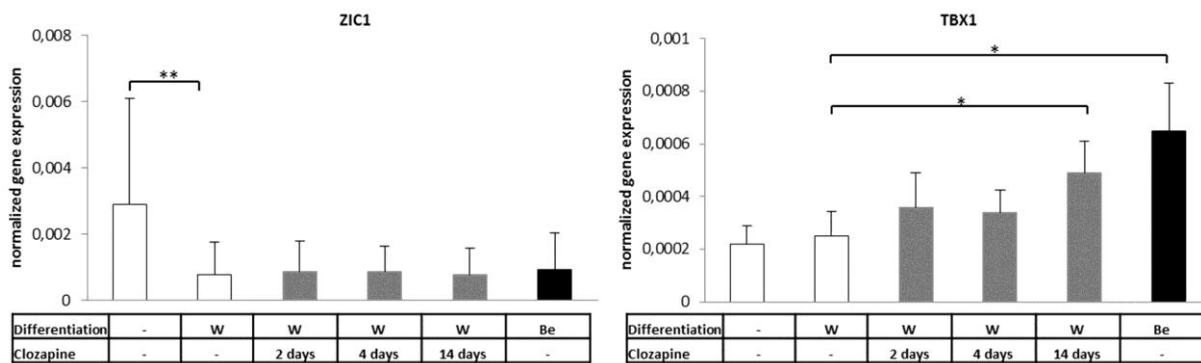


**Figure 23.** Normalized expression of classical brown and “beige”-selective genes in primary human adipocytes as a result of clozapine treatment during *ex vivo* white or “beige” adipocyte differentiation. SVF derived ADMSCs were differentiated and treated as in Figure 20-22. (Gene expression was determined by RT-qPCR, target genes were normalized to GAPDH) For multiple comparisons of groups statistical significance was evaluated by one-way ANOVA followed by Tukey post-hoc test.  $n=6$ ,  $*p<0.05$ ,  $**p<0.01$ .

When we investigated how short-term administration of clozapine affected the gene expression patterns of undifferentiated progenitors or completely differentiated white or “beige” adipocytes, we could not detect a significant response (except for the slight upregulation of TBX1 in differentiated “beige” adipocytes) to the 12-hour-long drug treatment (**Figure 25**).

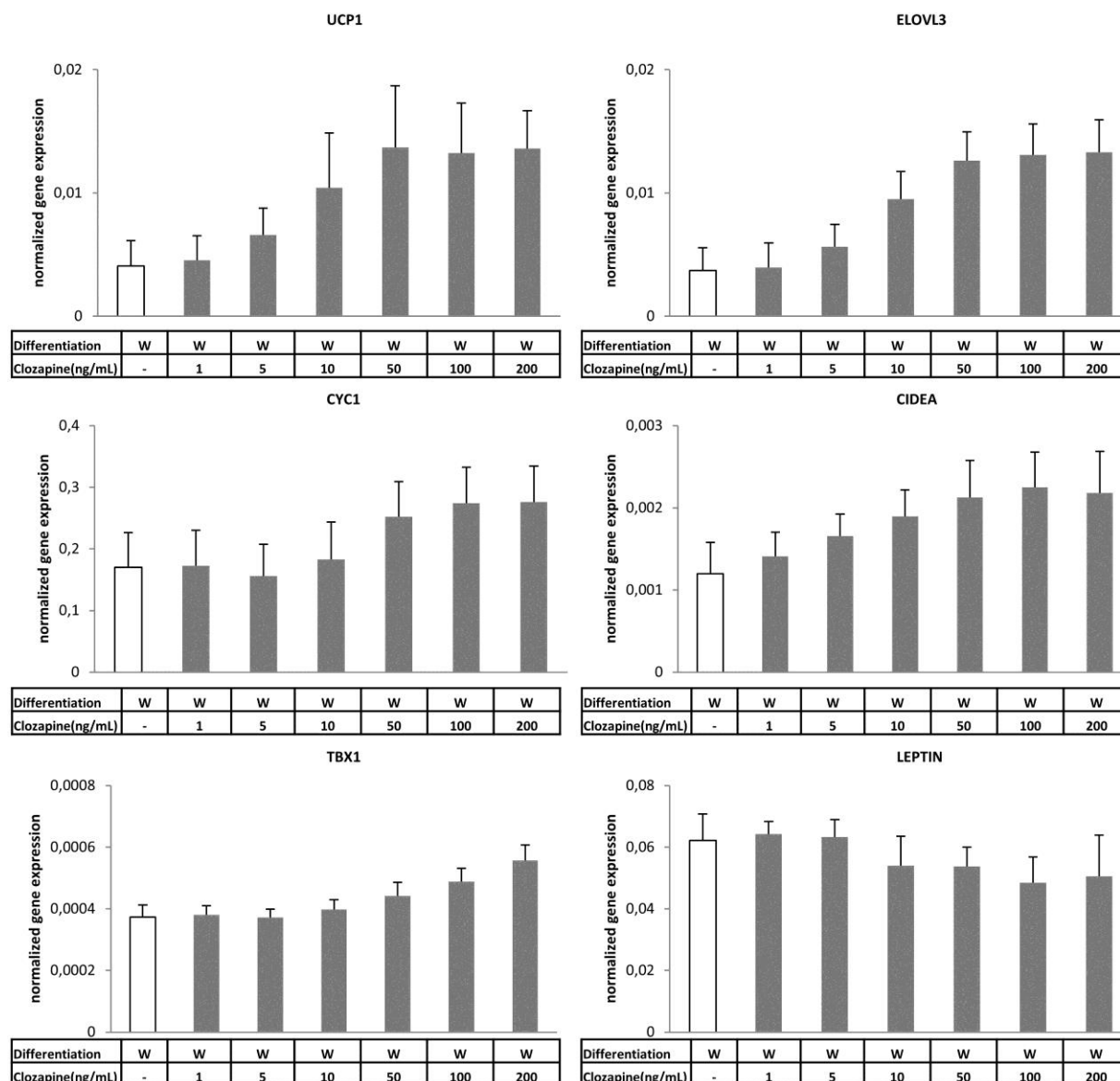


**Figure 24.** Dose dependence of clozapine treatment during ex vivo white adipocyte differentiation on the expression of browning and adipogenic marker genes in primary human adipocytes. SVF was differentiated for two weeks to white (W) adipocytes. 1-200 ng/mL clozapine (grey bars) was administered during the whole white adipogenic differentiation process. (Gene expression was determined by RT-qPCR, target genes were normalized to GAPDH); n=3.

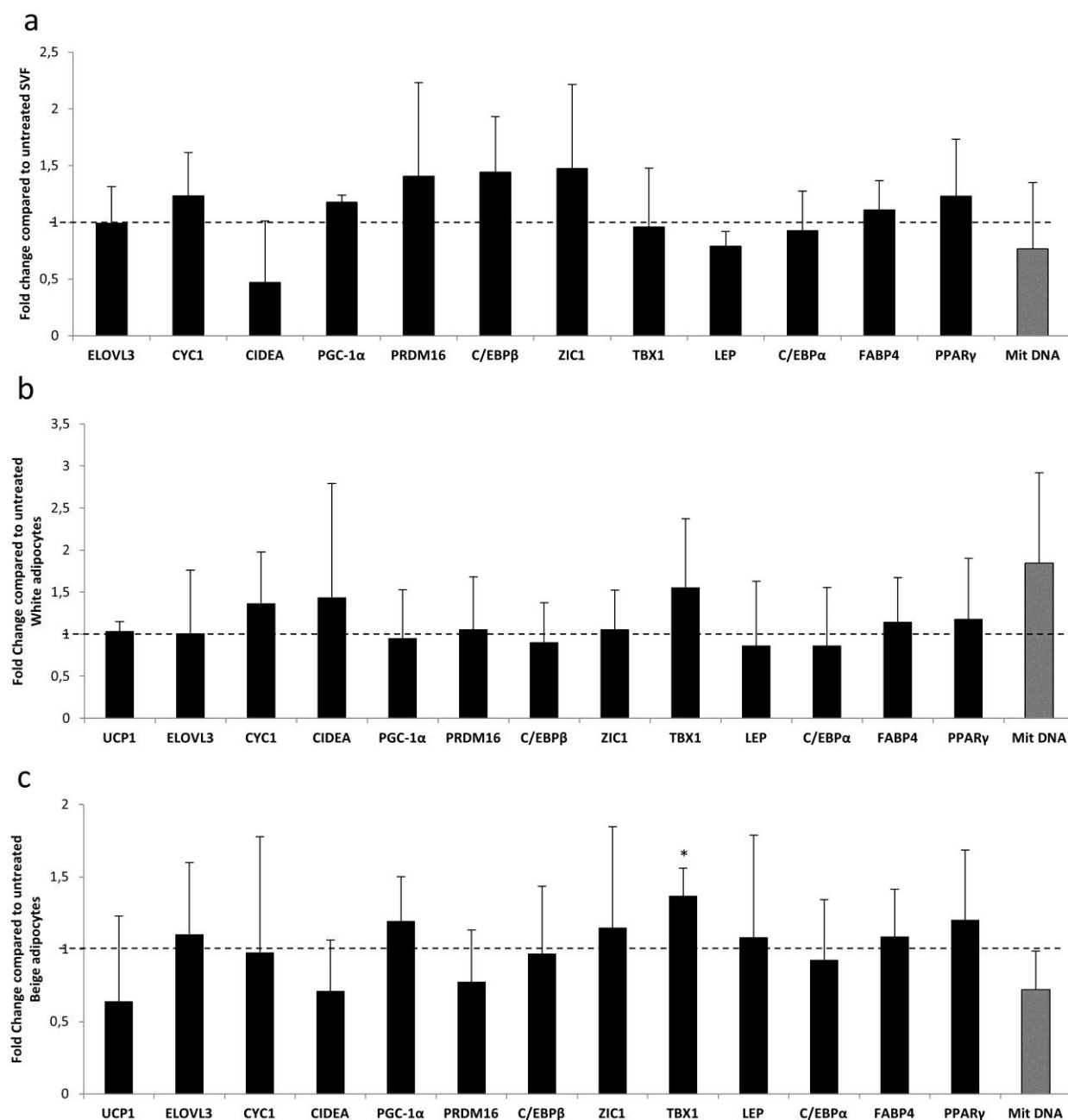


**Figure 25.** Effect of short-term clozapine treatment on the expression of selected adipocyte marker genes and amount of mitochondrial DNA in primary human SVF, white and “beige” adipocytes (as compared to untreated cells). 100 ng/mL clozapine was administered for 12 hours to undifferentiated SVF (**a**) or to fully differentiated white (**b**) or “beige” (**c**) adipocytes.  $n=4$ ,  $*p<0.05$  (The expression of UCP1 could not be detected in SVF).

Next, we wanted to learn if Ucp1 was upregulated at protein level in adipocytes that were differentiated in the presence of clozapine. In the collected whole cell lysates we found a 3-fold elevated Ucp1 protein level compared to the untreated cells (**Figure 26**). Thus, the induction of a “beige”-like gene expression pattern by direct clozapine administration during human white adipocyte differentiation was corroborated with the increased amount of Ucp1 protein.

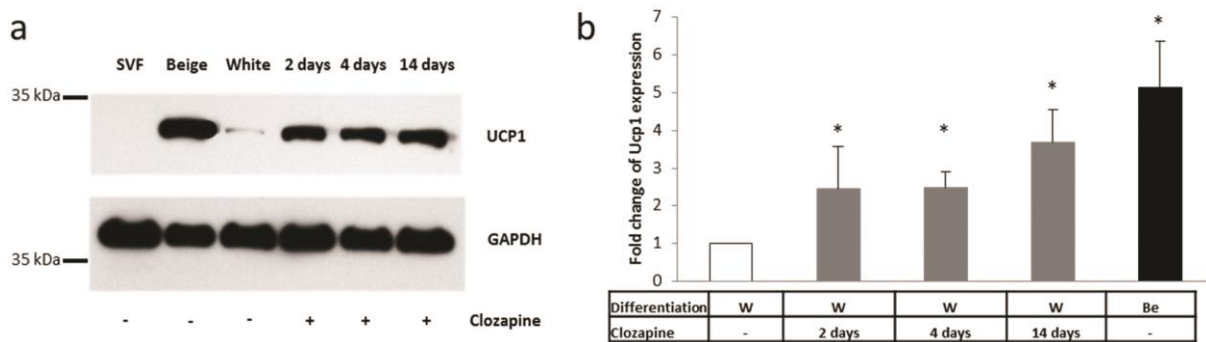


**Figure 26.** UCP1 protein expression in primary human adipocytes as a result of clozapine treatment during *ex vivo* white or “beige” adipocyte differentiation. SVF derived ADMSCs were differentiated and treated as in Figure 20-23. **(a)** Ucp1 protein expression in one representative adipocyte donor detected by immunoblotting. **(b)** Protein expression level of Ucp1 in the adipocytes of 3 different SVF donors quantified by densitometry (as compared to untreated white adipocytes). For comparison of two groups statistical significance was evaluated by Student’s *t*-test. \* $p < 0.05$ .

To obtain mechanistic data, we tested if browning induced by clozapine can be explained by its known pharmacological effect of antagonizing 5HT receptors. The expression of Tryptophan Hydroxylase 1 (TPH1), encoding the enzyme which catalyzes the rate-limiting step of 5HT synthesis, was detectable in hADMSCs and did not change as a result of white adipocyte differentiation, suggesting that these cells are capable of autonomously generating and secreting

5HT during adipogenesis. However, we found reduced TPH1 expression in clozapine treated and in “beige” adipocytes. In addition, we found that browning cells expressed 5HT receptors 2A, 1D and 7 at mRNA level (**Figure 27**) and the up-regulation of browning markers by clozapine was diminished in the presence of exogenous 5HT (**Figure 28**).

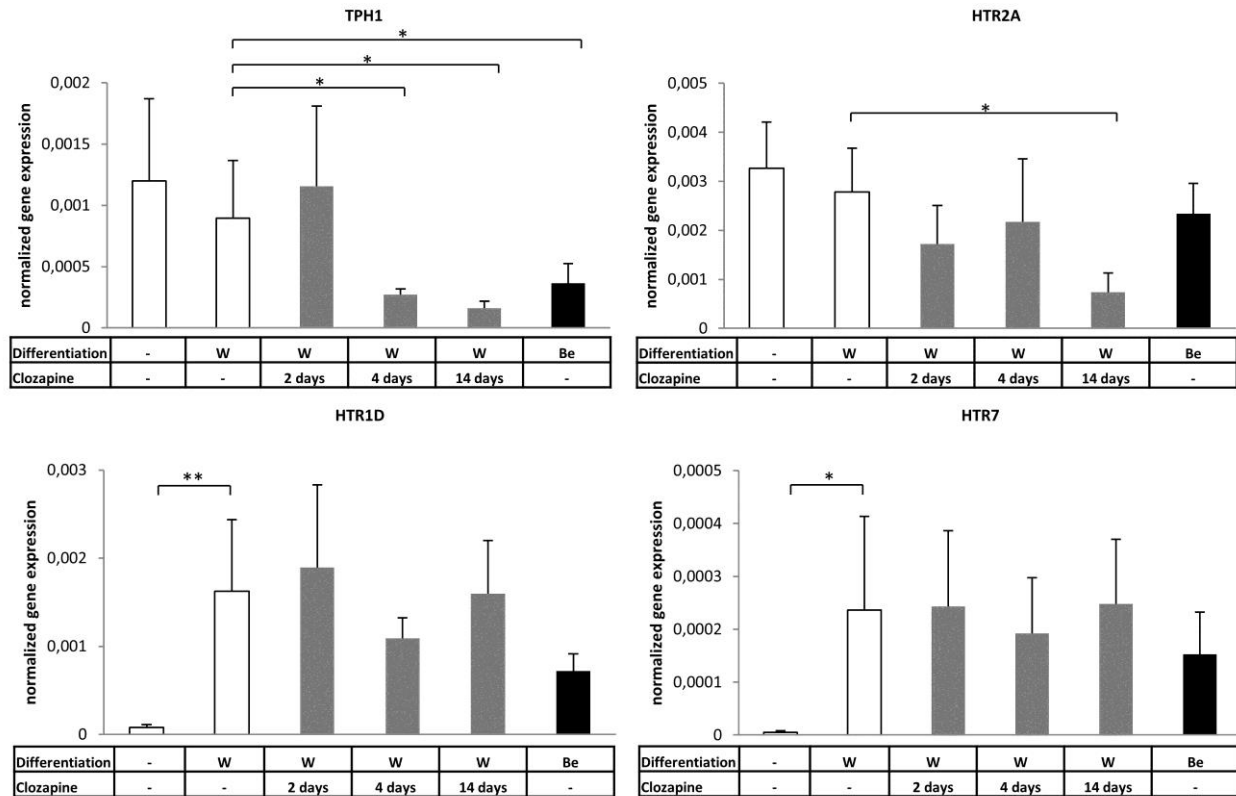


**Figure 27.** Normalized expression of Tryptophan Hydroxylase 1 and 5HT receptors in primary human adipocytes as a result of clozapine treatment during ex vivo white or “beige” adipocyte differentiation. SVF derived ADMSCs were differentiated and treated as in Figure 20-23. (Gene expression was determined by RT-qPCR, target genes were normalized to GAPDH) For multiple comparisons of groups statistical significance was evaluated by one-way ANOVA followed by Tukey post-hoc test.  $n=5$ ,  $*p<0.05$ ,  $**p<0.01$ .

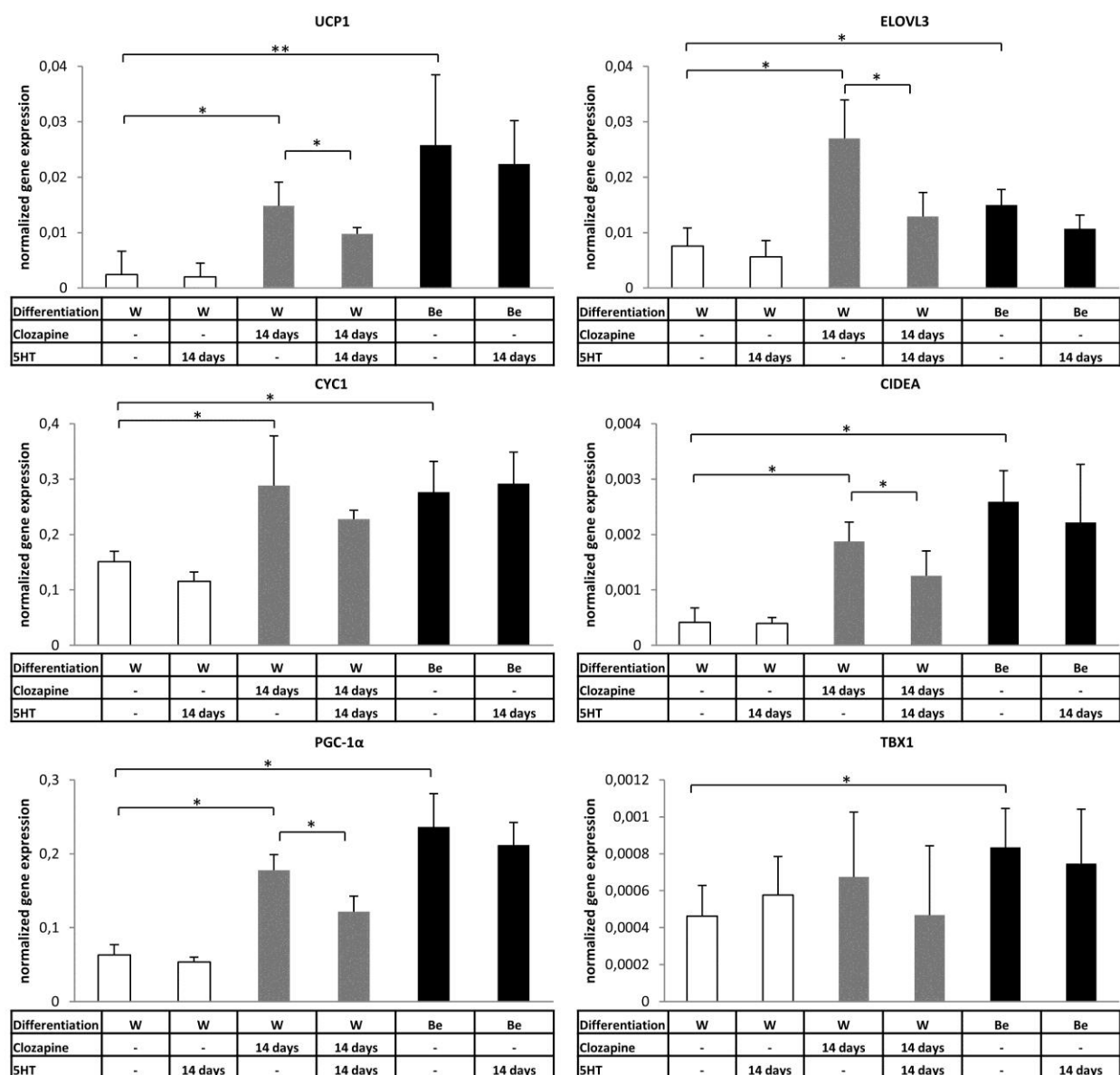


**Figure 28.** Effect of 5HT on the induction of browning marker genes in ex vivo differentiated primary human adipocytes treated with clozapine. SVF was differentiated for two weeks to white (W) or positive control “beige” (Be) adipocytes. 100 ng/mL clozapine (grey bars) and/or 10  $\mu$ M 5HT was administered on the last 2 and 4 days or during the whole adipogenic differentiation process. (Gene expression was determined by RT-qPCR, target genes were normalized to GAPDH) For multiple comparisons of groups statistical significance was evaluated by one-way ANOVA followed by Tukey post-hoc test.  $n=5$ ,  $*p<0.05$ ,  $**p<0.01$ .

The expression of classical brown, white and general adipogenic markers was not changed as a result of 5HT administration (**Figure 29**).

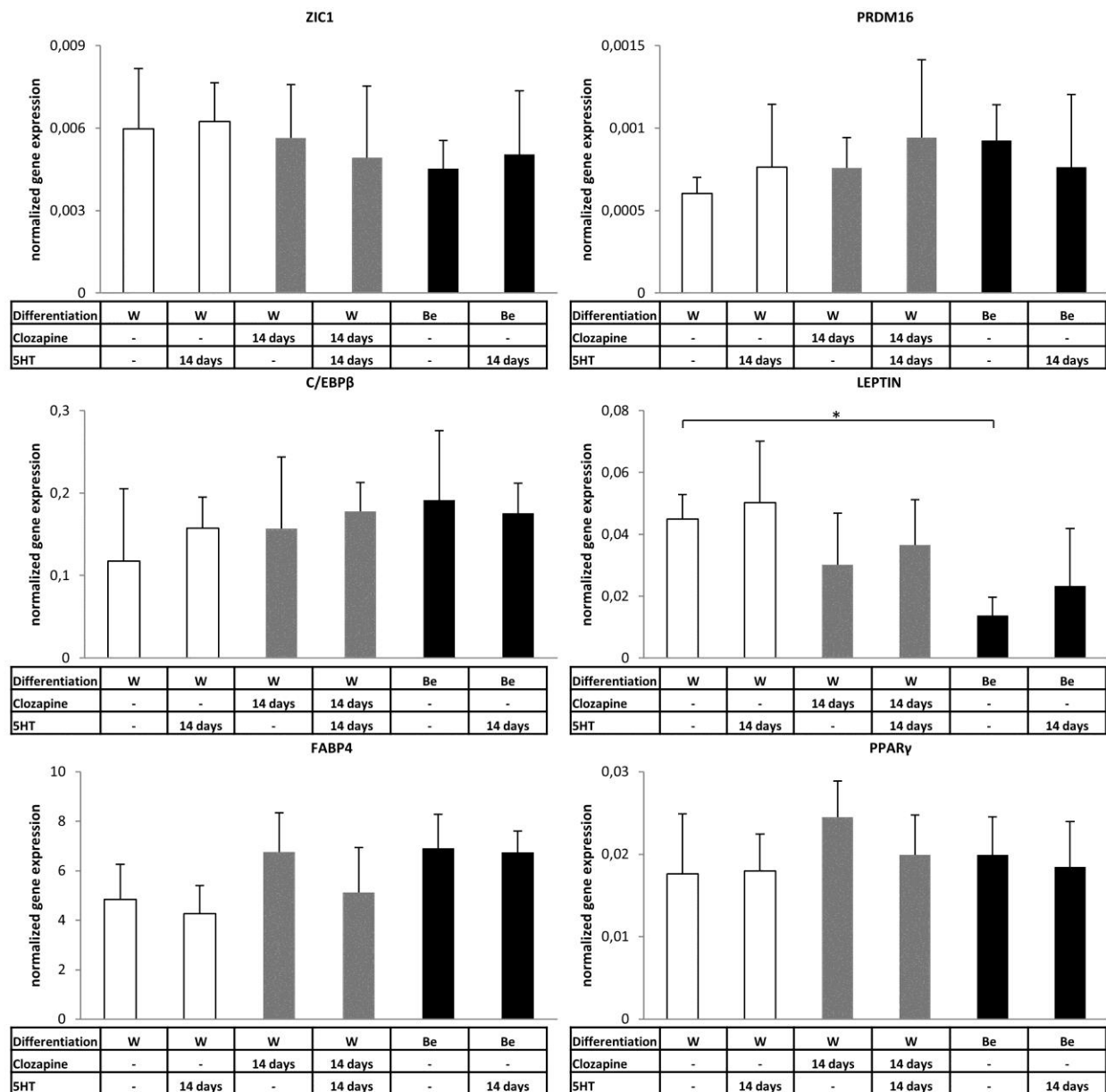


**Figure 29.** Effect of 5HT on the induction of selected adipogenic marker genes in ex vivo differentiated primary human adipocytes treated with clozapine. SVF derived ADMSCs were differentiated and treated as in Figure 28. (Gene expression was determined by RT-qPCR, target genes were normalized to GAPDH)  $n=5$ ,  $*p<0.05$ .



Out of the 5HT-receptors, HTR2A was expressed at the highest level in hADMSCs and in differentiated adipocytes. Interestingly, long-term clozapine administration resulted in the down-regulation of HTR2A gene (**Figure 27**). HTR2A initiates Gq signaling which was recently reported to abolish browning in mice and in human adipocytes [334]. Our data suggest that the disturbance of 5HT-production and 5HT-receptor-mediated signaling by clozapine might, at least partially, explain the browning effect of the drug described in the present dissertation.

#### **5.7. The “beige” adipogenic cocktail, irisin and BMP7 induce a functional browning program while clozapine treated adipocytes are less capable of responding to thermogenic cues**

As a next step, we intended to analyze the functional capacity of human primary adipocytes differentiated in the presence of the aforementioned browning-inducers. Irisin or BMP7 treated white adipocytes contained higher amount of mitochondrial DNA, to a similar extent as “beige” adipocytes. Clozapine treated primary adipocytes had a moderately increased mitochondrial DNA content compared to white cells but less than the adipocytes differentiated by the “beige” regimen (**Figure 30**).

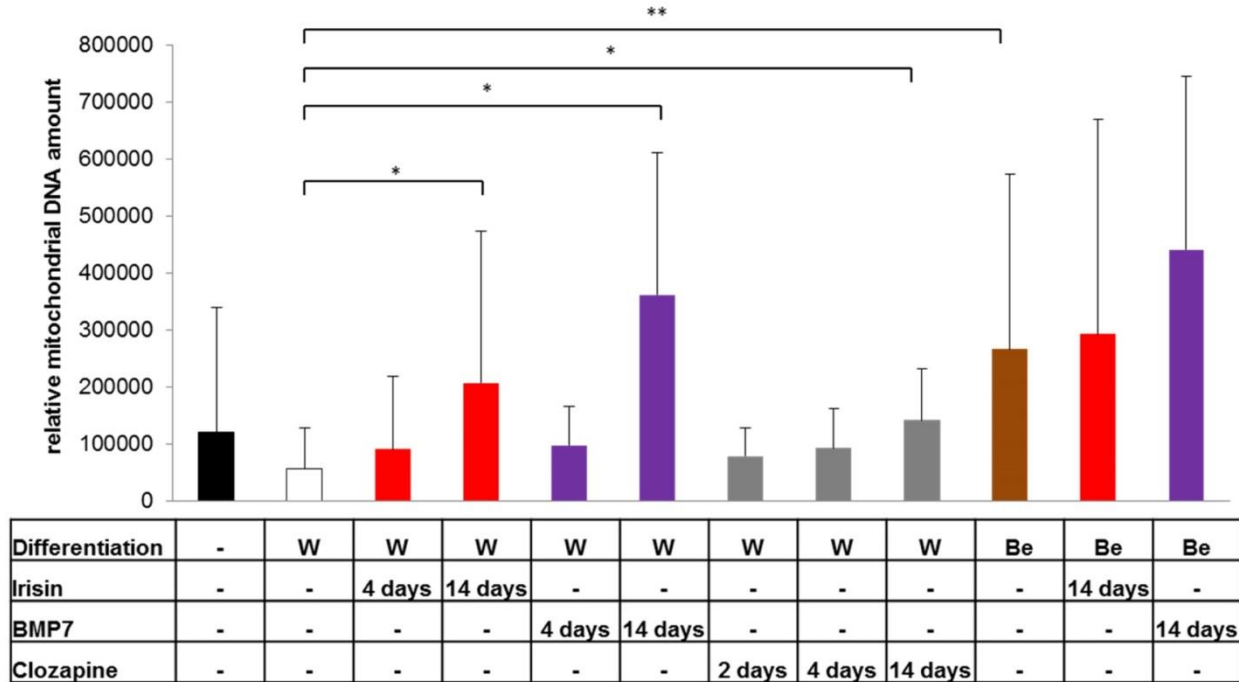


**Figure 30.** Relative mitochondrial DNA amount of *ex vivo* differentiated primary human adipocytes determined by qPCR. ADMSCs were differentiated for two weeks to white (W) or “beige” (Be) adipocytes. 250 ng/ml irisin (red bars), 50 ng/ml BMP7 (blue bars) or 100 ng/ml clozapine (grey bars) was administered on the last 2 or 4 days or during the whole differentiation process. For multiple comparisons of groups statistical significance was evaluated by one-way ANOVA followed by Tukey post-hoc test.  $n=5$ ,  $*p<0.05$ ,  $**p<0.01$ .

In accordance with the gene expression and morphological changes, *ex vivo* differentiated “beige” adipocytes had higher basal OCR than white adipocytes (**Figures 31 and 32**). Basal mitochondrial respiration of irisin (**Figure 31**) and clozapine (**Figure 32**) treated white adipocytes was also elevated as compared to the untreated white cells. The presence or absence of clozapine during the differentiation did not affect the basal OCR of “beige” adipocytes (**Figure 32**). After the cells received a single bolus dose of cell permeable dibutyryl-cAMP mimicking adrenergic stimulation, we found that adipocytes differentiated in the presence of

irisin, BMP7 or the “beige” adipogenic cocktail had significantly increased stimulated mitochondrial respiration compared to white adipocytes (**Figure 31**).

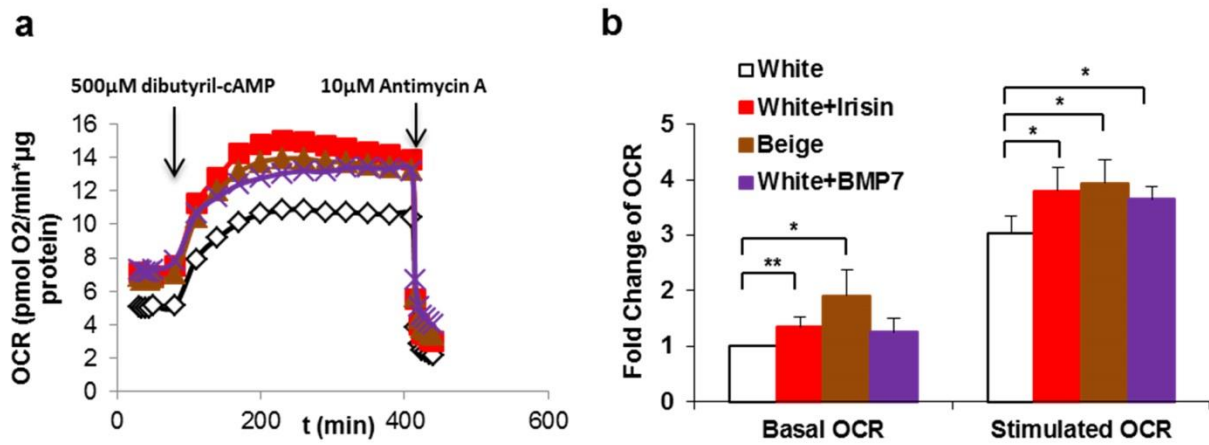


**Figure 31.** Functional analysis of ex vivo differentiated primary adipocytes treated with irisin or BMP7. (a) OC of one representative ADMSC derived adipocyte donor measured by an XF96 oxymeter. After recording the baseline OC, cells received a single bolus dose of dibutyryl-cAMP (500  $\mu$ M final concentration) modelling adrenergic stimulation. Then, stimulated OC was recorded every 30 min. The OCR was normalized to protein content and normalized readings were displayed. (b) Basal and stimulated OC level (as compared to basal OCR of white adipocytes) of adipocytes. Results are expressed as the mean  $\pm$  SD for the number of assays (adipocytes of 3 different SVF donors) indicated. For multiple comparisons of groups statistical significance was evaluated by one-way ANOVA followed by Tukey post-hoc test. \* $p < 0.05$ , \*\* $p < 0.01$

However, adipocytes that were differentiated in the presence of clozapine were less capable than the untreated cells to induce their respiration. At the maximal level of induced respiration, the difference in OCR demonstrated at basal level between clozapine treated and untreated white adipocytes was abolished (**Figure 32**).

ATP synthase activity was inhibited after adding oligomycin at 2  $\mu$ M concentration to detect proton leak respiration. Both basal and cAMP stimulated proton leak OCRs were significantly higher in “beige” than in white adipocytes. In the case of clozapine induced browning adipocytes elevated proton leak respiration could be only detected in basal conditions (**Figure 32**).

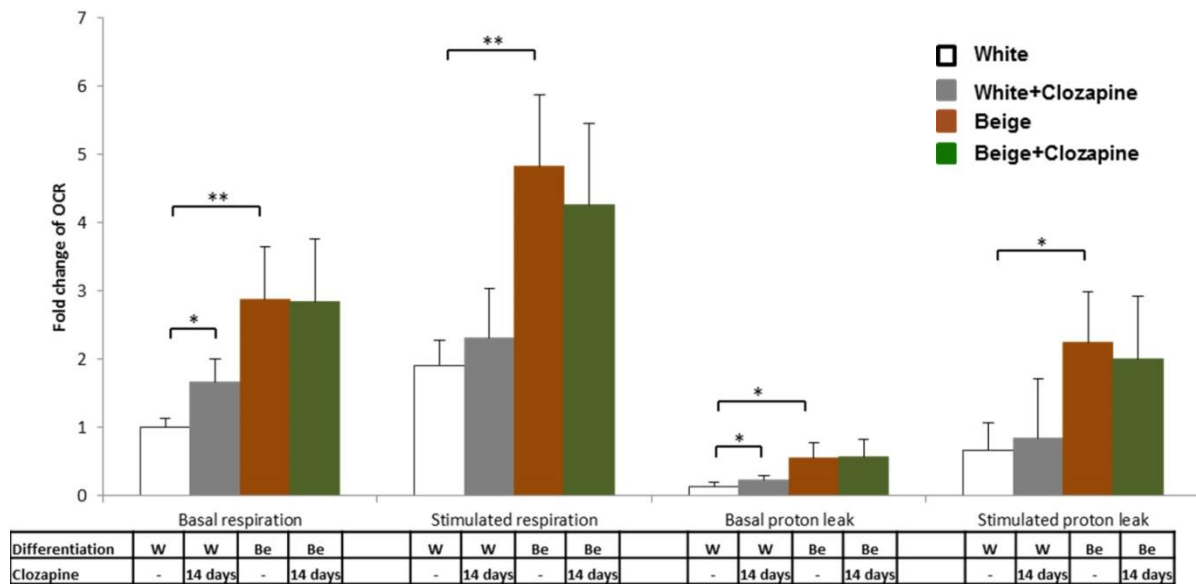


**Figure 32.** Functional analysis of *ex vivo* differentiated primary adipocytes treated with clozapine. Basal, cAMP stimulated and oligomycin inhibited oxygen consumption levels (as compared to basal OCR of white adipocytes) in 4 different SVF derived adipocyte donors. SVF derived ADMSCs were differentiated for two weeks to white (W) or “beige” (Be) adipocytes. 100 ng/mL clozapine was administered during the whole adipogenic differentiation process. OC was measured with an XF96 oxymeter. After recording the baseline OC, cells received a single bolus dose of dibutyryl-cAMP. Proton leak respiration was determined after adding oligomycin to block ATP synthase activity. For multiple comparisons of groups statistical significance was evaluated by one-way ANOVA followed by Tukey post-hoc test. \* $p < 0.05$ , \*\* $p < 0.01$ .

We also tested the involvement of fatty acid beta-oxidation and the recently described creatine-driven substrate cycle in the metabolism of *ex vivo* differentiated adipocytes. When “beige” cells and adipocytes differentiated in the presence of clozapine were treated with etomoxir (CPT-1 inhibitor) or  $\beta$ -GPA (creatine analogue which reduces creatine levels in the cells), basal and cAMP stimulated OCRs were decreased at a higher extent than in the case of white adipocytes (**Figure 33**). Our results show that the clozapine induced browning cells, similarly to “beige” adipocytes, consume more fatty acids by beta-oxidation compared to white adipocytes and further enhance their energy expenditure by activating the futile cycle of creatine metabolism.

We also analyzed the changes in UCP1 and PGC-1 $\alpha$  expression in response to a 4 h long dibutyryl-cAMP treatment that serves as an accepted model of thermogenic induction mimicking natural anti-obesity cues [159]. In line with the results described in section 5.1, white adipocytes expressed UCP1 gene at a moderate level. Adipocytes treated with clozapine on top of the white cocktail had a significantly elevated UCP1 expression than the untreated cells. “Beige” adipocytes expressed UCP1 mRNA at an even higher level; in this case clozapine administration did not affect UCP1 expression. A similar trend was found in the case of PGC-1 $\alpha$ . UCP1 and PGC-1 $\alpha$  expression showed a robust (10 and 5-fold, respectively) upregulation in response to cAMP treatment of white and “beige” adipocytes differentiated in the absence of clozapine. This effect of thermogenic induction was less manifested in clozapine generated “beige” adipocytes, with regard to UCP1. The responsiveness of “beige” adipocytes differentiated in the presence of clozapine was also reduced (**Figure 34**). Of note, beta-oxidation and creatine-driven futile cycle was enhanced by dibutyryl-cAMP in a similar extent in clozapine induced as in “beige” adipocytes (**Figure 33**).

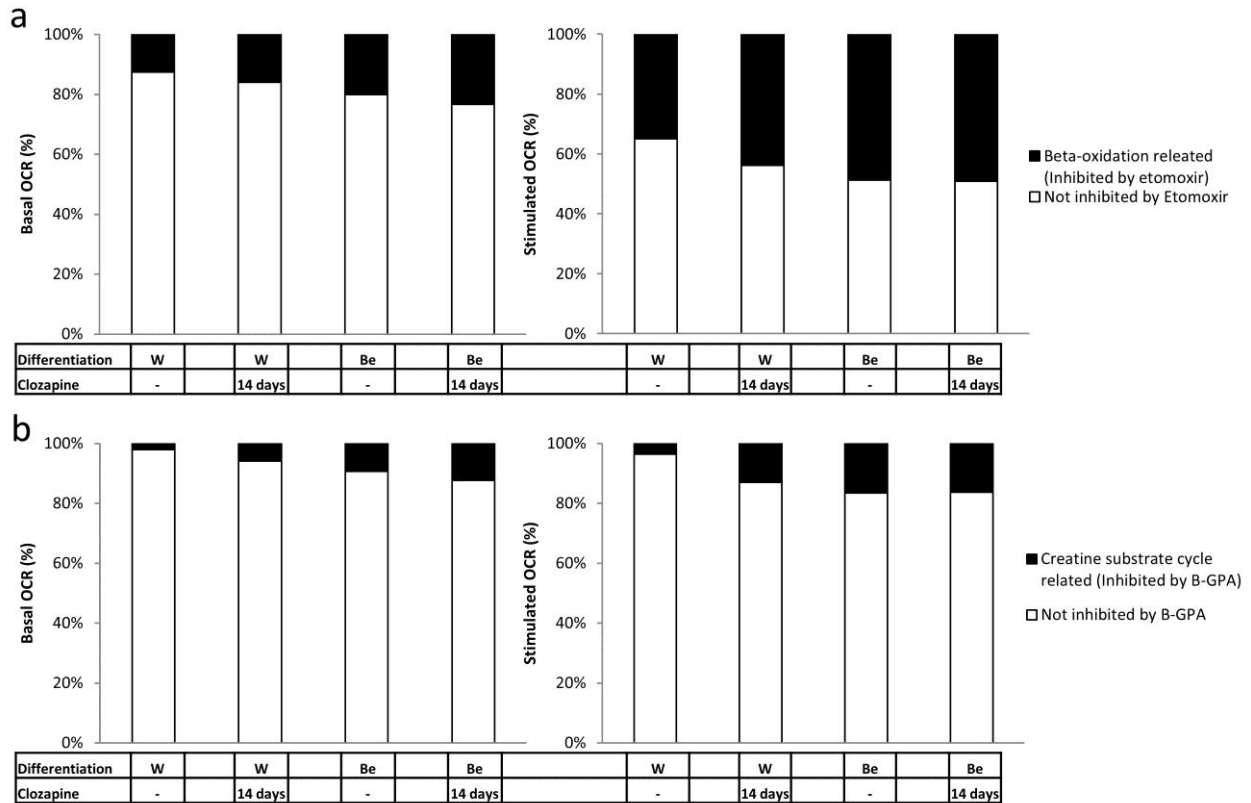


**Figure 33.** Involvement of beta-oxidation (**a**) and the creatine-driven futile cycle (**b**) in the metabolism of *ex vivo* differentiated primary adipocytes. SVF derived ADMSCs were differentiated and treated as in Figure 32. Etomoxir (5  $\mu$ M final concentration) (**a**) and  $\beta$ -GPA inhibited (2 mM final concentration) (**b**) relative OC levels (as compared to basal and cAMP stimulated OCR of each sample) measured by an XF96 oxymeter. The experiment was repeated four times with SVFs from independent healthy donors.

Our results suggest that browning induced by irisin, BMP7 or the “beige” adipogenic cocktail is coupled with enhanced mitochondrial biogenesis and elevated energy expenditure in response to thermogenic stimuli. Clozapine treatment induced the “beige” program in differentiating white adipocytes, these “masked beige” cells, however, were less capable to respond to  $\beta$ -adrenergic induction of thermogenesis.

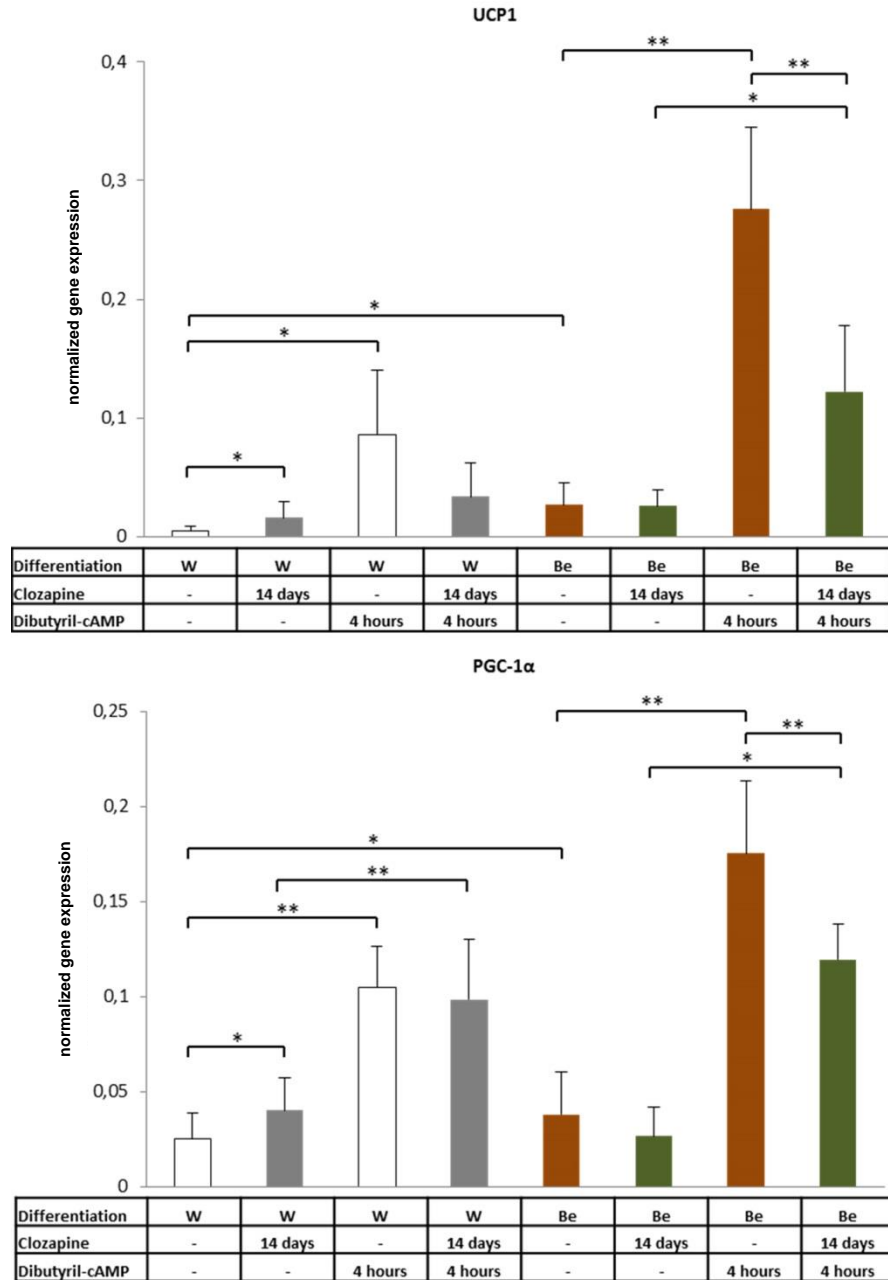


**Figure 34.** Effect of short-term cAMP treatment on the expression of UCP1 and PGC-1α genes in adipocytes that had been treated with clozapine. SVF derived ADMSCs were differentiated and treated as in Figure 32-33. Then cells received a single bolus dose of dibutyl-cAMP at 500 μM concentration modelling adrenergic stimulation. (Gene expression was determined by RT-qPCR, target genes were normalized to GAPDH) \* $p < 0.05$ , \*\* $p < 0.01$ ,  $n = 5$ .

### 5.8. Differentiating human browning adipocytes secrete cytokines (“batokines”)

Finally, we investigated the secretion of “batokines” by primary human white, brown and “beige” adipocytes. Conditioned differentiation media were collected during the regular replacement of the adipogenic cocktails and secreted IL-6, IL-8, TNF $\alpha$ , MCP-1 and IL-1 $\beta$  were measured by ELISA after samples stored on the 1<sup>st</sup> and 2<sup>nd</sup> week of differentiation were pooled. Neither hADMSCs nor differentiating adipocytes secreted TNF $\alpha$  and IL-1 $\beta$ . Interestingly, IL-6, MCP-1 and IL-8 secretion was significantly higher by “beige” compared to white adipocytes. In contrast to BMP7 administration (when “classical brown” adipocyte differentiation occurs), irisin treatment (which induced “beige” adipocyte differentiation) resulted in an increased total IL-6, MCP-1 and IL-8 production (**Figures 35 and 36**).

When we examined cytokine production in the time-course of adipocyte differentiation and therefore collected and replaced media daily we found that MCP-1 and IL-8 secretion was induced at the end of the first week of “beige” adipogenic differentiation and then declined. On the other hand, IL-6 production did not subside (**Figure 37**). Contrasting the daily measurements with the samples collected and pooled over longer periods reveals an interesting fact. While daily measurements may be expected to inform on the actual cytokine secreting activity on a given day and the pooled samples on the averaged cumulative amount of the cytokine in the milieu over a period, the two did not differ significantly either in the first or second half of the differentiation (**Figures 35-37**). This suggests that browning adipocytes quickly adjusted their production to replenish their environment in these cytokines to meet a level that was required in a particular period of their maturation.



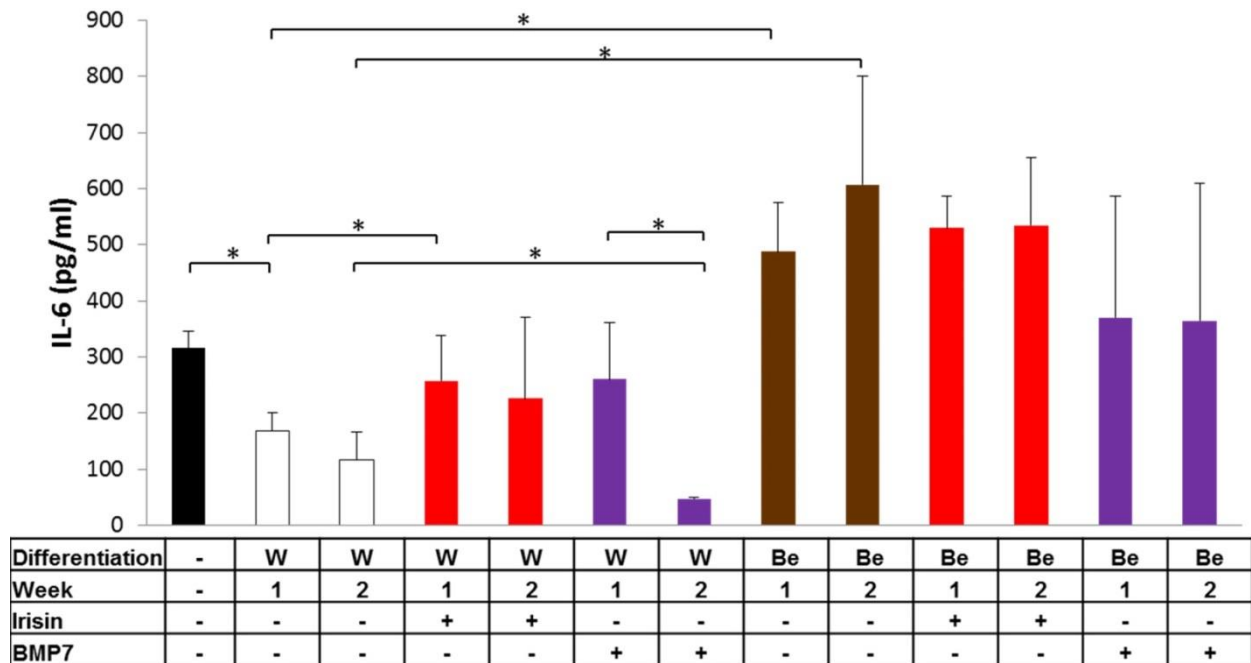


**Figure 35.** IL-6 secretion by ex vivo differentiated human adipocytes treated with irisin or BMP7. ADMSCs were differentiated for two weeks to white (W) or “beige” (Be) adipocytes. 250 ng/ml irisin (red bars) or 50 ng/ml BMP7 (blue bars) was administered during the whole differentiation process. Conditioned differentiation media were collected and pooled during the 1st and 2nd week of differentiation and secreted IL-6 was measured by sandwich ELISA. Results are expressed as the mean  $\pm$  SD for the number of assays (adipocytes of 6 different SVF donors) indicated. For multiple comparisons of groups statistical significance was evaluated by one-way ANOVA followed by Tukey post-hoc test. \* $p < 0.05$ . [Unpublished data]

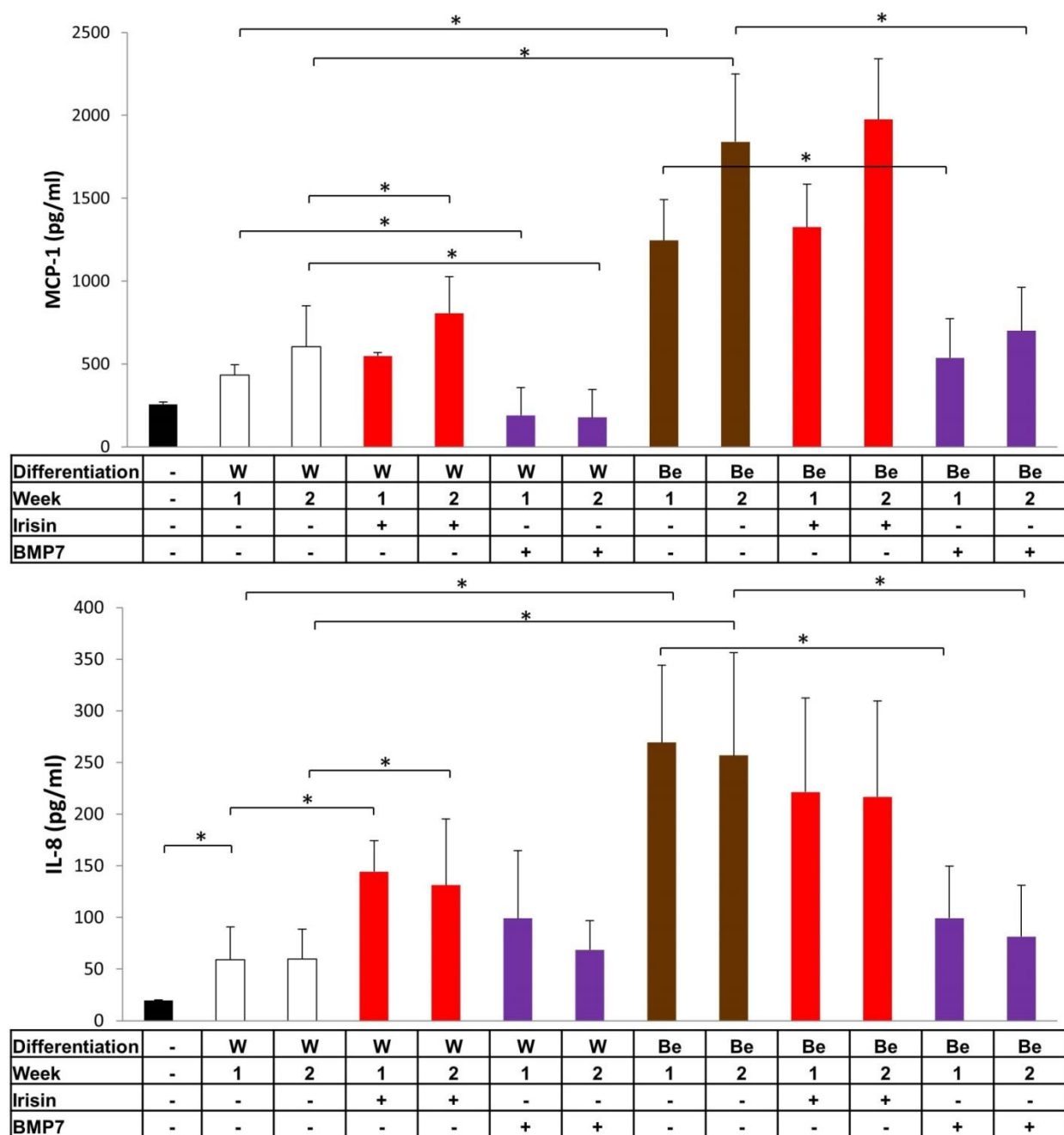


**Figure 36.** MCP-1 and IL-8 secretion by ex vivo differentiated human adipocytes treated with irisin or BMP7. SVF derived ADMSCs were differentiated and treated as in Figure 35. Results are expressed as the mean  $\pm$  SD for the number of assays (adipocytes of 6 different SVF donors) indicated. For multiple comparisons of groups statistical significance was evaluated by one-way ANOVA followed by Tukey post-hoc test. \* $p < 0.05$ . [Unpublished data]

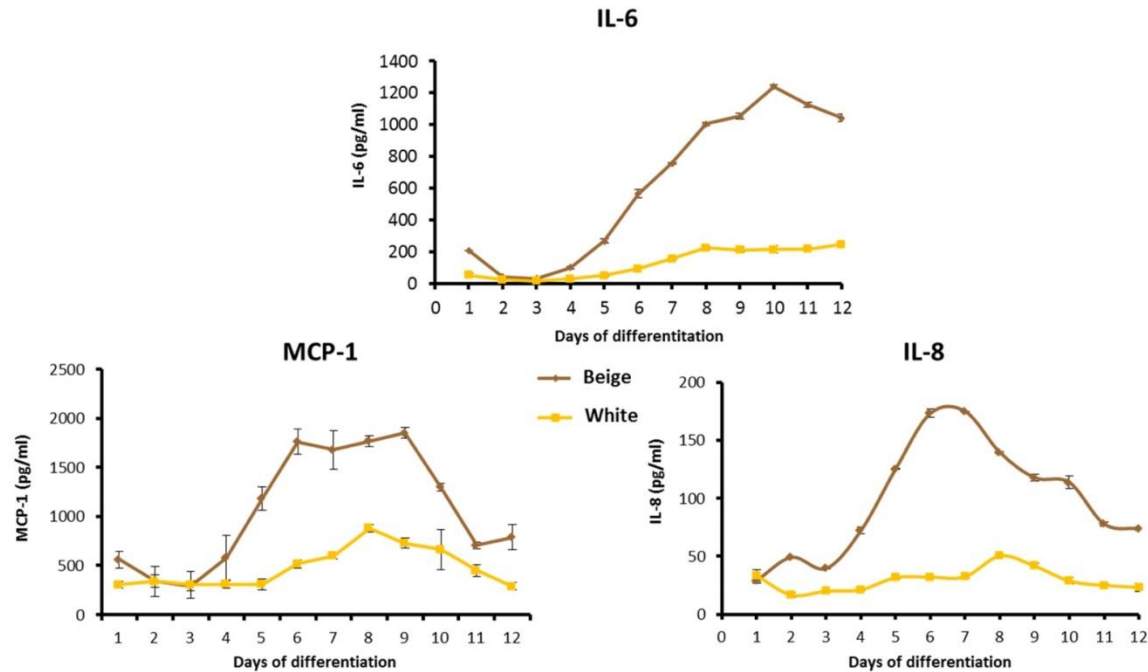


**Figure 37.** Daily cytokine production of *ex vivo* differentiated human adipocytes of one representative donor. ADMSCs were differentiated for two weeks to white (yellow lines) or “beige” (brown lines) adipocytes. Conditioned differentiation media were collected every day and secreted cytokines were measured by sandwich ELISA. SD means the experimental error of the technical replicates. [Unpublished data]

## 6. DISCUSSION

### 6.1. Methodological overview of analysis of *ex vivo* browning – an unsolved problem

Former studies focused on BAT differentiation in mouse models found that there are at least two types of thermogenic fat depots, classical brown and “beige”, which have different origins and tissue distribution. “Beige” cells are found interspersed in WAT depots as a result of cold-, diet or exercise induced thermogenesis. These induced cells express several browning marker genes and have a multilocular morphology as classical brown adipocytes (section 2.2). In parallel, the importance of BAT activity in controlling the energy homeostasis of the entire body of adult humans was shown in the past few years, highlighting a possible promising therapeutic application of BAT stimulation in the treatment of obesity and type 2 diabetes mellitus (section 2.3).

Although a protocol to induce human brown adipocyte differentiation in cell cultures was established several years ago [328], there is only limited data about regulatory networks that drive, or mediators that regulate “classical brown” or “beige” adipocyte differentiation in humans. Using cellular, in particular *ex vivo* human models, and performing population scale analysis to determine the heterogeneity of cultured and differentiated adipocytes in response to natural or artificial anti-obesity cues would be a valuable tool to understand the development of “classical brown” or “beige” adipocytes in distinct human adipose tissue depots and to validate novel findings obtained in mice.

Primarily, we aimed to optimize the aforementioned adipogenic differentiation protocol [328] to induce browning of hADMSCs cultivated from abdominal subcutaneous fat. Since populations of *ex vivo* differentiated adipocytes are heterogeneous regardless of whether white or brown

adipogenic differentiation was induced, we wished to examine human adipocyte browning not only by determining the expression of “classical brown”, “beige”, white or general adipocyte markers at the mRNA and protein levels using total cell lysates but also to specifically identify browning cells in mixed adipocyte populations according to their morphological parameters. On one hand, investigators have already successfully used flow cytometry to assess surface protein expression of human primary adipocytes or to sort out floating adipocytes from SVF cells including undifferentiated progenitors [335,336]. In spite of its analytical power, however, no concise protocol is available to identify browning adipocytes in a large population of cells by flow cytometry due to the fact that widely accepted surface markers have not been identified, and the collection of accurate morphological data (e.g. determination of the size or number of lipid droplets in single adipocytes) and the possibility to inspect adipocyte differentiation at consecutive time points are sacrificed under the experimental conditions flow cytometry requires. Furthermore, already attached adipocytes are too fragile to tolerate detachment by trypsinization before the analysis [337].

On the other hand, LSC, which combines scanning lasers, a microscope and automated image acquisition and inherits both the cytometric attributes of flow cytometry and the photographing operation of a microscope, allows automated examination of large population of cells with negligible perturbation [338-340]. Thus, LSC is not limited to analyzing cells in flowing fluids and it can perform high-content analysis of adherent cells cultured in chamber slides [341-343]. Considering the limitations of flow cytometry and the advantages of LSC, we decided to quantify *ex vivo* browning at a single cell level in a highly replicative manner by using the slide-based image cytometry approach. In our experiments, Hoechst labelled nuclei of cells were first recognized, and then cellular morphology, lipid droplet formation and Ucp1 or Cidea content of each cell were inspected simultaneously as illustrated in **Figures 8 and 11**.

## **6.2. Combined analysis of texture and Ucp1 by laser-scanning cytometry (LSC) effectively identifies browning adipocytes**

Browning adipocytes have small lipid droplets in multilocular arrangement and the highest number of mitochondria in mammalian organisms [344]. Lipid droplets can be quantified and analyzed directly by segmentation of a fluorescent signal (using Nile Red labelling for instance) [345]. However, this method showed its disadvantage in that the segmentation highly depends on the threshold algorithm as well as on the consistency of the staining. Moreover, Doan-Xuan et al. [331] showed that texture parameters were more sensitive in quantitating adipocyte differentiation or at least gave similar results compared to signals of fluorescent lipid staining. Due to possibilities of inconsistent sample preparations, different fluorescent signals among and within samples and errors in the segmentation of small objects (lipid droplets range from 1 to 40 pixels in size) we have chosen texture analysis as a reliable method to reflect the size of lipid droplets.

The idea of using texture parameters of the scatter signal stems from two roots. First, flow cytometers which were developed long time ago use the scatter signals of cells to be able to recognize cellular events reliably [346]. This is a very sensitive parameter and all, even unstained cells, can be detected based on their scatter signals. Furthermore, in flow cytometry a specific scatter parameter, the side scatter was recognized as a valuable parameter; and has been used to analyze and isolate fat cells based on their internal complexity [347]. This was quite similar to how blood cells can be distinguished by flow cytometry based on their internal complexity [348]. The second idea is that in LSC scatter signals are still measured sensitively, but here the side scatter parameter is missing. This is based on the nature of the measurement, hence we cannot detect light scatter in the plane of the glass slide. But replacing the side scatter of flow cytometry with the sensitive measurement of the interference pattern of forward scattered, refracted and

unchanged photons by imaging cytometry, lead us to the texture parameters of scatter signals to evaluate complexity of unstained samples [332].

In our model, not only texture parameters but also the expression of major browning marker proteins was detected at the same time in single adipocytes following the immunostaining against Ucp1 or Cidea. Then we plotted Ucp1 immunofluorescence intensity and texture SV for each differentiated adipocyte (**Figures 12-14**). Browning adipocytes were identified as the ones that contained small lipid droplets and high levels of Ucp1 protein (lower right quadrant of density plot images), in contrast to white adipocytes, which accumulated larger lipid droplets and expressed low amount of browning marker proteins (upper left quadrant of density plot images). With these combined approaches, we found that human ADMSCs from abdominal subcutaneous fat can be differentiated into “beige” adipocytes *ex vivo*. On one hand, we observed that after two weeks of differentiation 30-50% of the cells accumulated lipids and out of those 15-30%, depending on individual donors, had the characteristic morphological features of browning even in response to the white adipogenic cocktail. Most probably already committed “beige” precursors, which could not be differentiated into white adipocytes even in the presence of a white protocol, can be found in a significant amount in the SVFs isolated from subcutaneous WAT. Moreover, 30-70% of the differentiated adipocytes appeared as browning cells when they were differentiated by the browning cocktail. This regimen developed by Elabd et al. [328] was described originally as a brown adipocyte differentiation protocol and indeed resulted in a high expression level of browning markers, more mitochondrial DNA and elevated OC. On the other hand, we showed that these changes correspond more to a “beige” rather than a “classical brown” program, inasmuch as the “beige”-specific TBX1 was induced without the up-regulation of ZIC1. Since then, it has also been shown by gene expression and texture analyses that this protocol

effectively induced “beige”-like differentiation of progenitors isolated from human pericardial fat [349].

The observed shift in the mixed adipocyte populations indicates that the browning cocktail (long-term rosiglitazone treatment), most probably, induces the commitment of multi- or bipotent human mesenchymal progenitor cells to “beige” adipocytes at some point during the differentiation. The proportion of anti-obesity “beige” and lipid-storing white adipocytes (which fundamentally defines the thermogenic competency of each individual) is determined, at least partially, when mesenchymal progenitors are committed into white or “beige” preadipocyte subtypes from which mature fat cells are differentiated [96,130,131,135]. A key transcriptional machinery regulating this process was identified by Claussnitzer et al. [131] (introduced in detail in section 2.2). In this study, it was also described that carriers of a common risk-allele of the FTO locus fail to repress a mesenchymal super enhancer, and its targets leading to reduced energy expenditure by “beige” fat thermogenesis and to increased lipid storage in white adipocytes. Furthermore these results strengthen the hypothesis that “beige” adipocytes originate from distinct precursors. Another study showed that “beige” adipocyte progenitors can be found in association with expanding capillary networks in human fat biopsies and proliferate rapidly in response to pro-angiogenic factors [216]. We believe that these cells exist in the SVF isolated from subcutaneous WAT specimens and their differentiation can be followed in a time dependent manner by LSC.

In summary, we showed that LSC is a tool, which in combination with gene expression measurements of widely accepted adipocyte markers makes effective population scale analysis of *ex vivo* human brown or „beige” adipogenic differentiation possible. This method can help researchers to clarify how endogenous mediators or exogenous drugs affect human adipocyte browning directly. In our experiments, we validated mouse data in human samples demonstrating



the effectiveness of irisin and BMP7 to induce browning of subcutaneous white adipocytes. Using this method we also demonstrated that clozapine could shift the adipogenic differentiation program towards browning. Next, we are planning to investigate whether SVFs isolated from distinct fat depots which originate from different anatomical sites have different potentials to induce a browning program. In the future, this technique might allow to test the propensity of hADMSCs of each individual to differentiate into heat-generating brown or “beige” cells (thermogenic competency) or to sort out homogeneously differentiated hADMSC populations not only providing the possibility to understand the differences between “classical brown” or “beige” differentiation pathways in humans but also to “engineer” thermogenically active, transplantable browning adipocytes, as it was proposed by Min et al. recently [216], to aid weight reduction in obese individuals.

### **6.3. Gene expression pattern and “batokine” secretion distinguish irisin and BMP7 induced browning**

When human adipocytes were differentiated either in the presence of irisin, BMP7 or clozapine on top of the white adipogenic cocktail, similar morphological alterations were found. The simultaneous gene expression changes and functional consequences, however, were markedly different. In line with previous results obtained in mice [113], irisin induced a gene expression pattern which indicated the “beige” program (**Figure 17**). Irisin treated cells had more mitochondrial DNA and higher basal mitochondrial respiration than white adipocytes and responded robustly to dibutyryl-cAMP administration (**Figure 31**). Moreover, irisin treatment had an enhancing effect on IL-6, MCP-1 and IL-8 production during adipogenesis (**Figures 35-36**). “Beige” adipocytes differentiated following the regimen of Elabd et al. [328] also behaved similarly as irisin induced “beige” cells. Of note, irisin was administered in a concentration that

can be found in the blood plasma of exercise trained rodents [113,290]. In humans, however, much less irisin is secreted into the bloodstream, quantified recently by mass spectrometry [290]. Nevertheless, it is still possible that higher levels of irisin can be accumulated in discrete local tissue milieux in which browning are induced. In other studies, inconsistent effects were found when recombinant Fndc5 or irisin was administered directly to differentiating human adipocytes. Lee et al. found that Fndc5 treatment for 6 days after a 5 days long adipogenic differentiation of ADMSCs from the neck and subcutaneous WAT induced a browning program [350]. Progenitors from visceral fat did not respond to the Fndc5 treatment [350]. Contrarily, ADMSCs isolated from mediastinal fat could be differentiated into functional “beige” adipocytes in the presence of Fndc5 [351]. Zhang et al. found that differentiated adipocytes from mammary fat progenitors effectively induced browning as a result of a 4 days long irisin treatment, while the complete adipogenic differentiation process of these precursors was attenuated in response to irisin [352]. On the other hand, Raschke et al. did not find any effect of irisin or Fndc5 on differentiating adipocytes from the same anatomical origin [283]. In our experiments browning was induced by irisin on top of the white protocol in both, 4 and 14 day treatment regimens (**Figure 15**). This suggests that irisin induces browning of multipotent progenitors or already committed “beige” preadipocytes, respectively. Of note, the transdifferentiation of white to “beige” cells in response to irisin cannot be excluded either in regard of the abovementioned results. On the other hand, irisin did not further potentiate browning when it was added to the “beige” regimen. One reason behind the inconsistency in irisin effects in the different experiments might be the different origins of precursors that were isolated and differentiated. Some studies even restricted the adipocyte donors to females. Moreover, there were also significant differences between the obtained adipogenic differentiation protocols in these trials.

Contrarily, BMP7 treatment enhanced the expression of C/EBP $\beta$ , PRDM16, PPAR $\gamma$  and ZIC1 genes in human adipocytes suggesting that this mediator rather induced a “classical brown”-like differentiation (**Figures 16-17**). This program, similarly to irisin administration, resulted in increased mitochondrial DNA and Ucp1 levels and elevated OC both at basal and at cAMP stimulated conditions (**Figure 31**). On the other hand, BMP7 treatment decreased the secretion of IL-6, MCP-1 and IL-8 cytokines compared to untreated differentiating adipocytes (**Figures 35-36**).

Our results suggest that human SVFs isolated from subcutaneous WAT consist of a mixture of progenitors which have the potential to differentiate into white, “classical brown” or “beige” adipocytes in response to natural cues. In our experiments, the *ex vivo* differentiated thermogenic adipocytes, irrespectively of whether “classical brown” or “beige” gene expression program was induced, were active in a sense that they could prominently respond to an anti-obesity thermogenic cue with robustly enhanced energy expenditure. However, “classical brown” and “beige” adipocytes might have distinct non-thermogenic functions, with regard to the elevated secretion of IL-6, MCP-1 and IL-8 “batokines” by “beige” cells. Of note, the secretion of inflammatory mediators or the recruitment of M $\Phi$ s and eosinophil granulocytes is not only linked to the remodeling of WAT during obesity [353-355] but also to the differentiation and activation of browning adipocytes in special conditions [305]. For instance, eosinophils and type 2 cytokine signaling in M $\Phi$ s regulate the development of functional “beige” fat in rodents as summarized in 2.4.

#### **6.4. Clozapine, an unexpected novel inducer of browning**

When we unexpectedly observed that clozapine treated adipocytes had more and smaller lipid droplets and higher mitochondrial DNA amount than white fat cells, we found that the drug

significantly up-regulated ELOVL3, CIDEA, CYC1, PGC-1 $\alpha$  and TBX1 genes but not ZIC1, suggesting the induction of the “beige” and not the “classical brown” phenotype (**Figures 20 and 23**). In line with our observations in regard to elevated cytokine production during “beige” adipogenesis, Sárvári et al. [333] demonstrated that clozapine administration enhanced the secretion of MCP-1 and IL-8 by differentiating adipocytes. Of note, clozapine treatment on top of the white protocol was less effective in the induction of “beige” potential than either the browning cocktail or irisin administration. Moreover, a functional deficit of clozapine induced “beige” cells was detected by an XF96 oxymeter. Basal mitochondrial respiration (even basal proton leak OC) of clozapine treated cells was significantly elevated as compared to white adipocytes; however, the generated “masked beige” cells could not be efficiently stimulated by a cell permeable cAMP agonist (**Figure 32**). Additional gene expression results suggest that adipocytes differentiated in the presence of clozapine are less sensitive to cAMP activation (**Figure 34**). Previous studies, in which altered cAMP signaling was reported in the brain of rodents [356,357] and humans [358] in response to SGA treatment, further support these findings. On the other hand, clozapine could facilitate the energy expenditure of adipocytes by the induction of the recently identified substrate cycle of creatine-metabolism (**Figure 33**). The importance of this pathway in the metabolism of “beige” adipocytes was shown formerly in mice [179,359] and in human cell lines [179,360]; however, as far as we are aware, this is the first study in which a functional creatine-driven futile cycle was detected in primary human adipocytes.

The prevalence rate of obesity and its co-morbidities is at least two times higher in patients suffering in schizophrenia or in other SMIs compared to the general population [361,362].

Clozapine, a frequently administered SGA, induced browning in our *ex vivo* experiments in spite of its well documented effect to promote obesity in patients [270-272]. Different central and

peripheral mechanisms were suggested which might elucidate the molecular background of SGA-induced weight gain [273]. Kim et al. demonstrated that SGAs up-surged the appetite by the activation of hypothalamic AMP kinase via histamine H1 receptors in rodents [363]. It was also reported that these drugs decreased insulin sensitivity in rats [364], hampered insulin secretion or clearance in dogs [365] or rats [366], altered gut microbiota in rats [367] and humans [368], induced low-grade inflammation in WAT in rats [369,370] and directly stimulated adipogenesis in rodents [371,372].

Despite the aforementioned published data, the mechanisms underlying SGA-induced metabolic dysfunctions in humans remain barely understood [273]. To date, only a few studies investigated the direct effect of SGAs on human adipocytes [333,373,374]. It was reported formerly that clozapine enhanced the accumulation of lipids in differentiating human adipocytes which could stand in line with its documented effect to promote obesity [374]. However, we failed to detect more or larger lipid droplets in the clozapine treated adipocytes by LSC. When we examined how the propensity of hADMSCs to differentiate into thermogenic browning adipocytes is influenced by clozapine, we followed the practice of the study conducted by Sárvári et al. [333], where it was demonstrated that the long-term administration of SGAs enhanced the expression of several adipogenic marker genes and pro-inflammatory mediators in human adipocytes. In both studies, antipsychotic drugs were administered at doses comparable to their *in vivo* therapeutic plasma concentrations based on published information [373,375-377]. We also recorded dose-response curves which show the concentration dependent browning effect of clozapine (**Figure 24**).

Previously, it was reported that clozapine administration at 20-fold higher concentration than the upper limit of therapeutic reference range (TRR) resulted in a significant inhibition of the differentiation of a murine brown preadipocyte cell line [378]. However, toxic consequences of the treatment for the cultured cells cannot be excluded at this high clozapine concentration [373].

In line with our results, clozapine administration at the concentrations of TRR, however, had a slight positive effect on the expression of the selected BAT marker genes in the same *in vitro* mouse model [378].

The question may arise why *in vivo* administration of clozapine leads to fat gain and obesity. A similar discrepancy has been observed with thiazolidinediones (TZDs) which act through the nuclear receptor PPAR $\gamma$ . The long-term administration of some TZDs, including rosiglitazone which is the key component of the regimen developed by Elabd et al. [328], is not only capable of inducing browning of adipocytes *ex vivo* but also of increasing the thermogenic competency of WAT in rodents [125]. Rosiglitazone acts mostly directly on adipocytes or adipocyte precursor cells to promote browning [379-382]. Clinical trials implicated that TZDs increase the risk of weight gain, congestive heart failure and myocardial infarction in patients who received these drugs as oral medication for type 2 diabetes mellitus [383-385]. The underlying mechanisms of TZD-induced obesity remain under debate and have been linked either directly to the adipose tissue [386,387] or to the CNS [388-390].

Finally, we aimed to learn the molecular mechanism which can elucidate the browning effect of clozapine. To obtain mechanistic data, we tested if browning induced by clozapine can be explained by its known pharmacological effect of antagonizing 5HT receptors [267-269]. 14 different 5HT-receptor (HTR1-7) types have been already identified [391] and most of them are expressed by white [392,393] and brown adipocytes [84,106] in rodents. The release of 5HT by 3T3-L1 adipocytes was also reported formerly [265]. In cultivated subcutaneous hADMSCs, HTR2A and 7 were transcribed at significant levels detected by microarray [394]. Later, full RNA sequencing revealed that HTR1D, 2A and 3 were expressed by clonally derived human brown adipocytes and by their undifferentiated precursor counterparts isolated from “deep neck” fat [162]. In our experiments, the expression of TPH1, the gene encoding the enzyme which

catalyzes the rate-limiting step of 5HT synthesis outside the CNS [264], was detectable in hADMSCs of subcutaneous origin by RT-qPCR and did not change as a result of white adipocyte differentiation, suggesting that these cells are capable of autonomously generating and secreting 5HT during adipogenesis. However, we found decreased TPH1 expression in clozapine induced and in “beige” adipocytes (**Figure 27**). In addition, we showed that primary cells expressed HTR2A, 1D and 7 and the up-regulation of browning markers by clozapine was diminished in the presence of exogenous 5HT (**Figure 28**). Recently, two groups reported independently that peripheral 5HT reduced the “beige” potential and the sensitivity of browning adipocytes to thermogenic induction in a cell autonomous manner in mice [264,265]. Other studies showed that increased levels of peripheral 5HT [395] and polymorphisms in TPH1 gene were associated with obesity [396]. In our experiments, out of the 5HT-receptors, HTR2A to which clozapine can be bound with the strongest affinity [268], was expressed at the highest level in hADMSCs and in differentiated adipocytes. Gq signaling, which is otherwise initiated by HTR2A [391], was recently reported to abolish browning in mice and in human adipocytes [334]. Our results suggest that the disturbance of 5HT-receptor-mediated signaling by clozapine might, at least partially, explain the browning phenomenon described above.

In summary, we found that clozapine modified the differentiation program of human adipocyte progenitors; presumably via the inhibition of 5HT receptor mediated signaling, leading to generation of “beige” adipocytes with masked and not fully responsive thermogenic potential.

The detected incomplete acute thermogenic response to cAMP can be one of the reasons why these “masked beige” adipocytes function ineffectively also *in vivo*. Results from *in vivo* experiments focusing on the effect of SGAs on the SNS have been conflicting [397-400].

However, the  $\beta$ 3-adrenergic signaling pathway which plays a crucial role in the activation of thermogenesis in browning adipocytes [22-25] has never, to our knowledge, been studied in this

regard. Our data suggest that novel pharmacological stimulation of these “masked beige” adipocytes can be a future therapeutic target for treatment of SGA-induced obesity. We hope that our results initiate studies which identify the “masked beige” cells differentiated in response to clozapine treatment *in vivo* and find ways to induce their thermogenic function independently from the SNS.



## 7. SUMMARY

- By complementing measurements of gene expression changes from total cell lysates, Laser-scanning cytometry (LSC) was presented as a tool that made the population scale analysis of *ex vivo* browning possible. Our approach combined texture analysis which reflected the size and number of lipid droplets and detection of Ucp1 and Cidea protein content in single browning adipocytes of mixed cell populations.
- Irisin administration during white adipogenic differentiation resulted in a significant upregulation of several brown and “beige” adipocyte marker genes (UCP1, ELOVL3, CIDEA, CYC1, PGC-1 $\alpha$  and TBX1). Irisin treated cells had more and smaller lipid droplets, more mitochondrial DNA, higher mitochondrial respiration and contained more Ucp1 and Cidea protein than the untreated white adipocytes. By using the slide-based image cytometry method we could validate mouse data in human samples demonstrating the effectiveness of irisin to induce “beige” differentiation of subcutaneous white adipocytes.
- On the contrary, BMP7 treatment resulted in a functional browning in parallel with the gene expression pattern which indicated the classical brown program.
- Administration of second-generation antipsychotic drugs often leads to weight gain and consequent cardio-metabolic side effects. We unexpectedly observed that clozapine reprogrammed the gene expression pattern of differentiating human adipocytes *ex vivo*, leading to an elevated expression of the browning marker gene UCP1, more and smaller lipid droplets and more mitochondrial DNA than in the untreated white adipocytes. LSC showed that up to 40% of the differentiating single primary adipocytes had the

characteristic morphological features of browning cells. Furthermore, clozapine significantly up-regulated ELOVL3, CIDEA, CYC1, PGC-1 $\alpha$  and TBX1 genes but not ZIC1 suggesting induction of the “beige”-like and not the classical brown phenotype. The clozapine induced “beige” cells displayed increased basal and oligomycin inhibited (proton leak) oxygen consumption but these cells showed a lower response to cAMP stimulus as compared to control “beige” adipocytes indicating that they are less capable to respond to natural thermogenic anti-obesity cues.

- When we tested if browning induced by clozapine can be explained by its known pharmacological effect of antagonizing serotonin (5HT) receptors it was found that browning cells expressed 5HT receptors 2A, 1D, 7 and the up-regulation of browning markers was diminished in the presence of exogenous 5HT. Our results suggest that the disturbance of 5HT-receptor-mediated signaling by clozapine might, at least partially, explain the browning effect of the drug.
- When conditioned differentiation media were collected during the replacement of the adipogenic cocktails, we found that IL-6, MCP-1 and IL-8 secretion was significantly higher by “beige” compared to white adipocytes. Classical brown adipocyte differentiation, however, did not result in an increased production of these cytokines. Media replaced daily or in three day periods contained the same steady-state amount of IL-6 depending only on the phase of differentiation. This suggests that adipocytes adjust their production of the cytokine to reach an optimal level in the medium.

## ÖSSZEFOGLALÁS

- Statisztikailag releváns számú, differenciálódott humán adipocita vizsgálatát a Lézer Pásztázó Citométer (LSC) alkalmazásával értük el. Az LSC használata lehetővé tette számukra az adherens adipociták multiparametrikus vizsgálatát: a sejtek festése nélkül kvantifikáltuk az adipocitákban lévő lipid cseppek számát és méretét (ún. texture analízissel), majd a sejtek fixálását és permeabilizálását követően jelöltük az Ucp1 és Cidea barna zsírsejt marker fehérjéket, specifikus antitestekkel. A sejtek automatizált, precíz morfológiai vizsgálata és több szintű jelölése így választ adhatott arra a kérdésre is, hogy a sejtek milyen arányban léptek a barna zsírsejt differenciáció irányába különböző stimulusok hatására.
- Megfigyeltük, hogy mind az irisin, mind a BMP7 alkalmazása a fehér differenciációs protokoll alatt fokozta az UCP1 és CIDEA mellett az ELOVL3, CYC1 és PGC-1 $\alpha$  általános barna zsírsejt marker gének kifejeződését. A fokozott ZIC1 génexpresszió („klasszikus barna” adipocita marker) mellett a C/EBP $\beta$ , PRDM16, C/EBP $\alpha$  és PPAR $\gamma$  emelkedett kifejeződését figyeltük meg, hosszú távú BMP7 kezelés hatására. A TBX1 „beige” marker gén kifejeződését ugyanakkor csak az irisin kezelés fokozta szignifikánsan. Ez arra utal, hogy a bőr alatti zsírszövetből származó zsírsejt előalakok képesek lehetnek különböző jelek hatására egy „klasszikus barna”-szerű vagy egy „beige”-szerű differenciációs program beindítására is, melyekben általánosan megfigyelhető a barna zsírszöveti funkciót meghatározó legfontosabb gének fokozott kifejeződése.

- A második generációs antipszichotikumok alkalmazása gyakran vezet elhízáshoz. Humán szövetből izolált preadipociták clozapine kezelése ennek ellenére a barna és “beige” marker gének legtöbbjének, illetve az Ucp1 fehérje kifejeződését szignifikánsan fokozta, míg a fehér és általános zsírszöveti marker gének kifejeződése a kezelés hatására nem változott. Eredményeink arra utalnak, hogy clozapine kezelés képes “beige” zsírsejt differenciáció iniciálására humán *ex vivo* rendszerben, azonban az így létrejött sejtek reakciója természetes hőképző stimulusokra csökkent.
- Vizsgáltuk, hogy a clozapine kezelés “beige” programot kiváltó hatása összefügg-e a szer ismert, szerotonin (5HT) receptorokat gátló farmakológiai hatásával. A differenciálódó zsírsejtek kifejezték a 2A, 1D és 7-típusú 5HT receptorokat. Ezenfelül a barna marker gének fokozott kifejeződése clozapine hatására, szerotonin jelenlétében nem volt megfigyelhető. Eredményeink arra utalnak, hogy a clozapine “browning”-ot kiváltó hatása összefügg a szer 5HT receptorok által kiváltott jelátvitel-gátló képességével.
- Végül megfigyeltük, hogy az *ex vivo* differenciáltatott barna zsírsejtek és irisin kezelt fehér zsírsejtek nagymértékben termelnek IL-6, IL-8 és MCP-1 citokineket. A BMP7 kezelt sejtek ugyanakkor kevesebb mediátort szekretáltak. Ismert, hogy egerekben az IL-6 termelés kedvezően befolyásolhatja az inzulin szenzitivitást, míg a fokozott IL-8 és MCP-1 elősegítheti makrofágok odavándorlását a differenciálódó barna sejtek környezetébe. A makrofágok esetleges alternatív úton történő aktiválódása noradrenalin termelést válthat ki, mely fokozhatja a barna adipociták hő termelő képességét is.

## 8. REFERENCES

1. Gessner, K. (1551) Conradi Gesneri Medici Tigurine Historiae Animalium: Lib. I De Quadrupedibus Viviparis
2. Smith, R.E. (1961) Thermogenic activity of the hibernating gland in the cold-acclimated rat. *Physiologist* **4**: 113.
3. Smith, R. E., Hock, R. J. (1963) Brown fat: thermogenic effector of arousal in hibernators. *Science* **140**: 199-200.
4. Cannon, B., Nedergaard, J. (2004) Brown adipose tissue: function and physiological significance. *Physiol. Rev.* **84**: 277-359.
5. Afzelius, B.A. (1970) Brown Adipose Tissue: Its Gross Anatomy, Histology and Cytology, *In: Lindberg O., Ed., Brown Adipose Tissue, Elsevier, New York*, 1-28.
6. Cinti, S. (1999) The Adipose Organ. Kurtis SRL, Milan, Italy
7. Nechad, M., Barnard, T. (1979) Development of the interscapular brown adipose tissue in the hamster. I. Two pathways of adipocyte differentiation and the development of the sympathetic innervation. *Biol. Cell* **36**: 43–50.
8. Nedergaard, J., and Lindberg, O. (1982) The brown fat cell. *Int. Rev. Cytol.* **74**: 187–286.
9. Bukowiecki, L., Collet, A.J., Follea, N., Guay, G., Jahjah, L. (1982) Brown adipose tissue hyperplasia: a fundamental mechanism of adaptation to cold and hyperphagia. *Am. J. Physiol.* **242**: E353-359.
10. Cinti, S., Mitchell, G., Barbatelli, G., Murano, I., Ceresi, E., Faloia, E., Wang, S., Fortier, M., Greenberg, A.S., Obin, M.S. (2005) Adipocyte death defines macrophage localization and function in adipose tissue of obese mice and humans. *J. Lipid Res.* **46**: 2347-2355.
11. Heaton, G.M., Wagenvoort, R.J., Kemp, A.Jr., Nicholls, D.G. (1978) Brown-adipose-tissue mitochondria: photoaffinity labelling of the regulatory site of energy dissipation. *Eur. J. Biochem.* **82**: 515–521.
12. Nicholls, D.G. (1976) The bioenergetics of brown adipose tissue mitochondria. *FEBS Lett.* **61**: 103-110.
13. Ricquier, D., Mory, G., Hemon, P. (1979) Changes induced by cold adaptation in the brown adipose tissue from several species of rodents, with special reference to the mitochondrial components. *Can. J. Biochem.* **57**:1262-1266.
14. Lin, C.S., Klingenberg, M. (1980) Isolation of the uncoupling protein from brown adipose tissue mitochondria. *FEBS Lett.* **113**: 299-303.
15. Cannon, B., Hedin, A., Nedergaard, J. (1982) Exclusive occurrence of thermogenin antigen in brown adipose tissue. *FEBS Lett.* **150**:129-132.
16. Nicholls, D.G., Locke, R.M. (1984) Thermogenic mechanisms in brown fat. *Physiol. Rev.* **64**:1-64.
17. Jacobsson, A., Stadler, U., Glotzer, M.A., Kozak, L.P. (1985) Mitochondrial uncoupling protein from mouse brown fat. Molecular cloning, genetic mapping, and mRNA expression. *J. Biol. Chem.* **260**: 16250–16254.
18. Lindberg, O., DePierre, J., Rylander, E., Afzelius, B.A. (1967) Studies of the mitochondrial energy-transfer system of brown adipose tissue. *J. Cell. Biol.* **34**: 293–310.
19. Cannon, B., Vogel, G. (1977) The mitochondrial ATPase of brown adipose tissue. Purification and comparison with the mitochondrial ATPase from beef heart. *FEBS Lett.* **76**: 284–289.

20. Houstek, J., Andersson, U., Tvrdik, P., Nedergaard, J., Cannon, B. (1995) The expression of subunit c correlates with and thus may limit the biosynthesis of the mitochondrial F<sub>0</sub>F<sub>1</sub>-ATPase in brown adipose tissue. *J. Biol. Chem.* **270**: 7689–7694.
21. Kramarova, T.V., Shabalina, I.G., Andersson, U., Westerberg, R., Carlberg, I., Houstek, J., Nedergaard, J., Cannon, B. (2008) Mitochondrial ATP synthase levels in brown adipose tissue are governed by the c-Fo subunit P1 isoform. *FASEB J.* **22**:55-63.
22. Prusiner, S.B., Cannon, B., Lindberg, O. (1968) Oxidative metabolism in cells isolated from brown adipose tissue. I. Catecholamine and fatty acid stimulation of respiration. *Eur. J. Biochem.* **6**: 15–22.
23. Shih, M.F., Taberner, P.V. (1995) Selective activation of brown adipocyte hormone-sensitive lipase and cAMP production in the mouse by  $\beta$ 3-adrenoceptor agonists. *Biochem. Pharmacol.* **50**: 601–608.
24. Chaudhry, A., Granneman, J.G. (1999) Differential regulation of functional responses by  $\beta$ -adrenergic receptor subtypes in brown adipocytes. *Am. J. Physiol.* **277**: R147-53.
25. Matthias, A., Ohlson, K.E.B., Fredriksson, J.M., Jacobsson, A., Nedergaard, J., Cannon, B. (2000) Thermogenic responses in brown-fat cells are fully UCP1-dependent: UCP2 or UCP3 do not substitute for UCP1 in adrenergically or fatty-acid induced thermogenesis. *J. Biol. Chem.* **275**: 25073–25081.
26. Fedorenko, A., Lishko, P.V., Kirichok, Y. (2012) Mechanism of fatty-acid-dependent UCP1 uncoupling in brown fat mitochondria. *Cell* **151**:400-413.
27. Chouchani, E.T., Kazak, L., Jedrychowski, M.P., Lu, G.Z., Erickson, B.K., Szpyt, J., Pierce, K.A., Laznik-Bogoslavski, D., Vetrivelan, R., Clish, C.B., Robinson, A.J., Gygi, S.P., Spiegelman, B.M. (2016) Mitochondrial ROS regulate thermogenic energy expenditure and sulfenylation of UCP1. *Nature* **532**:112-116.
28. Aherne, W., Hull, D. (1966) Brown adipose tissue and heat production in the newborn infant. *J. Pathol. Bacteriol.* **91**:223-234.
29. Rothwell, N.J., Stock, M.J. (1985) Biological distribution and significance of brown adipose tissue. *Comp. Biochem. Physiol. A Comp. Physiol.* **82**:745-751.
30. Enerbäck, S., Jacobsson, A., Simpson, E.M., Guerra, C., Yamashita, H., Harper, M.E., Kozak, L.P. (1997) Mice lacking mitochondrial uncoupling protein are cold-sensitive but not obese. *Nature* **387**: 90-94.
31. Golozoubova, V., Hohtola, E., Matthias, A., Jacobsson, A., Cannon, B., Nedergaard, J. (2001) Only UCP1 can mediate adaptive nonshivering thermogenesis in the cold. *FASEB J.* **15**: 2048-2050.
32. Ukropec, J., Anunciado, R.P., Ravussin, Y., Hulver, M.W., Kozak, L.P. (2006) UCP1-independent thermogenesis in white adipose tissue of cold-acclimated Ucp1<sup>-/-</sup>-mice. *J. Biol. Chem.* **281**: 31894-31908.
33. Koza, R.A., Kozak, U.C., Brown, L.J., Leiter, E.H., MacDonald, M.J., Kozak, L.P. (1996) Sequence and tissue-dependent RNA expression of mouse FAD-linked glycerol-3-phosphate dehydrogenase. *Arch. Biochem. Biophys.* **336**: 97-104.
34. Shabalina, I.G., Hoeks, J., Kramarova, T.V., Schrauwen, P., Cannon, B., Nedergaard, J. (2010) Cold tolerance of UCP1-ablated mice: A skeletal muscle mitochondria switch toward lipid oxidation with marked UCP3 up-regulation not associated with increased basal, fatty acid- or ROS-induced uncoupling or enhanced GDP effects. *Biochim. Biophys. Acta* **1797**: 968-980.
35. Rothwell, N.J., Stock, M.J. (1979) A role for brown adipose tissue in diet-induced thermogenesis. *Nature* **281**: 31–35.
36. Liu, X., Rossmeisl, M., McClaine, J., Riachi, M., Harper, M.E., Kozak, L.P. (2003) Paradoxical resistance to diet-induced obesity in UCP1-deficient mice. *J. Clin. Invest.* **111**: 399–407.

37. Golozoubova, V., Gullberg, H., Matthias, A., Cannon, B., Vennström, B., Nedergaard, J. (2004) Depressed thermogenesis but competent brown adipose tissue recruitment in mice devoid of all hormone-binding thyroid hormone receptors. *Mol. Endocrinol.* **18**: 384-401.
38. Feldmann, H.M., Golozoubova, V., Cannon, B., Nedergaard, J. (2009) UCP1 ablation induces obesity and abolishes diet-induced thermogenesis in mice exempt from thermal stress by living at thermoneutrality. *Cell Metab.* **9**: 203-209.
39. Kopecky, J., Clarke, G., Enerbäck, S., Spiegelman, B., Kozak, L.P. (1995) Expression of the mitochondrial uncoupling protein gene from the aP2 gene promoter prevents genetic obesity. *J Clin. Invest.* **96**:2914-2923.
40. Cederberg, A., Grønning, L.M., Ahrén, B., Taskén, K., Carlsson, P., Enerbäck, S. (2001) FOXC2 is a winged helix gene that counteracts obesity, hypertriglyceridemia, and diet-induced insulin resistance. *Cell* **106**:563-573.
41. Tsukiyama-Kohara, K., Poulin, F., Kohara, M., DeMaria, C.T., Cheng, A., Wu, Z., Gingras, A.C., Katsume, A., Elchebly, M., Spiegelman, B.M., Harper, M.E., Tremblay, M.L., Sonenberg, N. (2001) Adipose tissue reduction in mice lacking the translational inhibitor 4E-BP1. *Nat. Med.* **7**:1128-1132.
42. Xue, B., Rim, J.S., Hogan, J.C., Coulter, A.A., Koza, R.A., Kozak, L.P. (2007) Genetic variability affects the development of brown adipocytes in white fat but not in interscapular brown fat. *J. Lipid Res.* **48**:41-51.
43. Hsieh, A.C., Carlson, L.D. (1957) Role of adrenaline and noradrenaline in chemical regulation of heat production. *Am. J. Physiol.* **190**: 243-246.
44. Depocas, F. (1960) The calorogenic response of cold-acclimated white rats to infused noradrenaline. *Can. J. Biochem. Physiol.* **38**: 107-114.
45. Foster, D.O., Frydman, M.L. (1979) Tissue distribution of cold-induced thermogenesis in conscious warm- or cold-acclimated rats reevaluated from changes in tissue blood flow: The dominant role of brown adipose tissue in the replacement of shivering by nonshivering thermogenesis. *Can. J. Physiol. Pharmacol.* **57**: 257-270.
46. Foster, D.O., Depocas, F., Zaror-Behrens, G. (1982) Unilaterality of the sympathetic innervation of each pad of rat interscapular brown adipose tissue. *Can. J. Physiol. Pharmacol.* **60**: 107-113.
47. Arch, J.R., Ainsworth, A.T., Cawthorne, M.A., Piercy, V., Sennitt, M.V., Thody, V.E., Wilson, C., Wilson, S. (1984) Atypical  $\beta$ -adrenoceptor on brown adipocytes as target for anti-obesity drugs. *Nature* **309**: 163-165.
48. Nånberg, E., Connolly, E., Nedergaard, J. (1985) Presence of a  $\text{Ca}^{2+}$ -dependent  $\text{K}^{+}$  channel in brown adipocytes. Possible role in maintenance of alpha 1-adrenergic stimulation. *Biochim. Biophys. Acta* **844**: 42-49.
49. Domínguez, M.J., Fernández, M., Elliott, K., Benito, M. (1986) Occurrence of alpha 2-adrenergic effects on adenylate cyclase activity and (3H)-clonidine specific binding in brown adipose tissue from foetal rats. *Biochem. Biophys. Res. Commun.* **138**:1390-1394.
50. Costain, W.J., Mainra, R., Desautels, M., Sulakhe, P.V. (1996) Expressed  $\alpha$ 1-adrenoceptors in adult rat brown adipocytes are primarily of  $\alpha$ 1A subtype. *Can. J. Physiol. Pharmacol.* **74**: 234-240.
51. Kikuchi-Utsumi, K., Kikuchi-Utsumi, M., Cannon, B., Nedergaard, J. (1997) Differential regulation of the expression of  $\alpha$ 1-adrenergic subtype genes in brown adipose tissue. *Biochem. J.* **322**: 417-424.
52. Revelli, J.P., Pescini, R., Muzzin, P., Seydoux, J., Fitzgerald, M.G., Fraser, C.M., Giacobino, J.P. (1991) Changes in  $\beta$ 1- and  $\beta$ 2-adrenergic receptor mRNA levels in brown adipose tissue and heart of hypothyroid rats. *Biochem. J.* **277**: 625-629.

53. Bronnikov, G., Bengtsson, T., Kramarova, L., Golozoubova, V., Cannon, B., Nedergaard, J. (1999)  $\beta$ 1 to  $\beta$ 3 switch in control of cAMP during brown adipocyte development explains distinct  $\beta$ -adrenoceptor subtype mediation of proliferation and differentiation. *Endocrinology* **140**: 4185–4197.
54. Bengtsson, T., Nedergaard, J., Cannon, B. (2000) Differential regulation of the gene expression of  $\beta$ -adrenoceptor subtypes in brown adipocytes. *Biochem. J.* **347**: 643–651.
55. Granneman, J.G. (1988) Norepinephrine infusions increase adenylate cyclase responsiveness in brown adipose tissue. *J. Pharmacol. Exp. Ther.* **245**: 1075–1080.
56. Chaudhry, A., Muffler, L.A., Yao, R., Granneman, J.G. (1996) Perinatal expression of adenylyl cyclase subtypes in rat brown adipose tissue. *Am. J. Physiol.* **270**: R755–R760.
57. Bourova, L., Pesanova, Z., Novotny, J., Bengtsson, T., Svoboda, P. (2000) Differentiation of cultured brown adipocytes is associated with a selective increase in the short variant of g(s)alpha protein. Evidence for higher functional activity of g(s)alphaS. *Mol. Cell Endocrinol.* **167**: 23–31.
58. Reed, N., Fain, J.N. (1968) Stimulation of respiration in brown fat cells by epinephrine, dibutyl-3',5'-adenosine monophosphate, and m-chloro-(carbonyl cyanide)phenylhydrazine. *J. Biol. Chem.* **243**: 2843–2848.
59. Scarpace, P.J., Matheny, M. (1996) Thermogenesis in brown adipose tissue with age: post-receptor activation by forskolin. *Pflügers Arch.* **431**: 388–394.
60. Tews, D., Schwar, V., Scheithauer, M., Weber, T., Fromme, T., Klingenspor, M., Barth, T.F., Möller, P., Holzmann, K., Debatin, K.M., Fischer-Posovszky, P., Wabitsch, M. (2014) Comparative gene array analysis of progenitor cells from human paired deep neck and subcutaneous adipose tissue. *Mol. Cell Endocrinol.* **395**: 41–50.
61. Holm, C., Fredrikson, G., Cannon, B., Belfrage, P. (1987) Hormonesensitive lipase in brown adipose tissue: identification and effect of cold exposure. *Biosci. Rep.* **7**: 897–904.
62. Lindquist, J.M., Fredriksson, J.M., Rehnmark, S., Cannon, B., Nedergaard, J. (2000)  $\beta$ 3- and  $\alpha$ 1-adrenergic Erk1/2 activation is Src but not Gi-mediated in brown adipocytes. *J. Biol. Chem.* **275**: 22670–22677.
63. Cao, W., Medvedev, A.V., Daniel, K.W., Collins, S. (2001)  $\beta$ -Adrenergic activation of p38 MAP kinase in adipocytes. cAMP induction of the uncoupling protein 1 (UCP1) gene requires p38 MAP kinase. *J. Biol. Chem.* **276**: 27077–27082.
64. Wang, S.P., Laurin, N., Himms-Hagen, J., Rudnicki, M.A., Levy, E., Robert, M.F., Pan, L., Oligny, L., Mitchell, G.A. (2001) The adipose tissue phenotype of hormone-sensitive lipase deficiency in mice. *Obesity Res.* **9**: 119–128.
65. Mohell, N., Wallace, M., Fain, J.N. (1984)  $\alpha$ 1-adrenergic stimulation of phosphatidylinositol turnover and respiration of brown fat cells. *Mol. Pharmacol.* **25**: 64–69.
66. Nånberg, E., Putney, J.Jr. (1986)  $\alpha$ -Adrenergic activation of brown adipocytes leads to an increased formation of inositol polyphosphates. *FEBS Lett.* **195**: 319–322.
67. Barge, R.M., Mills, I., Silva, E., Larsen, P.R. (1988) Phorbol esters, protein kinase C, and thyroxine 5'-deiodinase in brown adipocytes. *Am. J. Physiol.* **254**: E323–E327.
68. Wilcke, M., Nedergaard, J. (1989)  $\alpha$ 1- and  $\beta$ -adrenergic regulation of intracellular  $\text{Ca}^{2+}$  levels in brown adipocytes. *Biochem. Biophys. Res. Commun.* **163**: 292–300.
69. Shimizu, Y., Tanishita, T., Minokoshi, Y., Shimazu, T. (1997) Activation of mitogen-activated protein kinase by norepinephrine in brown adipocytes from rats. *Endocrinology* **138**: 248–253.
70. Thonberg, H., Nedergaard, J., Cannon, B. (2002) A novel pathway for adrenergic stimulation of cAMP-response-element-binding protein (CREB) phosphorylation: mediation via  $\alpha$ 1-adrenoceptors and protein kinase C activation. *Biochem. J.* **364**: 73–79.



71. N  chad, M., Nedergaard, J., Cannon, B. (1987) Noradrenergic stimulation of mitochondriogenesis in brown adipocytes differentiating in culture. *Am. J. Physiol.* **253**: C889–C894.
72. Bronnikov, G., Houstek, J., Nedergaard, J. (1992)  $\beta$ -Adrenergic, cAMP-mediated stimulation of proliferation of brown fat cells in primary culture. Mediation via  $\beta$ 1 but not via  $\beta$ 3 receptors. *J. Biol. Chem.* **267**: 2006–2013.
73. Rehnmark, S., Antonson, P., Xanthopoulos, K.G., Jacobsson, A. (1993) Differential adrenergic regulation of C/EBP $\alpha$  and C/EBP $\beta$  in brown adipose tissue. *FEBS Lett.* **318**: 235–241.
74. Lindquist, J.M., Rehnmark, S. (1998) Ambient temperature regulation of apoptosis in brown adipose tissue: Erk 1/2 promotes norepinephrine-dependent cell survival. *J. Biol. Chem.* **273**: 30147–30156.
75. Freytag, S.O., Paielli, D.L., Gilbert, J.D. (1994) Ectopic expression of the CCAAT/enhancer-binding protein alpha promotes the adipogenic program in a variety of mouse fibroblastic cells. *Genes Dev.* **8**:1654-1663.
76. Tontonoz, P., Hu, E., Spiegelman, B.M. (1994) Stimulation of adipogenesis in fibroblasts by PPAR gamma 2, a lipid-activated transcription factor. *Cell* **79**:1147-1156.
77. Hu, E., Tontonoz, P., Spiegelman, B.M. (1995) Transdifferentiation of myoblasts by the adipogenic transcription factors PPAR gamma and C/EBP alpha. *Proc. Natl. Acad. Sci. USA* **92**: 9856-9860.
78. Rosen, E.D., Sarraf, P., Troy, A.E., Bradwin, G., Moore, K., Milstone, D.S., Spiegelman, B.M., Mortensen, R.M. (1999) PPAR gamma is required for the differentiation of adipose tissue in vivo and in vitro. *Mol. Cell* **4**: 611-617.
79. Rosen, E.D., Spiegelman, B.M. (2001) PPARgamma : a nuclear regulator of metabolism, differentiation, and cell growth. *J. Biol. Chem.* **276**: 37731-37734.
80. Lowe, C.E., O’Rahilly, S., Rochford, J.J. (2011) Adipogenesis at a glance. *J. Cell Sci.* **124**: 2681-2686.
81. Rosen, E.D., Spiegelman, B.M. (2000) Molecular regulation of adipogenesis. *Annu. Rev. Cell. Dev. Biol.* **16**:145-171.
82. Gesta, S., Tseng, Y.H., Kahn, C.R. (2007) Developmental origin of fat: tracking obesity to its source. *Cell* **131**: 242-256.
83. Atit, R., Sgaier, S.K., Mohamed, O.A., Taketo, M.M., Dufort, D., Joyner, A.L., Niswander, L., Conlon, R.A. (2006) Beta-catenin activation is necessary and sufficient to specify the dorsal dermal fate in the mouse. *Dev. Biol.* **296**:164-176.
84. Timmons, J.A., Wennmalm, K., Larsson, O., Walden, T.B., Lassmann, T., Petrovic, N., Hamilton, D.L., Gimeno, R.E., Wahlestedt, C., Baar, K., Nedergaard, J., Cannon, B. (2007) Myogenic gene expression signature establishes that brown and white adipocytes originate from distinct cell lineages. *Proc. Natl. Acad. Sci. USA* **104**: 4401-4406.
85. Seale, P., Bjork, B., Yang, W., Kajimura, S., Chin, S., Kuang, S., Scim  , A., Devarakonda, S., Conroe, H.M., Erdjument-Bromage, H., Tempst, P., Rudnicki, M.A., Beier, D.R., Spiegelman, B.M. (2008) PRDM16 controls a brown fat/skeletal muscle switch. *Nature* **454**: 961-967.
86. Lepper, C., Fan, C.M. (2010) Inducible lineage tracing of Pax7-descendant cells reveals embryonic origin of adult satellite cells. *Genesis* **48**: 424-436.
87. Tseng, Y.H., Kokkotou, E., Schulz, T.J., Huang, T.L., Winnay, J.N., Taniguchi, C.M., Tran, T.T., Suzuki, R., Espinoza, D.O., Yamamoto, Y., Ahrens, M.J., Dudley, A.T., Norris, A.W., Kulkarni, R.N., Kahn, C.R. (2008) New role of bone morphogenetic protein 7 in brown adipogenesis and energy expenditure. *Nature* **454**:1000-1004.
88. Schulz, T.J., Huang, P., Huang, T.L., Xue, R., McDougall, L.E., Townsend, K.L., Cypess, A.M., Mishina, Y., Gussoni, E., Tseng, Y.H. (2013) Brown-fat paucity due to impaired BMP signalling induces compensatory browning of white fat. *Nature* **495**: 379-383.

89. Wang, W., Kissig, M., Rajakumari, S., Huang, L., Lim, H.W., Won, K.J., Seale, P. (2014) Ebf2 is a selective marker of brown and beige adipogenic precursor cells. *Proc. Natl. Acad. Sci. USA* **111**: 14466-14471.
90. Longo, K.A., Wright, W.S., Kang, S., Gerin, I., Chiang, S.H., Lucas, P.C., Opp, M.R., MacDougald, O.A. (2004) Wnt10b inhibits development of white and brown adipose tissues. *J. Biol. Chem.* **279**: 35503-35509.
91. Kang, S., Bajnok, L., Longo, K.A., Petersen, R.K., Hansen, J.B., Kristiansen, K., MacDougald, O.A. (2005) Effects of Wnt signaling on brown adipocyte differentiation and metabolism mediated by PGC-1alpha. *Mol. Cell Biol.* **25**: 1272-1282.
92. Sanchez-Gurmaches, J., Hung, C.M., Sparks, C.A., Tang, Y., Li, H., Guertin, D.A. (2012) PTEN loss in the Myf5 lineage redistributes body fat and reveals subsets of white adipocytes that arise from Myf5 precursors. *Cell Metab.* **16**: 348-362.
93. Seale, P., Kajimura, S., Spiegelman, B.M. (2009) Transcriptional control of brown adipocyte development and physiological function--of mice and men. *Genes Dev.* **23**: 788-797.
94. Kajimura, S., Seale, P., Spiegelman, B.M. (2010) Transcriptional control of brown fat development. *Cell Metab.* **11**: 257-262.
95. Rosen, E.D., Spiegelman, B.M. (2014) What we talk about when we talk about fat. *Cell* **156**: 20-44.
96. Kajimura, S., Spiegelman, B.M., Seale, P. (2015) Brown and Beige Fat: Physiological Roles beyond Heat Generation. *Cell Metab.* **22**: 546-559.
97. Inagaki, T., Sakai, J., Kajimura, S. (2016) Transcriptional and epigenetic control of brown and beige adipose cell fate and function. *Nat. Rev. Mol. Cell. Biol.* **17**: 480-495.
98. Seale, P., Kajimura, S., Yang, W., Chin, S., Rohas, L.M., Uldry, M., Tavernier, G., Langin, D., Spiegelman, B.M. (2007) Transcriptional control of brown fat determination by PRDM16. *Cell Metab.* **6**: 38-54.
99. Kajimura, S., Seale, P., Tomaru, T., Erdjument-Bromage, H., Cooper, M.P., Ruas, J.L., Chin, S., Tempst, P., Lazar, M.A., Spiegelman, B.M. (2008) Regulation of the brown and white fat gene programs through a PRDM16/CtBP transcriptional complex. *Genes Dev.* **22**: 1397-1409.
100. Park, J.H., Kang, H.J., Kang, S.I., Lee, J.E., Hur, J., Ge, K., Mueller, E., Li, H., Lee, B.C., Lee, S.B. (2013) A multifunctional protein, EWS, is essential for early brown fat lineage determination. *Dev. Cell* **26**: 393-404.
101. Ohno, H., Shinoda, K., Ohyama, K., Sharp, L.Z., Kajimura, S. (2013) EHMT1 controls brown adipose cell fate and thermogenesis through the PRDM16 complex. *Nature* **504**: 163-167.
102. Kim, J.K., Kim, H.J., Park, S.Y., Cederberg, A., Westergren, R., Nilsson, D., Higashimori, T., Cho, Y.R., Liu, Z.X., Dong, J., Cline, G.W., Enerback, S., Shulman, G.I. (2005) Adipocyte-specific overexpression of FOXC2 prevents diet-induced increases in intramuscular fatty acyl CoA and insulin resistance. *Diabetes* **54**: 1657-1663.
103. Xue, Y., Cao, R., Nilsson, D., Chen, S., Westergren, R., Hedlund, E.M., Martijn, C., Rondahl, L., Krauli, P., Walum, E., Enerbäck, S., Cao, Y. (2008) FOXC2 controls Ang-2 expression and modulates angiogenesis, vascular patterning, remodeling, and functions in adipose tissue. *Proc. Natl. Acad. Sci. USA* **105**: 10167-10172.
104. Puigserver, P., Wu, Z., Park, C.W., Graves, R., Wright, M., Spiegelman, B.M. (1998) A cold-inducible coactivator of nuclear receptors linked to adaptive thermogenesis. *Cell* **92**: 829-839.
105. Lin, J., Wu, P.H., Tarr, P.T., Lindenberg, K.S., St-Pierre, J., Zhang, C.Y., Mootha, V.K., Jäger, S., Vianna, C.R., Reznick, R.M., Cui, L., Manieri, M., Donovan, M.X., Wu, Z., Cooper, M.P., Fan, M.C., Rohas, L.M., Zavacki, A.M., Cinti, S., Shulman, G.I., Lowell, B.B., Krainc, D., Spiegelman, B.M.

- (2004) Defects in adaptive energy metabolism with CNS-linked hyperactivity in PGC-1alpha null mice. *Cell* **119**:121-135.
106. Uldry, M., Yang, W., St-Pierre, J., Lin, J., Seale, P., Spiegelman, B.M. (2006) Complementary action of the PGC-1 coactivators in mitochondrial biogenesis and brown fat differentiation. *Cell Metab.* **3**: 333-341;
  107. Kong, X., Banks, A., Liu, T., Kazak, L., Rao, R.R., Cohen, P., Wang, X., Yu, S., Lo, J.C., Tseng, Y.H., Cypess, A.M., Xue, R., Kleiner, S., Kang, S., Spiegelman, B.M., Rosen, E.D. (2014) IRF4 is a key thermogenic transcriptional partner of PGC-1 $\alpha$ . *Cell* **158**: 69-83.
  108. Lehman, J.J., Barger, P.M., Kovacs, A., Saffitz, J.E., Medeiros, D.M., Kelly, D.P. (2000) Peroxisome proliferator-activated receptor gamma coactivator-1 promotes cardiac mitochondrial biogenesis. *J. Clin. Invest.* **106**: 847-856.
  109. Lin, J., Wu, H., Tarr, P.T., Zhang, C.Y., Wu, Z., Boss, O., Michael, L.F., Puigserver, P., Isotani, E., Olson, E.N., Lowell, B.B., Bassel-Duby, R., Spiegelman, B.M. (2002) Transcriptional co-activator PGC-1 alpha drives the formation of slow-twitch muscle fibres. *Nature* **418**: 797-801.
  110. Leone, T.C., Lehman, J.J., Finck, B.N., Schaeffer, P.J., Wende, A.R., Boudina, S., Courtois, M., Wozniak, D.F., Sambandam, N., Bernal-Mizrachi, C., Chen, Z., Holloszy, J.O., Medeiros, D.M., Schmidt, R.E., Saffitz, J.E., Abel, E.D., Semenkovich, C.F., Kelly, D.P. (2005) PGC-1alpha deficiency causes multi-system energy metabolic derangements: muscle dysfunction, abnormal weight control and hepatic steatosis. *PLoS Biol.* **3**: e101.
  111. Lin, J., Handschin, C., Spiegelman, B.M. (2005) Metabolic control through the PGC-1 family of transcription coactivators. *Cell Metab.* **1**: 361-70.
  112. Finck, B.N., Kelly, D.P. (2006) PGC-1 coactivators: inducible regulators of energy metabolism in health and disease. *J. Clin. Invest.* **116**: 615-622.
  113. Boström, P., Wu, J., Jedrychowski, M.P., Korde, A., Ye, L., Lo, J.C., Rasbach, K.A., Boström, E.A., Choi, J.H., Long, J.Z., Kajimura, S., Zingaretti, M.C., Vind, B.F., Tu, H., Cinti, S., Højlund, K., Gygi, S.P., Spiegelman, B.M. (2012) A PGC1- $\alpha$ -dependent myokine that drives brown-fat-like development of white fat and thermogenesis. *Nature* **481**: 463-468.
  114. Picard, F., Géhin, M., Annicotte, J., Rocchi, S., Champy, M.F., O'Malley, B.W., Chambon, P., Auwerx, J. (2002) SRC-1 and TIF2 control energy balance between white and brown adipose tissues. *Cell* **111**: 931-941.
  115. Hansen, J.B., Jørgensen, C., Petersen, R.K., Hallenborg, P., De Matteis, R., Bøye, H.A., Petrovic, N., Enerbäck, S., Nedergaard, J., Cinti, S., te Riele, H., Kristiansen, K. (2004) Retinoblastoma protein functions as a molecular switch determining white versus brown adipocyte differentiation *Proc. Natl. Acad. Sci. USA* **101**: 4112-4117.
  116. Louet, J.F., Coste, A., Amazit, L., Tannour-Louet, M., Wu, R.C., Tsai, S.Y., Tsai, M.J., Auwerx, J., O'Malley, B.W. (2006) Oncogenic steroid receptor coactivator-3 is a key regulator of the white adipogenic program. *Proc. Natl. Acad. Sci. USA*. **103**: 17868-17873.
  117. Young, P., Arch, J.R., Ashwell, M. (1984) Brown adipose tissue in the parametrial fat pad of the mouse. *FEBS Lett.* **167**: 10-14.
  118. Cousin, B., Cinti, S., Morroni, M., Raimbault, S., Ricquier, D., Pénicaud, L., Casteilla, L. (1992) Occurrence of brown adipocytes in rat white adipose tissue: molecular and morphological characterization. *J. Cell. Sci.* **103**: 931-942.
  119. Granneman, J.G., Li, P., Zhu, Z., Lu, Y. (2005) Metabolic and cellular plasticity in white adipose tissue I: effects of beta3-adrenergic receptor activation. *Am. J. Physiol. Endocrinol. Metab.* **289**: E608-616.

120. Himms-Hagen, J., Melnyk, A., Zingaretti, M.C., Ceresi, E., Barbatelli, G., Cinti, S. (2000) Multilocular fat cells in WAT of CL-316243-treated rats derive directly from white adipocytes. *Am. J. Physiol. Cell Physiol.* **279**: C670-681.
121. De Matteis, R., Arch, J.R., Petroni, M.L., Ferrari, D., Cinti, S., Stock, M.J. (2002) Immunohistochemical identification of the beta(3)-adrenoceptor in intact human adipocytes and ventricular myocardium: effect of obesity and treatment with ephedrine and caffeine. *Int. J. Obes. Relat. Metab. Disord.* **26**: 1442-1450.
122. Collins, S., Daniel, K.W., Petro, A.E., Surwit, R.S. (1997) Strain-specific response to beta 3-adrenergic receptor agonist treatment of diet-induced obesity in mice. *Endocrinology* **138**: 405-413.
123. Ghorbani, M., Claus, T.H., Himms-Hagen, J. (1997) Hypertrophy of brown adipocytes in brown and white adipose tissues and reversal of diet-induced obesity in rats treated with a beta3-adrenoceptor agonist. *Biochem. Pharmacol.* **54**: 121-131.
124. Ghorbani, M., Himms-Hagen, J. (1997) Appearance of brown adipocytes in white adipose tissue during CL 316,243-induced reversal of obesity and diabetes in Zucker fa/fa rats. *Int. J. Obes. Relat. Metab. Disord.* **21**: 465-475.
125. Petrovic, N., Walden, T.B., Shabalina, I.G., Timmons, J.A., Cannon, B., Nedergaard, J. (2010) Chronic peroxisome proliferator-activated receptor gamma (PPARgamma) activation of epididymally derived white adipocyte cultures reveals a population of thermogenically competent, UCP1-containing adipocytes molecularly distinct from classic brown adipocytes. *J. Biol. Chem.* **285**: 7153-7164.
126. Seale, P., Conroe, H.M., Estall, J., Kajimura, S., Frontini, A., Ishibashi, J., Cohen, P., Cinti, S., Spiegelman, B.M. (2011) Prdm16 determines the thermogenic program of subcutaneous white adipose tissue in mice. *J. Clin. Invest.* **121**: 96-105.
127. Wu, J., Boström, P., Sparks, L.M., Ye, L., Choi, J.H., Giang, A.H., Khandekar, M., Virtanen, K.A., Nuutila, P., Schaart, G., Huang, K., Tu, H., van Marken Lichtenbelt, W.D., Hoeks, J., Enerbäck, S., Schrauwen, P., Spiegelman, B.M. (2012) Beige adipocytes are a distinct type of thermogenic fat cell in mouse and human. *Cell* **150**: 366-376.
128. Lee, Y.H., Petkova, A.P., Mottillo, E.P., Granneman, J.G. (2012) In vivo identification of bipotential adipocyte progenitors recruited by  $\beta$ 3-adrenoceptor activation and high-fat feeding. *Cell Metab.* **15**: 480-491.
129. Harms, M., Seale, P. (2013) Brown and beige fat: development, function and therapeutic potential. *Nat. Med.* **19**: 1252-1263.
130. Wang, Q.A., Tao, C., Gupta, R.K., Scherer, P.E. (2013) Tracking adipogenesis during white adipose tissue development, expansion and regeneration. *Nat. Med.* **19**: 1338-1344.
131. Claussnitzer, M., Dankel, S.N., Kim, K.H., Quon, G., Meuleman, W., Haugen, C., Glunk, V., Sousa, I.S., Beaudry, J.L., Puvion, V., Abdennur, N.A., Liu, J., Svensson, P.A., Hsu, Y.H., Drucker, D.J., Mellgren, G., Hui, C.C., Hauner, H., Kellis, M. (2015) FTO Obesity Variant Circuitry and Adipocyte Browning in Humans. *N. Engl. J. Med.* **373**: 895-907.
132. Ishibashi, J., Seale, P. (2010) Beige can be slimming. *Science* **328**: 1113-1114.
133. Berry, R., Rodeheffer, M.S. (2013) Characterization of the adipocyte cellular lineage in vivo. *Nat. Cell Biol.* **15**: 302-308.
134. Stine, R.R., Shapira, S.N., Lim, H.W., Ishibashi, J., Harms, M., Won, K.J., Seale, P. (2015) EBF2 promotes the recruitment of beige adipocytes in white adipose tissue. *Mol. Metab.* **5**: 57-65.
135. Lynes, M.D., Tseng, Y.H. (2015) The Thermogenic Circuit: Regulators of Thermogenic Competency and Differentiation. *Genes Dis.* **2**: 164-172.
136. Cohen, P., Levy, J.D., Zhang, Y., Frontini, A., Kolodin, D.P., Svensson, K.J., Lo, J.C., Zeng, X., Ye, L., Khandekar, M.J., Wu, J., Gunawardana, S.C., Banks, A.S., Camporez, J.P., Jurczak, M.J.,

- Kajimura, S., Piston, D.W., Mathis, D., Cinti, S., Shulman, G.I., Seale, P., Spiegelman, B.M. (2014) Ablation of PRDM16 and beige adipose causes metabolic dysfunction and a subcutaneous to visceral fat switch. *Cell* **156**: 304-316.
137. Dempersmier, J., Sambeat, A., Gulyaeva, O., Paul, S.M., Hudak, C.S., Raposo, H.F., Kwan, H.Y., Kang, C., Wong, R.H., Sul, H.S. (2015) Cold-inducible Zfp516 activates UCP1 transcription to promote browning of white fat and development of brown fat. *Mol. Cell*. **57**: 235-246.
  138. Hallberg, M., Morganstein, D.L., Kiskinis, E., Shah, K., Kralli, A., Dilworth, S.M., White, R., Parker, M.G., Christian, M. (2008) A functional interaction between RIP140 and PGC-1alpha regulates the expression of the lipid droplet protein CIDEA. *Mol. Cell Biol.* **28**: 6785-6795.
  139. Scimè, A., Grenier, G., Huh, M.S., Gillespie, M.A., Bevilacqua, L., Harper, M.E., Rudnicki, M.A. (2005) Rb and p107 regulate preadipocyte differentiation into white versus brown fat through repression of PGC-1alpha. *Cell Metab.* **2**: 283-295.
  140. Villanueva, C.J., Vergnes, L., Wang, J., Drew, B.G., Hong, C., Tu, Y., Hu, Y., Peng, X., Xu, F., Saez, E., Wroblewski, K., Hevener, A.L., Reue, K., Fong, L.G., Young, S.G., Tontonoz, P. (2013) Adipose subtype-selective recruitment of TLE3 or Prdm16 by PPAR $\gamma$  specifies lipid storage versus thermogenic gene programs. *Cell Metab.* **17**: 423-435.
  141. Galmozzi, A., Mitro, N., Ferrari, A., Gers, E., Gilardi, F., Godio, C., Cermenati, G., Gualerzi, A., Donetti, E., Rotili, D., Valente, S., Guerrini, U., Caruso, D., Mai, A., Saez, E., De Fabiani, E., Crestani, M. (2013) Inhibition of class I histone deacetylases unveils a mitochondrial signature and enhances oxidative metabolism in skeletal muscle and adipose tissue. *Diabetes* **62**: 732-742.
  142. Shinoda, K., Ohyama, K., Hasegawa, Y., Chang, H.Y., Ogura, M., Sato, A., Hong, H., Hosono, T., Sharp, L.Z., Scheel, D.W., Graham, M., Ishihama, Y., Kajimura, S. (2015) Phosphoproteomics Identifies CK2 as a Negative Regulator of Beige Adipocyte Thermogenesis and Energy Expenditure. *Cell Metab.* **22**: 997-1008.
  143. Liu, W., Bi, P., Shan, T., Yang, X., Yin, H., Wang, Y.X., Liu, N., Rudnicki, M.A., Kuang, S. (2013) miR-133a regulates adipocyte browning in vivo. *PLoS Genet.* **9**: e1003626.
  144. Sun, L., Xie, H., Mori, M.A., Alexander, R., Yuan, B., Hattangadi, S.M., Liu, Q., Kahn, C.R., Lodish, H.F. (2011) Mir193b-365 is essential for brown fat differentiation. *Nat. Cell Biol.* **13**: 958-965.
  145. Yin, H., Pasut, A., Soleimani, V.D., Bentzinger, C.F., Antoun, G., Thorn, S., Seale, P., Fernando, P., van Ijcken, W., Grosveld, F., Dekemp, R.A., Boushel, R., Harper, M.E., Rudnicki, M.A. (2013) MicroRNA-133 controls brown adipose determination in skeletal muscle satellite cells by targeting Prdm16. *Cell Metab.* **17**: 210-24.
  146. Mori, M., Nakagami, H., Rodriguez-Araujo, G., Nimura, K., Kaneda, Y. (2012) Essential role for miR-196a in brown adipogenesis of white fat progenitor cells. *PLoS Biol.* **10**: e1001314.
  147. Chen, Y., Siegel, F., Kipschull, S., Haas, B., Fröhlich, H., Meister, G., Pfeifer, A. (2013) miR-155 regulates differentiation of brown and beige adipocytes via a bistable circuit. *Nat. Commun.* **4**: 1769.
  148. Hu, F., Wang, M., Xiao, T., Yin, B., He, L., Meng, W., Dong, M., Liu, F. (2015) miR-30 promotes thermogenesis and the development of beige fat by targeting RIP140. *Diabetes* **64**: 2056-2068.
  149. Pan, D., Mao, C., Quattrochi, B., Friedline, R.H., Zhu, L.J., Jung, D.Y., Kim, J.K., Lewis, B., Wang, Y.X. (2014) MicroRNA-378 controls classical brown fat expansion to counteract obesity. *Nat. Commun.* **5**: 4725.
  150. Alvarez-Dominguez, J.R., Bai, Z., Xu, D., Yuan, B., Lo, K.A., Yoon, M.J., Lim, Y.C., Knoll, M., Slavov, N., Chen, S., Chen, P., Lodish, H.F., Sun, L. (2015) De Novo Reconstruction of Adipose

- Tissue Transcriptomes Reveals Long Non-coding RNA Regulators of Brown Adipocyte Development. *Cell Metab.* **21**: 764-776.
151. Zhao, X.Y., Li, S., Wang, G.X., Yu, Q., Lin, J.D. (2014) A long noncoding RNA transcriptional regulatory circuit drives thermogenic adipocyte differentiation. *Mol. Cell* **55**: 372-382.
  152. Fu, T., Seok, S., Choi, S., Huang, Z., Suino-Powell, K., Xu, H.E., Kemper, B., Kemper, J.K. (2014) MicroRNA 34a inhibits beige and brown fat formation in obesity in part by suppressing adipocyte fibroblast growth factor 21 signaling and SIRT1 function. *Mol. Cell Biol.* **34**: 4130-4142.
  153. Karbiener, M., Pisani, D.F., Frontini, A., Oberreiter, L.M., Lang, E., Vegiopoulos, A., Mössenböck, K., Bernhardt, G.A., Mayr, T., Hildner, F., Grillari, J., Ailhaud, G., Herzig, S., Cinti, S., Amri, E.Z., Scheideler, M. (2014) MicroRNA-26 family is required for human adipogenesis and drives characteristics of brown adipocytes. *Stem Cells* **32**: 1578-1590.
  154. Long, J.Z., Svensson, K.J., Tsai, L., Zeng, X., Roh, H.C., Kong, X., Rao, R.R., Lou, J., Lokurkar, I., Baur, W., Castellot, J.J. Jr., Rosen, E.D., Spiegelman, B.M. (2014) A smooth muscle-like origin for beige adipocytes. *Cell Metab.* **19**: 810-20.
  155. Waldén, T.B., Hansen, I.R., Timmons, J.A., Cannon, B., Nedergaard, J. (2012) Recruited vs. nonrecruited molecular signatures of brown, "brite," and white adipose tissues. *Am. J. Physiol. Endocrinol. Metab.* **302**: E19-31.
  156. Rosenwald, M., Perdikari, A., Rülcke, T., Wolfrum, C. (2013) Bi-directional interconversion of brite and white adipocytes. *Nat. Cell Biol.* **15**: 659-667.
  157. Tvrdik, P., Asadi, A., Kozak, L.P., Nedergaard, J., Cannon, B., Jacobsson, A. (1997) Cig30, a mouse member of a novel membrane protein gene family, is involved in the recruitment of brown adipose tissue. *J. Biol. Chem.* **272**: 31738-31746.
  158. Waldén, T.B., Petrovic, N., Nedergaard, J. (2010) PPARalpha does not suppress muscle-associated gene expression in brown adipocytes but does influence expression of factors that fingerprint the brown adipocyte. *Biochem. Biophys. Res. Commun.* **397**: 146-151.
  159. Cypess, A.M., White, A.P., Vernochet, C., Schulz, T.J., Xue, R., Sass, C.A., Huang, T.L., Roberts-Toler, C., Weiner, L.S., Sze, C., Chacko, A.T., Deschamps, L.N., Herder, L.M., Truchan, N., Glasgow, A.L., Holman, A.R., Gavrilu, A., Hasselgren, P.O., Mori, M.A., Molla, M., Tseng, Y.H. (2013) Anatomical localization, gene expression profiling and functional characterization of adult human neck brown fat. *Nat. Med.* **19**: 635-639.
  160. Lidell, M.E., Betz, M.J., Dahlqvist Leinhard, O., Heglind, M., Elander, L., Slawik, M., Mussack, T., Nilsson, D., Romu, T., Nuutila, P., Virtanen, K.A., Beuschlein, F., Persson, A., Borga, M., Enerbäck, S. (2013) Evidence for two types of brown adipose tissue in humans. *Nat. Med.* **19**: 631-634.
  161. Sharp, L.Z., Shinoda, K., Ohno, H., Scheel, D.W., Tomoda, E., Ruiz, L., Hu, H., Wang, L., Pavlova, Z., Gilsanz, V., Kajimura, S. (2012) Human BAT possesses molecular signatures that resemble beige/brite cells. *PLoS One* **7**: e49452.
  162. Shinoda, K., Luijten, I.H., Hasegawa, Y., Hong, H., Sonne, S.B., Kim, M., Xue, R., Chondronikola, M., Cypess, A.M., Tseng, Y.H., Nedergaard, J., Sidossis, L.S., Kajimura, S. (2015) Genetic and functional characterization of clonally derived adult human brown adipocytes. *Nat. Med.* **21**: 389-394.
  163. Ussar, S., Lee, K.Y., Dankel, S.N., Boucher, J., Haering, M.F., Kleinridders, A., Thomou, T., Xue, R., Macotela, Y., Cypess, A.M., Tseng, Y.H., Mellgren, G., Kahn, C.R. (2014) ASC-1, PAT2, and P2RX5 are cell surface markers for white, beige, and brown adipocytes. *Sci. Transl. Med.* **6**: 247ra103.

164. Shabalina, I.G., Petrovic, N., de Jong, J.M., Kalinovich, A.V., Cannon, B., Nedergaard, J. (2013) UCP1 in brite/beige adipose tissue mitochondria is functionally thermogenic. *Cell Rep.* **5**: 1196-1203.
165. Estabrook, R.W., Sacktor, B. (1958) alpha-Glycerophosphate oxidase of flight muscle mitochondria. *J. Biol. Chem.* **233**: 1014-1019.
166. Ringler, R.L., Singer, T.P. (1959) Studies on the mitochondrial alpha-glycerophosphate dehydrogenase. I. Reaction of the dehydrogenase with electron acceptors and the respiratory chain. *J. Biol. Chem.* **234**: 2211-2217.
167. Lee, Y.P., Lardy, H.A. (1965) Influence of thyroid hormones on L-alpha-glycerophosphate dehydrogenases and other dehydrogenases in various organs of the rat. *J. Biol. Chem.* **240**: 1427-1436.
168. Lardy, H., Shrago, E. (1990) Biochemical aspects of obesity. *Annu. Rev. Biochem.* **59**: 689-710.
169. Anunciado-Koza, R., Ukropec, J., Koza, R.A., Kozak, L.P. (2008) Inactivation of UCP1 and the glycerol phosphate cycle synergistically increases energy expenditure to resist diet-induced obesity. *J. Biol. Chem.* **283**: 27688-27697.
170. Block, B.A. (1994) Thermogenesis in muscle. *Annu. Rev. Physiol.* **56**:535-77.
171. Block, B.A., O'Brien, J., Meissner, G. (1994) Characterization of the sarcoplasmic reticulum proteins in the thermogenic muscles of fish. *J. Cell. Biol.* **127**: 1275-1287.
172. de Meis, L., Arruda, A.P., da Costa, R.M., Benchimol, M. (2006) Identification of a Ca<sup>2+</sup>-ATPase in brown adipose tissue mitochondria: regulation of thermogenesis by ATP and Ca<sup>2+</sup>. *J. Biol. Chem.* **281**: 16384-16390.
173. Bal, N.C., Maurya, S.K., Sopariwala, D.H., Sahoo, S.K., Gupta, S.C., Shaikh, S.A., Pant, M., Rowland, L.A., Bombardier, E., Goonasekera, S.A., Tupling, A.R., Molkentin, J.D., Periasamy, M. (2012) Sarcolipin is a newly identified regulator of muscle-based thermogenesis in mammals. *Nat. Med.* **18**: 1575-1579.
174. Dulloo, A.G., Gubler, M., Montani, J.P., Seydoux, J., Solinas, G. (2004) Substrate cycling between de novo lipogenesis and lipid oxidation: a thermogenic mechanism against skeletal muscle lipotoxicity and glucolipotoxicity. *Int. J. Obes. Relat. Metab. Disord.* **28 Suppl 4**:S29-37.
175. Flachs, P., Rühl, R., Hensler, M., Janovska, P., Zouhar, P., Kus, V., Macek Jilkova, Z., Papp, E., Kuda, O., Svobodova, M., Rossmeisl, M., Tsenov, G., Mohamed-Ali, V., Kopecky, J. (2011) Synergistic induction of lipid catabolism and anti-inflammatory lipids in white fat of dietary obese mice in response to calorie restriction and n-3 fatty acids. *Diabetologia* **54**: 2626-2638.
176. Jacobus, W.E., Lehninger, A.L. (1973) Creatine kinase of rat heart mitochondria. Coupling of creatine phosphorylation to electron transport. *J. Biol. Chem.* **248**: 4803-4810.
177. Berlet HH, Bonsmann I, Birringer H. (1976) Occurrence of free creatine, phosphocreatine and creatine phosphokinase in adipose tissue. *Biochim. Biophys. Acta.* **437**: 166-174.
178. Terblanche, S.E., Masondo, T.C., Nel, W. (1998) Effects of cold acclimation on the activity levels of creatine kinase, lactate dehydrogenase and lactate dehydrogenase isoenzymes in various tissues of the rat. *Cell Biol. Int.* **22**: 701-707.
179. Kazak, L., Chouchani, E.T., Jedrychowski, M.P., Erickson, B.K., Shinoda, K., Cohen, P., Vetrivelan, R., Lu, G.Z., Laznik-Bogoslavski, D., Hasenfuss, S.C., Kajimura, S., Gygi, S.P., Spiegelman, B.M. (2015) A creatine-driven substrate cycle enhances energy expenditure and thermogenesis in beige fat. *Cell* **163**: 643-655.
180. Haslam, D.W., James, W.P. (2005) Obesity. *Lancet* **366**: 1197-1209.
181. Park, J., Euhus, D.M., Scherer, P.E. (2011) Paracrine and endocrine effects of adipose tissue on cancer development and progression. *Endocr. Rev.* **32**: 550-570.
182. Steg, P.G., James, S.K., Atar, D., Badano, L.P., Blömqstrom-Lundqvist, C., Borger, M.A., Di Mario, C., Dickstein, K., Ducrocq, G., Fernandez-Aviles, F., Gershlick, A.H., Giannuzzi, P.,

- Halvorsen, S., Huber, K., Juni, P., Kastrati, A., Knuuti, J., Lenzen, M.J., Mahaffey, K.W., Valgimigli, M., van 't Hof, A., Widimsky, P., Zahger, D. (2012) ESC Guidelines for the management of acute myocardial infarction in patients presenting with ST-segment elevation. Task Force on the management of ST-segment elevation acute myocardial infarction of the European Society of Cardiology (ESC). *Eur. Heart J.* **33**: 2569-2619.
183. Balogh, S., Papp, R., Jozan, P., Csaszar, A. (2010) Continued improvement of cardiovascular mortality in Hungary--impact of increased cardio-metabolic prescriptions. *BMC Public Health* **10**:422.
184. Nagy, V. (2013) Epidemiology and treatment of chronic heart failure; use of bisoprolol. *Orv. Hetil.* **154**: 1731-1734.
185. Bényi, M., Kéki, Zs., Hangay, I., Kókai, Z. (2012) Obesity related increase in diseases in Hungary studied by the Health Interview Survey 2009. *Orv. Hetil.* **153**: 768-775.
186. Iski, G., Rurik, I. (2014) The estimated economic burden of overweight and obesity in Hungary. *Orv. Hetil.* **155**: 1406-1412.
187. Tóth, E., Nagy, B. (2009) Health economic approach to obesity. [Az elhízás egészség-gazdaságtani megközelítése.] *Egészségügyi Gazdasági Szemle* **47**: 41-48.
188. Harper, J.A., Dickinson, K., Brand, M.D. (2001) Mitochondrial uncoupling as a target for drug development for the treatment of obesity. *Obes. Rev.* **2**: 255-265.
189. Aherne, W., Hull, D. (1964) The site of heat production in the newborn infant. *Proc. R. Soc. Med.* **57**: 1172-1173.
190. Heim, T., Kellermayer, M., Dani, M. (1968) Thermal conditions and the mobilization of lipids from brown and white adipose tissue in the human neonate. *Acta Paediatr. Acad. Sci. Hung.* **9**: 109-120.
191. Heaton, J.M. (1972) The distribution of brown adipose tissue in the human. *J. Anat.* **112**: 35-39.
192. Huttunen, P., Hirvonen, J., Kinnula, V. (1981) The occurrence of brown adipose tissue in outdoor workers. *Eur. J. Appl. Physiol. Occup. Physiol.* **46**: 339-345.
193. Nedergaard, J., Bengtsson, T., Cannon, B. (2007) Unexpected evidence for active brown adipose tissue in adult humans. *Am. J. Physiol. Endocrinol. Metab.* **293**: E444-452.
194. Hany, T.F., Gharehpapagh, E., Kamel, E.M., Buck, A., Himms-Hagen, J., von Schulthess, G.K. (2002) Brown adipose tissue: a factor to consider in symmetrical tracer uptake in the neck and upper chest region. *Eur. J. Nucl. Med. Mol. Imaging* **29**: 1393-1398.
195. Cypess, A.M., Lehman, S., Williams, G., Tal, I., Rodman, D., Goldfine, A.B., Kuo, F.C., Palmer, E.L., Tseng, Y.H., Doria, A., Kolodny, G.M., Kahn, C.R. (2009) Identification and importance of brown adipose tissue in adult humans. *N. Engl. J. Med.* **360**: 1509-1517.
196. van Marken Lichtenbelt, W.D., Vanhommelrig, J.W., Smulders, N.M., Drossaerts, J.M., Kemerink, G.J., Bouvy, N.D., Schrauwen, P., Teule, G.J. (2009) Cold-activated brown adipose tissue in healthy men. *N. Engl. J. Med.* **360**: 1500-1508.
197. Virtanen, K.A., Lidell, M.E., Orava, J., Heglind, M., Westergren, R., Niemi, T., Taittonen, M., Laine, J., Savisto, N.J., Enerbäck, S., Nuutila, P. (2009) Functional brown adipose tissue in healthy adults. *N. Engl. J. Med.* **360**: 1518-1525.
198. Saito, M., Okamatsu-Ogura, Y., Matsushita, M., Watanabe, K., Yoneshiro, T., Nio-Kobayashi, J., Iwanaga, T., Miyagawa, M., Kameya, T., Nakada, K., Kawai, Y., Tsujisaki, M. (2009) High incidence of metabolically active brown adipose tissue in healthy adult humans: effects of cold exposure and adiposity. *Diabetes* **58**: 1526-1531.
199. Admiraal, W.M., Holleman, F., Bahler, L., Soeters, M.R., Hoekstra, J.B., Verberne, H.J. (2013) Combining 123I-metaiodobenzylguanidine SPECT/CT and 18F-FDG PET/CT for the assessment of brown adipose tissue activity in humans during cold exposure. *J. Nucl. Med.* **54**: 208-212.



200. Admiraal, W.M., Verberne, H.J., Karamat, F.A., Soeters, M.R., Hoekstra, J.B., Holleman, F. (2013) Cold-induced activity of brown adipose tissue in young lean men of South-Asian and European origin. *Diabetologia* **56**: 2231-2237.
201. Lee, P., Greenfield, J.R., Ho, K.K., Fulham, M.J. (2010) A critical appraisal of the prevalence and metabolic significance of brown adipose tissue in adult humans. *Am. J. Physiol. Endocrinol. Metab.* **299**: E601-606.
202. Matsushita, M., Yoneshiro, T., Aita, S., Kameya, T., Sugie, H., Saito, M. (2013) Impact of brown adipose tissue on body fatness and glucose metabolism in healthy humans. *Int. J. Obes. (Lond)*. **38**: 812-817.
203. Ouellet, V., Routhier-Labadie, A., Bellemare, W., Lakhal-Chaieb, L., Turcotte, E., Carpentier, A.C., Richard, D. (2011) Outdoor temperature, age, sex, body mass index, and diabetic status determine the prevalence, mass, and glucose-uptake activity of 18F-FDG-detected BAT in humans. *J. Clin. Endocrinol. Metab.* **96**: 192-199.
204. Yoneshiro, T., Aita, S., Matsushita, M., Kayahara, T., Kameya, T., Kawai, Y., Iwanaga, T., Saito, M. (2013) Recruited brown adipose tissue as an antiobesity agent in humans. *J. Clin. Invest.* **123**: 3404-3408.
205. Chondronikola, M., Volpi, E., Børsheim, E., Porter, C., Annamalai, P., Enerbäck, S., Lidell, M.E., Saraf, M.K., Labbe, S.M., Hurren, N.M., Yfanti, C., Chao, T., Andersen, C.R., Cesani, F., Hawkins, H., Sidossis, L.S. (2014) Brown adipose tissue improves whole-body glucose homeostasis and insulin sensitivity in humans. *Diabetes* **63**: 4089-4099.
206. Lee, P., Smith, S., Linderman, J., Courville, A.B., Brychta, R.J., Dieckmann, W., Werner, C.D., Chen, K.Y., Celi, F.S. (2014) Temperature-acclimated brown adipose tissue modulates insulin sensitivity in humans. *Diabetes* **63**: 3686-3698.
207. van Marken Lichtenbelt, W.D., Schrauwen, P. (2011) Implications of nonshivering thermogenesis for energy balance regulation in humans. *Am. J. Physiol. Regul. Integr. Comp. Physiol.* **301**: R285-296.
208. Yoneshiro, T., Aita, S., Matsushita, M., Okamatsu-Ogura, Y., Kameya, T., Kawai, Y., Miyagawa, M., Tsujisaki, M., Saito, M. (2011) Age-related decrease in cold-activated brown adipose tissue and accumulation of body fat in healthy humans. *Obesity (Silver Spring)*. **19**: 1755-1760.
209. Rogers, N.H., Landa, A., Park, S., Smith, R.G. (2012) Aging leads to a programmed loss of brown adipocytes in murine subcutaneous white adipose tissue. *Aging Cell* **11**: 1074-1083.
210. Whittle, A.J., López, M., Vidal-Puig, A. (2011) Using brown adipose tissue to treat obesity - the central issue. *Trends. Mol. Med.* **17**: 405-411.
211. Lee, P., Swarbrick, M.M., Ho, K.K. (2013) Brown adipose tissue in adult humans: a metabolic renaissance. *Endocr. Rev.* **34**: 413-438.
212. van Marken Lichtenbelt, W.D., Kingma, B., van der Lans, A., Schellen, L. (2014) Cold exposure - an approach to increasing energy expenditure in humans. *Trends. Endocrinol. Metab.* **25**: 165-167.
213. Schrauwen, P., van Marken Lichtenbelt, W.D., Spiegelman, B.M. (2015) The future of brown adipose tissues in the treatment of type 2 diabetes. *Diabetologia* **58**: 1704-1707.
214. Svensson, P.A., Jernås, M., Sjöholm, K., Hoffmann, J.M., Nilsson, B.E., Hansson, M., Carlsson, L.M. (2011) Gene expression in human brown adipose tissue. *Int. J. Mol. Med.* **27**: 227-232.
215. Lee, P., Werner, C.D., Kebebew, E., Celi, F.S. (2014) Functional thermogenic beige adipogenesis is inducible in human neck fat. *Int. J. Obes. (Lond)*. **38**: 170-176.
216. Min, S.Y., Kady, J., Nam, M., Rojas-Rodriguez, R., Berkenwald, A., Kim, J.H., Noh, H.L., Kim, J.K., Cooper, M.P., Fitzgibbons, T., Brehm, M.A., Corvera, S. (2016) Human 'brite/beige' adipocytes

- develop from capillary networks, and their implantation improves metabolic homeostasis in mice. *Nat. Med.* **22**: 312-318.
217. Vosselman, M.J., van der Lans, A.A., Brans, B., Wierts, R., van Baak, M.A., Schrauwen, P., van Marken Lichtenbelt, W.D. (2012) Systemic  $\beta$ -adrenergic stimulation of thermogenesis is not accompanied by brown adipose tissue activity in humans. *Diabetes* **61**: 3106-3113.
  218. Cypess, A.M., Chen, Y.C., Sze, C., Wang, K., English, J., Chan, O., Holman, A.R., Tal, I., Palmer, M.R., Kolodny, G.M., Kahn, C.R. (2012) Cold but not sympathomimetics activates human brown adipose tissue in vivo. *Proc. Natl. Acad. Sci. USA* **109**: 10001-10005.
  219. Cypess, A.M., Weiner, L.S., Roberts-Toler, C., Franquet Elia, E., Kessler, S.H., Kahn, P.A., English, J., Chatman, K., Trauger, S.A., Doria, A., Kolodny, G.M. (2015) Activation of human brown adipose tissue by a  $\beta$ 3-adrenergic receptor agonist. *Cell Metab.* **21**: 33-38.
  220. Yoneshiro, T., Aita, S., Kawai, Y., Iwanaga, T., Saito, M. (2012) Nonpungent capsaicin analogs (capsinoids) increase energy expenditure through the activation of brown adipose tissue in humans. *Am. J. Clin. Nutr.* **95**: 845-850.
  221. Saito, M., Yoneshiro, T. (2013) Capsinoids and related food ingredients activating brown fat thermogenesis and reducing body fat in humans. *Curr. Opin. Lipidol.* **24**: 71-77.
  222. Yoneshiro, T., Saito, M. (2013) Transient receptor potential activated brown fat thermogenesis as a target of food ingredients for obesity management. *Curr. Opin. Clin. Nutr. Metab. Care.* **16**: 625-631.
  223. Saito, M., Yoneshiro, T., Matsushita, M. (2015) Food Ingredients as Anti-Obesity Agents. *Trends. Endocrinol. Metab.* **26**: 585-587.
  224. Ohyama, K., Nogusa, Y., Shinoda, K., Suzuki, K., Bannai, M., Kajimura, S. (2016) A Synergistic Antiobesity Effect by a Combination of Capsinoids and Cold Temperature Through Promoting Beige Adipocyte Biogenesis. *Diabetes* **65**: 1410-1423.
  225. Wang, G.X., Zhao, X.Y., Meng, Z.X., Kern, M., Dietrich, A., Chen, Z., Cozacov, Z., Zhou, D., Okunade, A.L., Su, X., Li, S., Blüher, M., Lin, J.D. (2014) The brown fat-enriched secreted factor Nrg4 preserves metabolic homeostasis through attenuation of hepatic lipogenesis. *Nat. Med.* **20**: 1436-1443.
  226. Stanford, K.I., Middelbeek, R.J., Townsend, K.L., An, D., Nygaard, E.B., Hitchcox, K.M., Markan, K.R., Nakano, K., Hirshman, M.F., Tseng, Y.H., Goodyear, L.J. (2013) Brown adipose tissue regulates glucose homeostasis and insulin sensitivity. *J. Clin. Invest.* **123**: 215-223.
  227. Stanford, K.I., Middelbeek, R.J., Townsend, K.L., Lee, M.Y., Takahashi, H., So, K., Hitchcox, K.M., Markan, K.R., Hellbach, K., Hirshman, M.F., Tseng, Y.H., Goodyear, L.J. (2015) A novel role for subcutaneous adipose tissue in exercise-induced improvements in glucose homeostasis. *Diabetes* **64**: 2002-2014.
  228. Collins, S. (2012)  $\beta$ -Adrenoceptor Signaling Networks in Adipocytes for Recruiting Stored Fat and Energy Expenditure. *Front. Endocrinol. (Lausanne)* **2**:102.
  229. Nguyen, K.D., Qiu, Y., Cui, X., Goh, Y.P., Mwangi, J., David, T., Mukundan, L., Brombacher, F., Locksley, R.M., Chawla, A. (2011) Alternatively activated macrophages produce catecholamines to sustain adaptive thermogenesis. *Nature* **480**: 104-108.
  230. Hogan, S., Himms-Hagen, J. (1983) Brown adipose tissue of mice with gold thioglucose-induced obesity: effect of cold and diet. *Am. J. Physiol.* **244**: E581-588.
  231. Sakaguchi, T., Takahashi, M., Bray, G.A. (1988) Diurnal changes in sympathetic activity. Relation to food intake and to insulin injected into the ventromedial or suprachiasmatic nucleus. *J. Clin. Invest.* **82**: 282-286.

232. Shido, O., Yoneda, Y., Nagasaka, T. (1989) Changes in brown adipose tissue metabolism following intraventricular vasoactive intestinal peptide and other gastrointestinal peptides in rats. *Jpn. J. Physiol.* **39**: 359-369.
233. Erlanson-Albertsson, C., Larsson, A. (1988) A possible physiological function of pancreatic pro-colipase activation peptide in appetite regulation. *Biochimie* **70**: 1245-1250.
234. Slot, J.W., Geuze, H.J., Gigengack, S., Lienhard, G.E., James, D.E. (1991) Immuno-localization of the insulin regulatable glucose transporter in brown adipose tissue of the rat. *J. Cell Biol.* **113**: 123-135.
235. Omatsu-Kanbe, M., Zarnowski, M.J., Cushman, S.W. (1996) Hormonal regulation of glucose transport in a brown adipose cell preparation isolated from rats that shows a large response to insulin. *Biochem. J.* **315**: 25-31.
236. Teruel, T., Valverde, A.M., Benito, M., Lorenzo, M. (1996) Insulin-like growth factor I and insulin induce adipogenic-related gene expression in fetal brown adipocyte primary cultures. *Biochem. J.* **319**: 627-632.
237. Fasshauer, M., Klein, J., Kriauciunas, K.M., Ueki, K., Benito, M., Kahn, C.R. (2001) Essential role of insulin receptor substrate 1 in differentiation of brown adipocytes. *Mol. Cell Biol.* **21**: 319-329.
238. Mur, C., Arribas, M., Benito, M., Valverde, A.M. (2003) Essential role of insulin-like growth factor I receptor in insulin-induced fetal brown adipocyte differentiation. *Endocrinology* **144**: 581-593.
239. Tseng, Y.H., Kriauciunas, K.M., Kokkotou, E., Kahn, C.R. (2004) Differential roles of insulin receptor substrates in brown adipocyte differentiation. *Mol. Cell Biol.* **24**: 1918-1929.
240. Tseng, Y.H., Butte, A.J., Kokkotou, E., Yeheor, V.K., Taniguchi, C.M., Kriauciunas, K.M., Cypess, A.M., Niinobe, M., Yoshikawa, K., Patti, M.E., Kahn, C.R. (2005) Prediction of preadipocyte differentiation by gene expression reveals role of insulin receptor substrates and necdin. *Nat. Cell Biol.* **7**: 601-611.
241. Yadav, H., Quijano, C., Kamaraju, A.K., Gavrilova, O., Malek, R., Chen, W., Zervas, P., Zhigang, D., Wright, E.C., Stuelten, C., Sun, P., Lonning, S., Skarulis, M., Sumner, A.E., Finkel, T., Rane, S.G. (2011) Protection from obesity and diabetes by blockade of TGF- $\beta$ /Smad3 signaling. *Cell Metab.* **14**: 67-79.
242. Koncarevic, A., Kajimura, S., Cornwall-Brady, M., Andreucci, A., Pullen, A., Sako, D., Kumar, R., Grinberg, A.V., Liharska, K., Ucran, J.A., Howard, E., Spiegelman, B.M., Sehra, J., Lachey J. (2012) A novel therapeutic approach to treating obesity through modulation of TGF $\beta$  signaling. *Endocrinology* **153**: 3133-3146.
243. Pelleymounter, M.A., Cullen, M.J., Baker, M.B., Hecht, R., Winters, D., Boone, T., Collins, F. (1995) Effects of the obese gene product on body weight regulation in ob/ob mice. *Science* **269**: 540-543.
244. Halaas, J.L., Gajiwala, K.S., Maffei, M., Cohen, S.L., Chait, B.T., Rabinowitz, D., Lallone, R.L., Burley, S.K., Friedman, J.M. (1995) Weight-reducing effects of the plasma protein encoded by the obese gene. *Science* **269**: 543-546.
245. Satoh, N., Ogawa, Y., Katsuura, G., Numata, Y., Masuzaki, H., Yoshimasa, Y., Nakao, K. (1998) Satiety effect and sympathetic activation of leptin are mediated by hypothalamic melanocortin system. *Neurosci. Lett.* **249**: 107-110.
246. Minokoshi, Y., Haque, M.S., Shimazu, T. (1999) Microinjection of leptin into the ventromedial hypothalamus increases glucose uptake in peripheral tissues in rats. *Diabetes* **48**: 287-291.

247. Commins, S.P., Watson, P.M., Frampton, I.C., Gettys, T.W. (2001) Leptin selectively reduces white adipose tissue in mice via a UCP1-dependent mechanism in brown adipose tissue. *Am. J. Physiol. Endocrinol. Metab.* **280**: E372-377.
248. Fischer, A.W., Hoefig, C.S., Abreu-Vieira, G., de Jong, J.M., Petrovic, N., Mittag, J., Cannon, B., Nedergaard, J. (2016) Leptin Raises Defended Body Temperature without Activating Thermogenesis. *Cell Rep.* **14**: 1621-1631.
249. Feldman D. (1978) Evidence that brown adipose tissue is a glucocorticoid target organ. *Endocrinology* **103**: 2091-2097.
250. Madiehe, A.M., Lin, L., White, C., Braymer, H.D., Bray, G.A., York, D.A. (2001) Constitutive activation of STAT-3 and downregulation of SOCS-3 expression induced by adrenalectomy. *Am. J. Physiol. Regul. Integr. Comp. Physiol.* **281**: R2048-2058.
251. Heick, H.M., Vachon, C., Kallai, M.A., Bégin-Heick, N., LeBlanc, J. (1973) The effects of thyroxine and isopropylnoradrenaline on cytochrome oxidase activity in brown adipose tissue. *Can. J. Physiol. Pharmacol.* **51**: 751-758.
252. Sundin, U. (1981) GDP binding to rat brown fat mitochondria: effects of thyroxine at different ambient temperatures. *Am. J. Physiol.* **241**: C134-139.
253. Abelenda, M., Puerta, M.L. (1992) Brown adipose tissue thermogenesis in T3-treated rats. *Horm. Metab. Res.* **24**: 60-62.
254. Branco, M., Ribeiro, M., Negrão, N., Bianco, A.C. (1999) 3,5,3'-Triiodothyronine actively stimulates UCP in brown fat under minimal sympathetic activity. *Am. J. Physiol.* **276**: E179-187.
255. Székely, M. (1970) Effects of thyroxine treatment of different duration on oxygen consumption and body temperature at different ambient temperatures in the rat. *Acta Physiol. Acad. Sci. Hung.* **37**: 51-55.
256. Nedergaard, J., Dicker, A., Cannon, B. (1997) The interaction between thyroid and brown-fat thermogenesis. Central or peripheral effects? *Ann. NY Acad. Sci.* **813**: 712-717.
257. López, M., Varela, L., Vázquez, M.J., Rodríguez-Cuenca, S., González, C.R., Velagapudi, V.R., Morgan, D.A., Schoenmakers, E., Agassandian, K., Lage, R., Martínez de Morentin, P.B., Tovar, S., Nogueiras, R., Carling, D., Lelliott, C., Gallego, R., Oresic, M., Chatterjee, K., Saha, A.K., Rahmouni, K., Diéguez, C., Vidal-Puig, A. (2010) Hypothalamic AMPK and fatty acid metabolism mediate thyroid regulation of energy balance. *Nat. Med.* **16**: 1001-1008.
258. Alvarez-Crespo, M., Csikasz, R.I., Martínez-Sánchez, N., Diéguez, C., Cannon, B., Nedergaard, J., López, M. (2016) Essential role of UCP1 modulating the central effects of thyroid hormones on energy balance. *Mol. Metab.* **5**: 271-282.
259. Tecott, L.H. (2007) Serotonin and the orchestration of energy balance. *Cell Metab.* **6**: 352-361.
260. Hodges, M.R., Tattersall, G.J., Harris, M.B., McEvoy, S.D., Richerson, D.N., Deneris, E.S., Johnson, R.L., Chen, Z.F., Richerson, G.B. (2008) Defects in breathing and thermoregulation in mice with near-complete absence of central serotonin neurons. *J. Neurosci.* **28**: 2495-2505.
261. Heal, D.J., Aspley, S., Prow, M.R., Jackson, H.C., Martin, K.F., Cheetham, S.C. (1998) Sibutramine: a novel anti-obesity drug. A review of the pharmacological evidence to differentiate it from d-amphetamine and d-fenfluramine. *Int. J. Obes. Relat. Metab. Disord.* **22 Suppl 1**: S18-28.
262. Connolly, H.M., Crary, J.L., McGoon, M.D., Hensrud, D.D., Edwards, B.S., Edwards, W.D., Schaff, H.V. (1997) Valvular heart disease associated with fenfluramine-phentermine. *N. Engl. J. Med.* **337**: 581-588.
263. James, W.P., Caterson, I.D., Coutinho, W., Finer, N., Van Gaal, L.F., Maggioni, A.P., Torp-Pedersen, C., Sharma, A.M., Shepherd, G.M., Rode, R.A., Renz, C.L.; SCOUT Investigators. (2010)

- Effect of sibutramine on cardiovascular outcomes in overweight and obese subjects. *N. Engl. J. Med.* **363**: 905-917.
264. Crane, J.D., Palanivel, R., Mottillo, E.P., Bujak, A.L., Wang, H., Ford, R.J., Collins, A., Blümer, R.M., Fullerton, M.D., Yabut, J.M., Kim, J.J., Ghia, J.E., Hamza, S.M., Morrison, K.M., Schertzer, J.D., Dyck, J.R., Khan, W.I., Steinberg, G.R. (2015) Inhibiting peripheral serotonin synthesis reduces obesity and metabolic dysfunction by promoting brown adipose tissue thermogenesis. *Nat. Med.* **21**: 166-172.
  265. Oh, C.M., Namkung, J., Go, Y., Shong, K.E., Kim, K., Kim, H., Park, B.Y., Lee, H.W., Jeon, Y.H., Song, J., Shong, M., Yadav, V.K., Karsenty, G., Kajimura, S., Lee, I.K., Park, S., Kim, H. (2015) Regulation of systemic energy homeostasis by serotonin in adipose tissues. *Nat. Commun.* **6**: 6794.
  266. Namkung, J., Kim, H., Park, S. (2015) Peripheral Serotonin: a New Player in Systemic Energy Homeostasis. *Mol. Cells* **38**: 1023-1028.
  267. Naheed, M., Green, B. (2001) Focus on clozapine. *Curr. Med. Res. Opin.* **17**: 223-229.
  268. Correll, C.U. (2010) From receptor pharmacology to improved outcomes: individualising the selection, dosing, and switching of antipsychotics. *Eur. Psychiatry* **25 Suppl 2**:S12-21.
  269. Taly, A. (2013) Novel approaches to drug design for the treatment of schizophrenia. *Expert Opin. Drug Discov.* **8**: 1285-1296.
  270. Casey, D.E., Haupt, D.W., Newcomer, J.W., Henderson, D.C., Sernyak, M.J., Davidson, M., Lindenmayer, J.P., Manoukian, S.V., Banerji, M.A., Lebovitz, H.E., Hennekens, C.H. (2004) Antipsychotic-induced weight gain and metabolic abnormalities: implications for increased mortality in patients with schizophrenia. *J. Clin. Psychiatry* **65 Suppl 7**:4-18.
  271. Newcomer, J.W. (2005) Second-generation (atypical) antipsychotics and metabolic effects: a comprehensive literature review. *CNS Drugs* **19 Suppl 1**:1-93.
  272. De Hert, M., Schreurs, V., Sweers, K., Van Eyck, D., Hanssens, L., Sinko, S., Wampers, M., Scheen, A., Peuskens, J., van Winkel, R. (2008) Typical and atypical antipsychotics differentially affect long-term incidence rates of the metabolic syndrome in first-episode patients with schizophrenia: a retrospective chart review. *Schizophr. Res.* **101**: 295-303.
  273. Gohlke, J.M., Dhurandhar, E.J., Correll, C.U., Morrato, E.H., Newcomer, J.W., Remington, G., Nasrallah, H.A., Crystal, S., Nicol, G; Adipogenic and Metabolic Effects of APDs Conference Speakers, Allison, D.B. (2012) Recent advances in understanding and mitigating adipogenic and metabolic effects of antipsychotic drugs. *Front. Psychiatry* **3**: 62.
  274. Mathur, N., Pedersen, B.K. (2008) Exercise as a mean to control low-grade systemic inflammation. *Mediators. Inflamm.* **2008**:109502
  275. Brandt, C., Pedersen, B.K. (2010) The role of exercise-induced myokines in muscle homeostasis and the defense against chronic diseases. *J. Biomed. Biotechnol.* **2010**:520258.
  276. Febbraio, M.A., Pedersen, B.K. (2002) Muscle-derived interleukin-6: mechanisms for activation and possible biological roles. *FASEB J.* **16**: 1335-1347.
  277. Pedersen, B.K., Febbraio, M.A. (2012) Muscles, exercise and obesity: skeletal muscle as a secretory organ. *Nat. Rev. Endocrinol.* **8**: 457-465.
  278. Contreras, C., Gonzalez, F., Fernø, J., Diéguez, C., Rahmouni, K., Nogueiras, R., López, M. (2015) The brain and brown fat. *Ann. Med.* **47**: 150-168.
  279. Gamas, L., Matafome, P., Seica, R. (2015) Irisin and Myonectin Regulation in the Insulin Resistant Muscle: Implications to Adipose Tissue: Muscle Crosstalk. *J. Diabetes Res.* **2015**: 359159.
  280. Kozak, L.P., Young, M.E. (2012) Heat from calcium cycling melts fat. *Nat. Med.* **18**: 1458-1459.

281. Aydin, S., Kuloglu, T., Aydin, S., Eren, M.N., Celik, A., Yilmaz, M., Kalayci, M., Sahin, I., Gungor, O., Gurel, A., Ogeturk, M., Dabak, O. (2014) Cardiac, skeletal muscle and serum irisin responses to with or without water exercise in young and old male rats: cardiac muscle produces more irisin than skeletal muscle. *Peptides* **52**: 68-73.
282. Zhang, Y., Li, R., Meng, Y., Li, S., Donelan, W., Zhao, Y., Qi, L., Zhang, M., Wang, X., Cui, T., Yang, L.J., Tang, D. (2014) Irisin stimulates browning of white adipocytes through mitogen-activated protein kinase p38 MAP kinase and ERK MAP kinase signaling. *Diabetes* **63**: 514-525.
283. Raschke, S., Elsen, M., Gassenhuber, H., Sommerfeld, M., Schwahn, U., Brockmann, B., Jung, R., Wisløff, U., Tjønn, A.E., Raastad, T., Hallén, J., Norheim, F., Drevon, C.A., Romacho, T., Eckardt, K., Eckel, J. (2013) Evidence against a beneficial effect of irisin in humans. *PLoS One* **8**: e73680.
284. Park, K.H., Zaichenko, L., Brinkoetter, M., Thakkar, B., Sahin-Efe, A., Joung, K.E., Tsoukas, M.A., Geladari, E.V., Huh, J.Y., Dincer, F., Davis, C.R., Crowell, J.A., Mantzoros, C.S. (2013) Circulating irisin in relation to insulin resistance and the metabolic syndrome. *J. Clin. Endocrinol. Metab.* **98**: 4899-4907.
285. Liu, J.J., Wong, M.D., Toy, W.C., Tan, C.S., Liu, S., Ng, X.W., Tavintharan, S., Sum, C.F., Lim, S.C. (2013) Lower circulating irisin is associated with type 2 diabetes mellitus. *J. Diabetes Complications* **27**: 365-369.
286. Wu, J., Spiegelman, B.M. (2014) Irisin ERKs the fat. *Diabetes* **63**: 381-383.
287. Ebert, T., Focke, D., Petroff, D., Wurst, U., Richter, J., Bachmann, A., Lössner, U., Kralisch, S., Kratzsch, J., Beige, J., Bast, I., Anders, M., Blüher, M., Stumvoll, M., Fasshauer, M. (2014) Serum levels of the myokine irisin in relation to metabolic and renal function. *Eur. J. Endocrinol.* **170**: 501-506.
288. Huh, J.Y., Siopi, A., Mougios, V., Park, K.H., Mantzoros, C.S. (2015) Irisin in response to exercise in humans with and without metabolic syndrome. *J. Clin. Endocrinol. Metab.* **100**: E453-457.
289. Albrecht, E., Norheim, F., Thiede, B., Holen, T., Ohashi, T., Schering, L., Lee, S., Brenmoehl, J., Thomas, S., Drevon, C.A., Erickson, H.P., Maak, S. (2015) Irisin - a myth rather than an exercise-inducible myokine. *Sci. Rep.* **5**: 8889.
290. Jedrychowski, M.P., Wrann, C.D., Paulo, J.A., Gerber, K.K., Szpyt, J., Robinson, M.M., Nair, K.S., Gygi, S.P., Spiegelman, B.M. (2015) Detection and Quantitation of Circulating Human Irisin by Tandem Mass Spectrometry. *Cell Metab.* **22**: 734-740.
291. Phillips, C., Baktir, M.A., Srivatsan, M., Salehi, A. (2014) Neuroprotective effects of physical activity on the brain: a closer look at trophic factor signaling. *Front. Cell. Neurosci.* **8**: 170.
292. Wrann, C.D., White, J.P., Salogiannis, J., Laznik-Bogoslavski, D., Wu, J., Ma, D., Lin, J.D., Greenberg, M.E., Spiegelman, B.M. (2013) Exercise induces hippocampal BDNF through a PGC-1 $\alpha$ /FNDC5 pathway. *Cell Metab.* **18**: 649-659.
293. Cao, L., Choi, E.Y., Liu, X., Martin, A., Wang, C., Xu, X., During, M.J. (2011) White to brown fat phenotypic switch induced by genetic and environmental activation of a hypothalamic-adipocyte axis. *Cell Metab.* **14**: 324-338.
294. Zsuga, J., Tajti, G., Papp, C., Juhasz, B., Gesztelyi, R. (2016) FNDC5/irisin, a molecular target for boosting reward-related learning and motivation. *Med. Hypotheses* **90**: 23-28.
295. Rao, R.R., Long, J.Z., White, J.P., Svensson, K.J., Lou, J., Lokurkar, I., Jedrychowski, M.P., Ruas, J.L., Wrann, C.D., Lo, J.C., Camera, D.M., Lachey, J., Gygi, S., Seehra, J., Hawley, J.A., Spiegelman, B.M. (2014) Meteorin-like is a hormone that regulates immune-adipose interactions to increase beige fat thermogenesis. *Cell* **157**: 1279-1291.

296. Roberts, L.D., Boström, P., O'Sullivan, J.F., Schinzel, R.T., Lewis, G.D., Dejam, A., Lee, Y.K., Palma, M.J., Calhoun, S., Georgiadi, A., Chen, M.H., Ramachandran, V.S., Larson, M.G., Bouchard, C., Rankinen, T., Souza, A.L., Clish, C.B., Wang, T.J., Estall, J.L., Soukas, A.A., Cowan, C.A., Spiegelman, B.M., Gerszten, R.E. (2014)  $\beta$ -Aminoisobutyric acid induces browning of white fat and hepatic  $\beta$ -oxidation and is inversely correlated with cardiometabolic risk factors. *Cell Metab.* **19**: 96-108.
297. Carrière, A., Jeanson, Y., Berger-Müller, S., André, M., Chenouard, V., Arnaud, E., Barreau, C., Walther, R., Galinier, A., Wdziekonski, B., Villageois, P., Louche, K., Collas, P., Moro, C., Dani, C., Villarroja, F., Casteilla, L. (2014) Browning of white adipose cells by intermediate metabolites: an adaptive mechanism to alleviate redox pressure. *Diabetes* **63**: 3253-3265.
298. Mauer, J., Denson, J.L., Brüning, J.C. (2015) Versatile functions for IL-6 in metabolism and cancer. *Trends Immunol.* **36**: 92-101.
299. Steensberg, A., van Hall, G., Osada, T., Sacchetti, M., Saltin, B., Klarlund Pedersen, B. (2000) Production of interleukin-6 in contracting human skeletal muscles can account for the exercise-induced increase in plasma interleukin-6. *J. Physiol.* **529**: 237-242.
300. Kelly, M., Gauthier, M.S., Saha, A.K., Ruderman, N.B. (2009) Activation of AMP-activated protein kinase by interleukin-6 in rat skeletal muscle: association with changes in cAMP, energy state, and endogenous fuel mobilization. *Diabetes* **58**: 1953-1960.
301. Ellingsgaard, H., Hauselmann, I., Schuler, B., Habib, A.M., Baggio, L.L., Meier, D.T., Eppler, E., Bouzakri, K., Wueest, S., Muller, Y.D., Hansen, A.M., Reinecke, M., Konrad, D., Gassmann, M., Reimann, F., Halban, P.A., Gromada, J., Drucker, D.J., Gribble, F.M., Ehse, J.A., Donath, M.Y. (2011) Interleukin-6 enhances insulin secretion by increasing glucagon-like peptide-1 secretion from L cells and alpha cells. *Nat. Med.* **17**: 1481-1489.
302. White, P.J., St-Pierre, P., Charbonneau, A., Mitchell, P.L., St-Amand, E., Marcotte, B., Marette, A. (2014) Protectin DX alleviates insulin resistance by activating a myokine-liver glucoregulatory axis. *Nat. Med.* **20**: 664-669.
303. Knudsen, J.G., Murholm, M., Carey, A.L., Biensø, R.S., Basse, A.L., Allen, T.L., Hidalgo, J., Kingwell, B.A., Febbraio, M.A., Hansen, J.B., Pilegaard, H. (2014) Role of IL-6 in exercise training- and cold-induced UCP1 expression in subcutaneous white adipose tissue. *PLoS One* **9**: e84910.
304. Mauer, J., Chaurasia, B., Goldau, J., Vogt, M.C., Ruud, J., Nguyen, K.D., Theurich, S., Hausen, A.C., Schmitz, J., Brönneke, H.S., Estevez, E., Allen, T.L., Mesaros, A., Partridge, L., Febbraio, M.A., Chawla, A., Wunderlich, F.T., Brüning, J.C. (2014) Signaling by IL-6 promotes alternative activation of macrophages to limit endotoxemia and obesity-associated resistance to insulin. *Nat. Immunol.* **15**: 423-430.
305. Qiu, Y., Nguyen, K.D., Odegaard, J.I., Cui, X., Tian, X., Locksley, R.M., Palmiter, R.D., Chawla, A. (2014) Eosinophils and type 2 cytokine signaling in macrophages orchestrate development of functional beige fat. *Cell* **157**: 1292-1308.
306. Lee, M.W., Odegaard, J.I., Mukundan, L., Qiu, Y., Molofsky, A.B., Nussbaum, J.C., Yun, K., Locksley, R.M., Chawla, A. (2015) Activated type 2 innate lymphoid cells regulate beige fat biogenesis. *Cell* **160**: 74-87.
307. Brestoff, J.R., Kim, B.S., Saenz, S.A., Stine, R.R., Monticelli, L.A., Sonnenberg, G.F., Thome, J.J., Farber, D.L., Lutfy, K., Seale, P., Artis, D. (2015) Group 2 innate lymphoid cells promote beiging of white adipose tissue and limit obesity. *Nature* **519**: 242-246.
308. Bordicchia, M., Liu, D., Amri, E.Z., Ailhaud, G., Dessì-Fulgheri, P., Zhang, C., Takahashi, N., Sarzani, R., Collins, S. (2012) Cardiac natriuretic peptides act via p38 MAPK to induce the brown fat thermogenic program in mouse and human adipocytes. *J. Clin. Invest.* **122**: 1022-1036.

309. Collins, S., Bordicchia, M. (2013) Heart hormones fueling a fire in fat. *Adipocyte* **2**: 104-108.
310. Petrović, V., Buzadžić, B., Korać, A., Vasiljević, A., Janković, A., Korać, B. (2010) NO modulates the molecular basis of rat interscapular brown adipose tissue thermogenesis. *Comp. Biochem. Physiol. C. Toxicol. Pharmacol.* **152**: 147-159.
311. Mitschke, M.M., Hoffmann, L.S., Gnad, T., Scholz, D., Kruithoff, K., Mayer, P., Haas, B., Sassmann, A., Pfeifer, A., Kilic, A. (2013) Increased cGMP promotes healthy expansion and browning of white adipose tissue. *FASEB J.* **27**: 1621-1630.
312. Hoffmann, L.S., Etzrodt, J., Willkomm, L., Sanyal, A., Scheja, L., Fischer, A.W., Stasch, J.P., Bloch, W., Friebe, A., Heeren, J., Pfeifer, A. (2015) Stimulation of soluble guanylyl cyclase protects against obesity by recruiting brown adipose tissue. *Nat. Commun.* **6**: 7235.
313. Schulz, T.J., Huang, T.L., Tran, T.T., Zhang, H., Townsend, K.L., Shadrach, J.L., Cerletti, M., McDougall, L.E., Giorgadze, N., Tchkonina, T., Schrier, D., Falb, D., Kirkland, J.L., Wagers, A.J., Tseng, Y.H. (2011) Identification of inducible brown adipocyte progenitors residing in skeletal muscle and white fat. *Proc. Natl. Acad. Sci. USA* **108**: 143-148.
314. Whittle, A.J., Carobbio, S., Martins, L., Slawik, M., Hondares, E., Vázquez, M.J., Morgan, D., Csikasz, R.I., Gallego, R., Rodriguez-Cuenca, S., Dale, M., Virtue, S., Villarroya, F., Cannon, B., Rahmouni, K., López, M., Vidal-Puig, A. (2012) BMP8B increases brown adipose tissue thermogenesis through both central and peripheral actions. *Cell* **149**: 871-885.
315. Qian, S.W., Tang, Y., Li, X., Liu, Y., Zhang, Y.Y., Huang, H.Y., Xue, R.D., Yu, H.Y., Guo, L., Gao, H.D., Liu, Y., Sun, X., Li, Y.M., Jia, W.P., Tang, Q.Q. (2013) BMP4-mediated brown fat-like changes in white adipose tissue alter glucose and energy homeostasis. *Proc. Natl. Acad. Sci. USA* **110**: E798-807.
316. Hinoi, E., Nakamura, Y., Takada, S., Fujita, H., Iezaki, T., Hashizume, S., Takahashi, S., Odaka, Y., Watanabe, T., Yoneda, Y. (2014) Growth differentiation factor-5 promotes brown adipogenesis in systemic energy expenditure. *Diabetes* **63**: 162-175.
317. Ogawa, Y., Kurosu, H., Yamamoto, M., Nandi, A., Rosenblatt, K.P., Goetz, R., Eliseenkova, A.V., Mohammadi, M., Kuro-o, M. (2007) BetaKlotho is required for metabolic activity of fibroblast growth factor 21. *Proc. Natl. Acad. Sci. USA* **104**: 7432-7437.
318. Hondares, E., Rosell, M., Gonzalez, F.J., Giralt, M., Iglesias, R., Villarroya, F. (2010) Hepatic FGF21 expression is induced at birth via PPARalpha in response to milk intake and contributes to thermogenic activation of neonatal brown fat. *Cell Metab.* **11**: 206-212.
319. Fisher, F.M., Kleiner, S., Douris, N., Fox, E.C., Mepani, R.J., Verdeguer, F., Wu, J., Kharitonkov, A., Flier, J.S., Maratos-Flier, E., Spiegelman, B.M. (2012) FGF21 regulates PGC-1 $\alpha$  and browning of white adipose tissues in adaptive thermogenesis. *Genes Dev.* **26**: 271-281.
320. Emanuelli, B., Vienberg, S.G., Smyth, G., Cheng, C., Stanford, K.I., Arumugam, M., Michael, M.D., Adams, A.C., Kharitonkov, A., Kahn, C.R. (2014) Interplay between FGF21 and insulin action in the liver regulates metabolism. *J. Clin. Invest.* **124**: 515-527.
321. So, W.Y., Leung, P.S (2016) Fibroblast Growth Factor 21 As an Emerging Therapeutic Target for Type 2 Diabetes Mellitus. *Med. Res. Rev.* **36**: 672-704.
322. Bailey, C.J., Tahrani, A.A., Barnett, A.H. (2016) Future glucose-lowering drugs for type 2 diabetes. *Lancet Diabetes Endocrinol.* **4**: 350-359.
323. Svensson, K.J., Long, J.Z., Jedrychowski, M.P., Cohen, P., Lo, J.C., Serag, S., Kir, S., Shinoda, K., Tartaglia, J.A., Rao, R.R., Chédotal, A., Kajimura, S., Gygi, S.P., Spiegelman, B.M. (2016) A Secreted Slit2 Fragment Regulates Adipose Tissue Thermogenesis and Metabolic Function. *Cell Metab.* **23**: 454-466.



324. Gnad, T., Scheibler, S., von Kügelgen, I., Scheele, C., Kilić, A., Glöde, A., Hoffmann, L.S., Reverte-Salisa, L., Horn, P., Mutlu, S., El-Tayeb, A., Kranz, M., Deuther-Conrad, W., Brust, P., Lidell, M.E., Betz, M.J., Enerbäck, S., Schrader, J., Yegutkin, G.G., Müller, C.E., Pfeifer, A. (2014) Adenosine activates brown adipose tissue and recruits beige adipocytes via A2A receptors. *Nature* **516**: 395-399.
325. Vegiopoulos, A., Müller-Decker, K., Strzoda, D., Schmitt, I., Chichelnitskiy, E., Ostertag, A., Berriel Diaz, M., Rozman, J., Hrabe de Angelis, M., Nüsing, R.M., Meyer, C.W., Wahli, W., Klingenspor, M., Herzig, S. (2010) Cyclooxygenase-2 controls energy homeostasis in mice by de novo recruitment of brown adipocytes. *Science* **328**: 1158-1161.
326. Fischer-Posovszky, P., Newell, F.S., Wabitsch, M., Tornqvist, H.E. (2008) Human SGBS cells - a unique tool for studies of human fat cell biology. *Obes. Facts* **1**:184-189.
327. Sárvári, A.K., Doan-Xuan, Q.M., Bacsó, Z., Csomós, I., Balajthy, Z., Fésüs, L. (2015) Interaction of differentiated human adipocytes with macrophages leads to trogocytosis and selective IL-6 secretion. *Cell Death Dis.* **6**: e1613.
328. Elabd, C., Chiellini, C., Carmona, M., Galitzky, J., Cochet, O., Petersen, R., Pénicaud, L., Kristiansen, K., Bouloumié, A., Casteilla, L., Dani, C., Ailhaud, G., Amri, E.Z. (2009) Human multipotent adipose-derived stem cells differentiate into functional brown adipocytes. *Stem Cells* **27**: 2753-2760.
329. Taube, M., Andersson-Assarsson, J.C., Lindberg, K., Pereira, M.J., Gäbel, M., Svensson, M.K., Eriksson, J.W., Svensson, P.A. (2015) Evaluation of reference genes for gene expression studies in human brown adipose tissue. *Adipocyte* **4**: 280-285.
330. Szántó, M., Rutkai, I., Hegedus, C., Czikora, Á., Rózsahegyi, M., Kiss, B., Virág, L., Gergely, P., Tóth, A., Bai, P. (2011) Poly(ADP-ribose) polymerase-2 depletion reduces doxorubicin-induced damage through SIRT1 induction. *Cardiovasc. Res.* **92**: 430-438.
331. Doan-Xuan, Q.M., Sarvari, A.K., Fischer-Posovszky, P., Wabitsch, M., Balajthy, Z., Fesus, L., Bacso Z. (2013) High content analysis of differentiation and cell death in human adipocytes. *Cytometry A* **83**: 933-943.
332. Haralick, R.M., Shanmugam, K., Dinstein, I. (1973) Textural features for image classification. *IEEE Trans. Syst. Man Cybern.* **SMC-3**: 610-621.
333. Sárvári, A.K., Veréb, Z., Uray, I.P., Fésüs, L., Balajthy, Z. (2014) Atypical antipsychotics induce both proinflammatory and adipogenic gene expression in human adipocytes in vitro. *Biochem. Biophys. Res. Commun.* **450**: 1383-1389.
334. Klepac, K., Kilić, A., Gnad, T., Brown, L.M., Herrmann, B., Wilderman, A., Balkow, A., Glöde, A., Simon, K., Lidell, M.E., Betz, M.J., Enerbäck, S., Wess, J., Freichel, M., Blüher, M., König, G., Kostenis, E., Insel, P.A., Pfeifer, A. (2016) The Gq signalling pathway inhibits brown and beige adipose tissue. *Nat. Commun.* **7**: 10895.
335. Majka, S.M., Miller, H.L., Helm, K.M., Acosta, A.S., Childs, C.R., Kong, R., Klemm, D.J. (2014) Analysis and isolation of adipocytes by flow cytometry. *Methods Enzymol.* **537**: 281-296.
336. Festy, F., Hoareau, L., Bes-Houtmann, S., Péquin, A.M., Gonthier, M.P., Munstun, A., Hoarau, J.J., Césari, M., Roche, R. (2005) Surface protein expression between human adipose tissue-derived stromal cells and mature adipocytes. *Histochem. Cell Biol.* **124**: 113-121.
337. Lin, J., Page, K.A., Della-Fera, M.A., Baile, C.A. (2004) Evaluation of adipocyte apoptosis by laser scanning cytometry. *Int. J. Obes. Relat. Metab. Disord.* **28**: 1535-1540.
338. Kamensky, L.A., Kamensky, L.D. (1991) Microscope-based multiparameter laser scanning cytometer yielding data comparable to flow cytometry data. *Cytometry* **12**: 381-387.
339. Rew, D.A., Woltmann, G., Wardlaw, A.J. (1999) Laser-scanning cytometry. *Lancet* **353**: 255-256.

340. Holden, E., Luther, E., Henriksen, M. (2005) New developments in quantitative imaging cytometry. *Nat. Methods* **2**: doi:10.1038/nmeth773.
341. Darzynkiewicz, Z., Bedner, E., Li, X., Gorczyca, W., Melamed, M.R. (1999) Laser-scanning cytometry: A new instrumentation with many applications. *Exp. Cell Res.* **249**: 1-12.
342. Henriksen, M. (2010) Quantitative imaging cytometry: instrumentation of choice for automated cellular and tissue analysis. *Nat. Methods* **7**: doi:10.1038/nmeth.f.302.
343. Henriksen, M., Miller, B., Newmark, J., Al-Kofahi, Y., Holden, E. (2011) Laser scanning cytometry and its applications: a pioneering technology in the field of quantitative imaging cytometry. *Methods Cell Biol.* **102**:161-205.
344. Scheffler, I. E. (1999) Biogenesis, in *Mitochondria, John Wiley & Sons, Inc., New York, USA*.
345. McDonough, P.M., Agustin, R.M., Ingermanson, R.S., Loy, P.A., Buehrer, B.M., Nicoll, J.B., Prigozhina, N.L., Mikic, I., Price, J.H. (2009) Quantification of lipid droplets and associated proteins in cellular models of obesity via high-content/high-throughput microscopy and automated image analysis. *Assay Drug Dev. Technol.* **7**:440-460.
346. Kamentsky, L.A. (1973) Cytology automation. *Adv. Biol. Med. Phys.* **14**: 93-161.
347. Lee, Y.H., Chen, S.Y., Wiesner, R.J., Huang, Y.F. (2004) Simple flow cytometric method used to assess lipid accumulation in fat cells. *J. Lipid Res.* **45**: 1162-1167.
348. Kristóf, E., Zahuczky, G., Katona, K., Doró, Z., Nagy, É., Fésüs, L. (2013) Novel role of ICAM3 and LFA-1 in the clearance of apoptotic neutrophils by human macrophages. *Apoptosis* **18**: 1235-1251.
349. Abdul-Rahman, O., Kristóf, E., Doan-Xuan, Q.M., Vida, A., Nagy, L., Horváth, A., Simon, J., Maros, T., Szentkirályi, I., Palotás, L., Debreceni, T., Csizmadia, P., Szerafin, T., Fodor, T., Szántó, M., Tóth, A., Kiss, B., Bacsó, Z., Bai, P. (2016) AMP-Activated Kinase (AMPK) Activation by AICAR in Human White Adipocytes Derived from Pericardial White Adipose Tissue Stem Cells Induces a Partial Beige-Like Phenotype. *PLoS One* **11**: e0157644.
350. Lee, P., Linderman, J.D., Smith, S., Brychta, R.J., Wang, J., Idelson, C., Perron, R.M., Werner, C.D., Phan, G.Q., Kammula, U.S., Kebebew, E., Pacak, K., Chen, K.Y., Celi, F.S. (2014) Irisin and FGF21 are cold-induced endocrine activators of brown fat function in humans. *Cell Metab.* **19**: 302-309.
351. Silva, F.J., Holt, D.J., Vargas, V., Yockman, J., Boudina, S., Atkinson, D., Grainger, D.W., Revelo, M.P., Sherman, W., Bull, D.A., Patel, A.N. (2014) Metabolically active human brown adipose tissue derived stem cells. *Stem Cells* **32**: 572-581.
352. Zhang, Y., Xie, C., Wang, H., Foss, R.M., Clare, M., George, E.V., Li, S., Katz, A., Cheng, H., Ding, Y., Tang, D., Reeves, W.H., Yang, L.J. (2016) Irisin exerts dual effects on browning and adipogenesis of human white adipocytes. *Am. J. Physiol. Endocrinol. Metab.* **311**: E530-541.
353. Xu, H., Barnes, G.T., Yang, Q., Tan, G., Yang, D., Chou, C.J., Sole, J., Nichols, A., Ross, J.S., Tartaglia, L.A., Chen, H. (2003) Chronic inflammation in fat plays a crucial role in the development of obesity-related insulin resistance. *J. Clin. Invest.* **112**: 1821–1830.
354. Weisberg, S.P., Mccann, D., Desai, M., Rosenbaum, M., Leibel, R.L., Ferrante, A.W. Jr. (2003) Obesity is associated with macrophage accumulation. *J. Clin. Invest.* **112**: 1796–1808.
355. Lee, Y.H., Pratley, R.E. (2005) The evolving role of inflammation in obesity and the metabolic syndrome. *Curr. Diab. Rep.* **5**: 70-75.
356. Dwivedi, Y., Rizavi, H.S., Pandey, G.N. (2002) Differential effects of haloperidol and clozapine on [(3)H]cAMP binding, protein kinase A (PKA) activity, and mRNA and protein expression of selective regulatory and catalytic subunit isoforms of PKA in rat brain. *J. Pharmacol. Exp. Ther.* **301**: 197-209.

357. Turalba, A.V., Leite-Morris, K.A., Kaplan, G.B. (2004) Antipsychotics regulate cyclic AMP-dependent protein kinase and phosphorylated cyclic AMP response element-binding protein in striatal and cortical brain regions in mice. *Neurosci. Lett.* **357**: 53-57.
358. Marazziti, D., Baroni, S., Palego, L., Betti, L., Giannaccini, G., Castagna, M., Naccarato, A.G., Luccachini, A., Catena-Dell'Osso, M., Dell'Osso, L. (2014) Clozapine effects on adenylyl cyclase activity and serotonin type 1A receptors in human brain post-mortem. *J. Psychopharmacol.* **28**: 320-328.
359. Stockebrand, M., Nejad, A.S., Neu, A., Kharbanda, K.K., Sauter, K., Schillemeit, S., Isbrandt, D., Choe, C.U. (2016) Transcriptomic and metabolic analyses reveal salvage pathways in creatine-deficient AGAT(-/-) mice. *Amino Acids* **48**: 2025-2039.
360. Müller, S., Balaz, M., Stefanicka, P., Varga, L., Amri, E.Z., Ukropec, J., Wollscheid, B., Wolfrum, C. (2016) Proteomic Analysis of Human Brown Adipose Tissue Reveals Utilization of Coupled and Uncoupled Energy Expenditure Pathways. *Sci. Rep.* **6**: 30030.
361. Hennekens, C.H., Hennekens, A.R., Hollar, D., Casey, D.E. (2005) Schizophrenia and increased risks of cardiovascular disease. *Am. Heart J.* **150**: 1115-1121.
362. De Hert, M., Schreurs, V., Vancampfort, D., Van Winkel, R. (2009) Metabolic syndrome in people with schizophrenia: a review. *World Psychiatry* **8**: 15-22.
363. Kim, S.F., Huang, A.S., Snowman, A.M., Teuscher, C., Snyder, S.H. (2007) From the Cover: Antipsychotic drug-induced weight gain mediated by histamine H1 receptor-linked activation of hypothalamic AMP-kinase. *Proc. Natl. Acad. Sci. USA* **104**: 3456-3459.
364. Houseknecht, K.L., Robertson, A.S., Zavadoski, W., Gibbs, E.M., Johnson, D.E., Rollema, H. (2007) Acute effects of atypical antipsychotics on whole-body insulin resistance in rats: implications for adverse metabolic effects. *Neuropsychopharmacology* **32**: 289-297.
365. Ader, M., Kim, S.P., Catalano, K.J., Ionut, V., Hucking, K., Richey, J.M., Kabir, M., Bergman, R.N. (2005) Metabolic dysregulation with atypical antipsychotics occurs in the absence of underlying disease: a placebo-controlled study of olanzapine and risperidone in dogs. *Diabetes* **54**: 862-871.
366. Chintoh, A.F., Mann, S.W., Lam, L., Giacca, A., Fletcher, P., Nobrega, J., Remington, G. (2009) Insulin resistance and secretion in vivo: effects of different antipsychotics in an animal model. *Schizophr. Res.* **108**: 127-133.
367. Davey, K.J., Cotter, P.D., O'Sullivan, O., Crispie, F., Dinan, T.G., Cryan, J.F., O'Mahony, S.M. (2013) Antipsychotics and the gut microbiome: olanzapine-induced metabolic dysfunction is attenuated by antibiotic administration in the rat. *Transl. Psychiatry* **3**: e309.
368. Bahr, S.M., Tyler, B.C., Wooldridge, N., Butcher, B.D., Burns, T.L., Teesch, L.M., Oltman, C.L., Azcarate-Peril, M.A., Kirby, J.R., Calarge, C.A. (2015) Use of the second-generation antipsychotic, risperidone, and secondary weight gain are associated with an altered gut microbiota in children. *Transl. Psychiatry* **5**: e652.
369. Victoriano, M., de Beaupaire, R., Naour, N., Guerre-Millo, M., Quignard-Boulangé, A., Huneau, J.F., Mathé, V., Tomé, D., Hermier, D. (2010) Olanzapine-induced accumulation of adipose tissue is associated with an inflammatory state. *Brain Res.* **1350**: 167-175.
370. Zhang, Q., He, M., Deng, C., Wang, H., Huang, X.F. (2014) Effects of olanzapine on the elevation of macrophage infiltration and pro-inflammatory cytokine expression in female rats. *J. Psychopharmacol.* **28**: 1161-1169.
371. Vestri, H.S., Maianu, L., Moellerling, D.R., Garvey, W.T. (2007) Atypical antipsychotic drugs directly impair insulin action in adipocytes: effects on glucose transport, lipogenesis, and antilipolysis. *Neuropsychopharmacology* **32**: 765-772.

372. Yang, L.H., Chen, T.M., Yu, S.T., Chen, Y.H. (2007) Olanzapine induces SREBP-1-related adipogenesis in 3T3-L1 cells. *Pharmacol. Res.* **56**: 202-208.
373. Sertié, A.L., Suzuki, A.M., Sertié, R.A., Andreotti, S., Lima, F.B., Passos-Bueno, M.R., Gattaz, W.F. (2011) Effects of antipsychotics with different weight gain liabilities on human in vitro models of adipose tissue differentiation and metabolism. *Prog. Neuropsychopharmacol. Biol. Psychiatry* **35**: 1884-1890.
374. Hemmrich, K., Gummersbach, C., Pallua, N., Luckhaus, C., Fehsel, K. (2006) Clozapine enhances differentiation of adipocyte progenitor cells. *Mol. Psychiatry* **11**: 980-981.
375. Coryell, W., Miller, D.D., Perry, P.J. (1998) Haloperidol plasma levels and dose optimization. *Am. J. Psychiatry* **155**: 48-53.
376. Broich, K., Heinrich, S., Marneros, A. (1998) Acute clozapine overdose: plasma concentration and outcome. *Pharmacopsychiatry* **31**: 149-151.
377. Bergemann, N., Frick, A., Parzer, P., Kopitz, J. (2004) Olanzapine plasma concentration, average daily dose, and interaction with co-medication in schizophrenic patients. *Pharmacopsychiatry* **37**: 63-68.
378. Oh, J.E., Cho, Y.M., Kwak, S.N., Kim, J.H., Lee, K.W., Jung, H., Jeong, S.W., Kwon, O.J. (2012) Inhibition of mouse brown adipocyte differentiation by second-generation antipsychotics. *Exp. Mol. Med.* **44**: 545-553.
379. Ahmadian, M., Suh, J.M., Hah, N., Liddle, C., Atkins, A.R., Downes, M., Evans, R.M. (2013) PPAR $\gamma$  signaling and metabolism: the good, the bad and the future. *Nat. Med.* **19**: 557-566.
380. Nedergaard, J., Petrovic, N., Lindgren, E.M., Jacobsson, A., Cannon, B. (2005) PPAR $\gamma$  in the control of brown adipocyte differentiation. *Biochim. Biophys. Acta* **1740**: 293-304.
381. Ohno, H., Shinoda, K., Spiegelman, B.M., Kajimura, S. (2012) PPAR $\gamma$  agonists induce a white-to-brown fat conversion through stabilization of PRDM16 protein. *Cell Metab.* **15**: 395-404.
382. Qiang, L., Wang, L., Kon, N., Zhao, W., Lee, S., Zhang, Y., Rosenbaum, M., Zhao, Y., Gu, W., Farmer, S.R., Accili, D. (2012) Brown remodeling of white adipose tissue by SirT1-dependent deacetylation of Ppar $\gamma$ . *Cell* **150**: 620-632.
383. Kung, J., Henry, R.R. (2012) Thiazolidinedione safety. *Expert Opin. Drug Saf.* **11**: 565-579.
384. Nissen, S.E., Wolski, K. (2007) Effect of rosiglitazone on the risk of myocardial infarction and death from cardiovascular causes. *N. Engl. J. Med.* **356**: 2457-2471.
385. Graham, D.J., Ouellet-Hellstrom, R., MaCurdy, T.E., Ali, F., Sholley, C., Worrall, C., Kelman, J.A. (2010) Risk of acute myocardial infarction, stroke, heart failure, and death in elderly Medicare patients treated with rosiglitazone or pioglitazone. *JAMA* **304**: 411-418.
386. Iwaki, M., Matsuda, M., Maeda, N., Funahashi, T., Matsuzawa, Y., Makishima, M., Shimomura, I. (2003) Induction of adiponectin, a fat-derived antidiabetic and antiatherogenic factor, by nuclear receptors. *Diabetes* **52**: 1655-1663.
387. Tomaru, T., Steger, D.J., Lefterova, M.I., Schupp, M., Lazar, M.A. (2009) Adipocyte-specific expression of murine resistin is mediated by synergism between peroxisome proliferator-activated receptor gamma and CCAAT/enhancer-binding proteins. *J. Biol. Chem.* **284**: 6116-6125.
388. Sarruf, D.A., Yu, F., Nguyen, H.T., Williams, D.L., Printz, R.L., Niswender, K.D., Schwartz, M.W. (2009) Expression of peroxisome proliferator-activated receptor-gamma in key neuronal subsets regulating glucose metabolism and energy homeostasis. *Endocrinology* **150**: 707-712.
389. Ryan, K.K., Li, B., Grayson, B.E., Matter, E.K., Woods, S.C., Seeley, R.J. (2011) A role for central nervous system PPAR- $\gamma$  in the regulation of energy balance. *Nat. Med.* **17**: 623-626.
390. Lu, M., Sarruf, D.A., Talukdar, S., Sharma, S., Li, P., Bandyopadhyay, G., Nalbandian, S., Fan, W., Gayen, J.R., Mahata, S.K., Webster, N.J., Schwartz, M.W., Olefsky, J.M. (2011) Brain PPAR- $\gamma$

- promotes obesity and is required for the insulin-sensitizing effect of thiazolidinediones. *Nat. Med.* **17**: 618-622.
391. Nichols, D.E., Nichols, C.D. (2008) Serotonin receptors. *Chem. Rev.* **108**: 1614-1641.
  392. Kinoshita, M., Ono, K., Horie, T., Nagao, K., Nishi, H., Kuwabara, Y., Takanabe-Mori, R., Hasegawa, K., Kita, T., Kimura, T. (2010) Regulation of adipocyte differentiation by activation of serotonin (5-HT) receptors 5-HT<sub>2A</sub>R and 5-HT<sub>2C</sub>R and involvement of microRNA-448-mediated repression of KLF5. *Mol. Endocrinol.* **24**: 1978-1987.
  393. Stunes, A.K., Reseland, J.E., Hauso, O., Kidd, M., Tømmerås, K., Waldum, H.L., Syversen, U., Gustafsson, B.I. (2011) Adipocytes express a functional system for serotonin synthesis, reuptake and receptor activation. *Diabetes Obes. Metab.* **13**: 551-558.
  394. Tchkonina, T., Lenburg, M., Thomou, T., Giorgadze, N., Frampton, G., Pirtskhalava, T., Cartwright, A., Cartwright, M., Flanagan, J., Karagiannides, I., Gerry, N., Forse, R.A., Tchoukalova, Y., Jensen, M.D., Pothoulakis, C., Kirkland, J.L. (2007) Identification of depot-specific human fat cell progenitors through distinct expression profiles and developmental gene patterns. *Am. J. Physiol. Endocrinol. Metab.* **292**: E298-307.
  395. Kim, H.J., Kim, J.H., Noh, S., Hur, H.J., Sung, M.J., Hwang, J.T., Park, J.H., Yang, H.J., Kim, M.S., Kwon, D.Y., Yoon, S.H. (2011) Metabolomic analysis of livers and serum from high-fat diet induced obese mice. *J. Proteome. Res.* **10**: 722-731.
  396. Kwak, S.H., Park, B.L., Kim, H., German, M.S., Go, M.J., Jung, H.S., Koo, B.K., Cho, Y.M., Choi, S.H., Cho, Y.S., Shin, H.D., Jang, H.C., Park, K.S. (2012) Association of variations in TPH1 and HTR2B with gestational weight gain and measures of obesity. *Obesity (Silver Spring)* **20**: 233-238.
  397. Elman, I., Goldstein, D.S., Green, A.I., Eisenhofer, G., Folio, C.J., Holmes, C.S., Pickar, D., Breier, A. (2002) Effects of risperidone on the peripheral noradrenergic system in patients with schizophrenia: a comparison with clozapine and placebo. *Neuropsychopharmacology* **27**: 293-300.
  398. Blessing, W.W., Seaman, B., Pedersen, N.P., Ootsuka, Y. (2003) Clozapine reverses hyperthermia and sympathetically mediated cutaneous vasoconstriction induced by 3,4-methylenedioxymethamphetamine (ecstasy) in rabbits and rats. *J. Neurosci.* **23**: 6385-6391.
  399. Monda, M., Viggiano, A., Viggiano, A., Fuccio, F., De, Luca V. (2004) Clozapine blocks sympathetic and thermogenic reactions induced by orexin A in rat. *Physiol. Res.* **53**: 507-513.
  400. Savoy, Y.E., Ashton, M.A., Miller, M.W., Nedza, F.M., Spracklin, D.K., Hawthorn, M.H., Rollema, H., Matos, F.F., Hajos-Korcsok, E. (2010) Differential effects of various typical and atypical antipsychotics on plasma glucose and insulin levels in the mouse: evidence for the involvement of sympathetic regulation. *Schizophr. Bull.* **36**: 410-418.

## **9. KEYWORDS**

adipocyte, beige, browning, clozapine, irisin, laser-scanning cytometry, obesity, serotonin, thermogenesis, UCP1

## **TÁRGYSZAVAK**

adipocita, beige, browning, clozapine, irisin, lézer-pásztázó citometria, elhízás, szerotonin, termogenezis, UCP1

## 10. ACKNOWLEDGEMENTS

First of all, I would like to express my sincere gratitude to my supervisor, Prof. Dr. László Fésüs, for the excellent training, continuous support and motivation, and the scientific discussions during my Ph.D. candidacy period. I am thankful that he gave me the opportunity to learn and work in his research group.

Many thanks to all of the former and present members of the Cellular Biochemistry Research Group and MTA-DE Stem Cells, Apoptosis and Genomics Research Group of the Hungarian Academy of Sciences for the friendly working atmosphere. I am especially thankful to Dr. Máté Demény for helping me with his constructive advices and scientific discussions.

I also would like to thank Jennifer Nagy, Attiláné Klem and Szilvia Szalóki for their technical assistance.

I am especially grateful to our long-term collaborators: Dr. Zsolt Bacsó, Dr. Quang-Minh Doan-Xuan and Dr. Péter Bai, for their excellent help in Laser-scanning image acquisition and analysis or in cellular respiration measurements and valuable suggestions.

Special thanks to Dr. Zoltán Balajthy and Dr. Anitta Kinga Sárvári for opening studies in regard to many aspects of human adipocyte biology.

I am also thankful to Dr. Gábor Zahuczky for sharing his knowledge and experience with me when I was an undergraduate student.

I wish to express my gratitude to Dr. Goran Petrovski and his colleagues (Dr. Réka Albert, Mária Szatmári-Tóth, Dr. Zoltán Veréb) for a continuous collaboration and friendship.

I am also thankful to former and current undergraduate students (Ágnes Klusóczy, Roland Veress, Zsolt Combi and Klára Varga) who worked/are working with me on experiments related to human adipocyte browning.

I am also grateful to Prof. Dr. József Tőzsér, current Head of the Department of Biochemistry and Molecular Biology for the opportunity to work in a well-equipped institute.

Furthermore, I would like to thank all my colleagues from the Department of Biochemistry and Molecular Biology.

Special thanks to Dr. Ferenc Győry and the surgery group at the Augusztia Surgery Center of the University of Debrecen, Faculty of Medicine, for providing adipose tissue samples.

The research was financially supported by the European Union and the State of Hungary, co-financed by the European Social Fund in the framework of TÁMOP-4.2.4.A/2-11/1-2012-0001 ‘National Excellence Program’ which provided personal support, TÁMOP-4.2.2.A-11/1/KONV-2012-0023, GINOP-2.3.2-15-2016-00006 grant, the European Union Framework Programme 7 TRANSCOM IAPP 251506, OTKA K108308, and the Hungarian Academy of Sciences.

Most importantly and dearly, I would like to thank my beloved family and to all of my dear friends helping me get through the difficult times, and for their continuous encouragement.





Registry number:  
Subject:

DEENK/283/2016.PL  
PhD Publikációs Lista

Candidate: Endre Kristóf

Neptun ID: N64U4X

Doctoral School: Doctoral School of Molecular Cellular and Immune Biology

### List of publications related to the dissertation

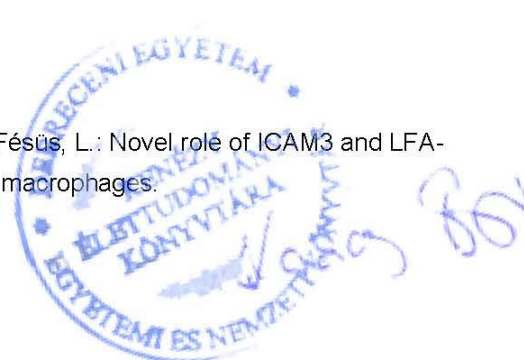
1. **Kristóf, E.**, Doan-Xuan, Q. M., Sárvári, A. K., Klusóczki, Á., Fischer-Posovszky, P., Wabitsch, M., Bacsó, Z., Bai, P., Balajthy, Z., Fésüs, L.: Clozapine modifies the differentiation program of human adipocytes inducing browning.  
*Transl. Psychiatry*. "Accepted by Publisher", 2016.  
IF: 5.538 (2015)
2. **Kristóf, E.**, Doan-Xuan, Q. M., Bai, P., Bacsó, Z., Fésüs, L.: Laser-scanning cytometry can quantify human adipocyte browning and proves effectiveness of irisin.  
*Sci. Rep.* 5, 1-9, 2015.  
DOI: <http://dx.doi.org/10.1038/srep12540>  
IF: 5.228





### List of other publications

3. Abdul-Rahman, O., **Kristóf, E.**, Doan-Xuan, Q. M., Vida, A., Nagy, L., Horváth, A., Simon, J., Maros, T. M., Szentkirályi, I., Palotás, L., Debreceni, T., Csizmadia, P., Szerafin, T., Fodor, T., Szántó, M., Tóth, A., Kiss, B. K., Bacsó, Z., Bai, P.: AMP-Activated Kinase (AMPK) Activation by AICAR in Human White Adipocytes Derived from Pericardial White Adipose Tissue Stem Cells Induces a Partial Beige-Like Phenotype.  
*PLoS One*. 11 (6), e0157644, 2016.  
DOI: <http://dx.doi.org/10.1371/journal.pone.0157644>  
IF: 3.057 (2015)
4. Szatmári-Tóth, M., **Kristóf, E.**, Veréb, Z., Akhtar, S., Facskó, A., Fésüs, L., Kauppinen, A., Kaarniranta, K., Petrovski, G.: Clearance of autophagy-associated dying retinal pigment epithelial cells - a possible source for inflammation in age-related macular degeneration.  
*Cell Death Dis.* 7 (9), e2367, 2016.  
DOI: <http://dx.doi.org/10.1038/cddis.2016.133>  
IF: 5.378 (2015)
5. Csomós, K., **Kristóf, E.**, Jakob, B., Csomós, I., Kovács, G., Rotem, O., Hodrea, J., Bagoly, Z., Muszbek, L., Csósz, É., Fésüs, L.: Protein cross-linking by chlorinated polyamines and transglutamylation stabilizes neutrophil extracellular traps.  
*Cell Death Dis.* 7 (8), e2332, 2016.  
DOI: <http://dx.doi.org/10.1038/cddis.2016.200>  
IF: 5.378 (2015)
6. Albert, R.\*, **Kristóf, E.\***, Zahuczky, G., Szatmári-Tóth, M., Veréb, Z., Oláh, B., Moe, M. C., Facskó, A., Fésüs, L., Petrovski, G.: Triamcinolone regulated apopto-phagocytic gene expression patterns in the clearance of dying retinal pigment epithelial cells. A key role of Mertk in the enhanced phagocytosis.  
*Biochim. Biophys. Acta-Gen. Subj.* 1850 (2), 435-446, 2015.  
\*These authors contributed equally in this work.  
DOI: <http://dx.doi.org/10.1016/j.bbagen.2014.10.026>  
IF: 5.083
7. **Kristóf, E.**, Zahuczky, G., Katona, K., Doró, Z., Nagy, É., Fésüs, L.: Novel role of ICAM3 and LFA-1 in the clearance of apoptotic neutrophils by human macrophages.  
*Apoptosis*. 18 (10), 1235-1251, 2013.  
DOI: <http://dx.doi.org/10.1007/s10495-013-0873-z>  
IF: 3.614





8. Zahuczky, G., **Kristóf, E.**, Majai, G., Fésüs, L.: Differentiation and Glucocorticoid Regulated Apopto-Phagocytic Gene Expression Patterns in Human Macrophages: role of Mertk in Enhanced Phagocytosis.  
*PLoS One*. 6 (6), e21349, 2011.  
DOI: <http://dx.doi.org/10.1371/journal.pone.0021349>  
IF: 4.092

**Total IF of journals (all publications): 37,368**

**Total IF of journals (publications related to the dissertation): 10,766**

The Candidate's publication data submitted to the iDEa Tudóstér have been validated by DEENK on the basis of Web of Science, Scopus and Journal Citation Report (Impact Factor) databases.

26 October, 2016



## CONFERENCES

### Oral presentations:

Endre Kristóf, Quang-Minh Doan-Xuan, Anitta Kinga Sárvári, Zoltán Balajthy, Zsolt Bacsó and László Fésüs. **Effect of second generation antipsychotic (SGA) drugs on the differentiation program of human adipocytes** (6th Molecular Cell and Immune Biology Winter Symposium, 2013, Galyatető)

Endre Kristóf, Quang-Minh Doan-Xuan, Anitta Kinga Sárvári, Zoltán Balajthy, Zsolt Bacsó and László Fésüs. **Second generation antipsychotic (SGA) drugs modify the differentiation program of human adipocytes inducing ‘browning’ markers** (Hungarian Molecular Life Sciences Conference, 2013, Siófok)

Endre Kristóf, Quang-Minh Doan-Xuan, Anitta Kinga Sárvári, Zoltán Balajthy, Zsolt Bacsó and László Fésüs. **Second generation antipsychotic (SGA) drugs modify the differentiation program of human adipocytes inducing “browning” markers** (7th Molecular Cell and Immune Biology Winter Symposium, 2014, Galyatető)

Endre Kristóf, Quang-Minh Doan-Xuan, Péter Bai, Zsolt Bacsó and László Fésüs. **Irisin modifies the differentiation program of subcutaneous human adipocytes and induces “browning” *ex vivo*** (Magyar Biokémiai Egyesület Vándorgyűlése, 2014, Debrecen)

Endre Kristóf, Quang-Minh Doan-Xuan, Péter Bai, Zsolt Bacsó and László Fésüs. **Laser-scanning cytometry can quantify human adipocyte browning and proves effectiveness of irisin** (8th Molecular Cell and Immune Biology Winter Symposium, 2015, Debrecen)

Endre Kristóf, Ferenc Győry, Quang-Minh Doan-Xuan, Péter Bai, Zsolt Bacsó and László Fésüs. **Functional characterization and gene expression patterns of *ex vivo* differentiated human white, “beige” and brown adipocytes** (FEBS 3+ Meeting; Molecules of Life, 2015, Portoroz, Slovenia)

Endre Kristóf, Ágnes Klusóczki, Roland Veress, Ferenc Győry, Zsolt Bacsó and László Fésüs. **Functions of brown and beige fat in energy homeostasis in humans** (9th Molecular Cell and Immune Biology Winter Symposium, 2016, Debrecen)

Endre Kristóf, Ágnes Klusóczki, Zsolt Combi, Roland Veress, Ferenc Győry, Szilárd Póliska, Zsolt Bacsó and László Fésüs. **Differentiating human beige adipocytes secrete cytokines (“batokines”)** (Magyar Biokémiai Egyesület Vándorgyűlése, 2016, Szeged)

Endre Kristóf, Quang-Minh Doan-Xuan, Ágnes Klusóczki, Ferenc Győry, Szilárd Póliska, Zsolt Bacsó, Péter Bai, László Fésüs. **Browning-inducers modify the differentiation of human adipocytes from different anatomical sites and enhance their mitochondrial respiration** (7th World Congress on Targeting Mitochondria, 2016, Berlin, Germany)

#### **Poster presentations:**

Endre Kristóf, Quang-Minh Doan-Xuan, Anitta Kinga Sárvári, Zoltán Balajthy, Zsolt Bacsó and László Fésüs. **Second generation antipsychotic (SGA) drugs modify the differentiation program of human adipocytes inducing ‘browning’ markers** (13th Young Scientists Forum & 38th FEBS Congress, 2013, Saint Petersburg, Russia)

Endre Kristóf, Quang-Minh Doan-Xuan, Anitta Kinga Sárvári, Zoltán Balajthy, Zsolt Bacsó and László Fésüs. **Second generation antipsychotic (SGA) drugs modify the differentiation program of human adipocytes inducing “browning” markers** (Keystone Symposia, Obesity: A Multisystems Perspective, 2014, Vancouver, Canada)

Endre Kristóf, Quang-Minh Doan-Xuan, Péter Bai, Zsolt Bacsó and László Fésüs. **Irisin modifies the differentiation program of subcutaneous human adipocytes and induces “browning”** (FEBS EMBO 2014 Conference, Paris, France)

Endre Kristóf, Quang-Minh Doan-Xuan, Péter Bai, Zsolt Bacsó and László Fésüs. **Laser-scanning cytometry can quantify human adipocyte browning and proves effectiveness of irisin** (Keystone Symposia, Beige and Brown Fat: Basic Biology and Novel Therapeutics, 2015, Snowbird, UT, USA)

Ágnes Klusóczki, Endre Kristóf, Quang-Minh Doan-Xuan, Zsolt Bacsó, Péter Bai and László Fésüs. **Human SGBS preadipocyte cell line can serve as a model for beige differentiation** (Magyar Biokémiai Egyesület Vándorgyűlése, 2016, Szeged)